

https://dspace.org/

Geometric induction of bone formation

Chidarikire, Thato Nelly

2007-02-16T12:34:16Z
http://hdl.handle.net/10539/2035

Downloaded from a DSpace repository. https://dspace.org/

GEOMETRIC INDUCTION OF BONE FORMATION

THATO NELLY CHIDARIKIRE

A thesis submitted to the Faculty of Health Sciences, University of the Witwatersrand, Johannesburg, in fulfilment of the requirements for the degree of Master of Science in Medicine.

Johannesburg, 2006

DECLARATION

I, Thato Nelly Chidarikire declare that this thesis is my own work and has not been submitted before for any degree or examination at this or any other University.

Thato Nelly Chidarikire

.....

.....day of ....., 2006

DEDICATION

To my husband, my son and my daughter……with all my love

PUBLICATIONS ARISEN FROM MATERIAL PRESENTED IN THIS THESIS

1. Michael Thomas, Paul W. Richter, **Thato Matsaba**, Nathaniel Ramoshebi, June Teare, Louise Renton and Ugo Ripamonti. 2003. Gene Expression and Bone Induction Regulated by Bioceramic Substratum. Key Engineering Materials. 240-242: 639-642.

2. **Abstract and Poster:** in the Proceedings of the 15th Bioceramics Symposium on Ceramics in Medicine, Key Engineering Materials, Sydney (Australia). December 4-5, 2002.

Title: Gene Expression and Bone Induction Regulated by Bioceramic Substratum.
Michael Thomas, Paul W. Richter, **Thato Matsaba**, Nathaniel Ramoshebi, June Teare, Louise Renton and Ugo Ripamonti.

3. **Abstract:** in the 4th International Conference on Bone Morphogenetic Proteins. Sacramento (USA). October 17-21, 2002.

Title: Intrinsic Osteoinductivity by Smart Biomimetic Matrices.

Ugo Ripamonti, **Thato Matsaba**, June Teare, Nathaniel Ramoshebi, Louise Renton, Janet Patton, Michael Thomas and Wim Richter.

ABSTRACT

An exciting and novel concept of tissue engineering and morphogenesis is the generation of bone by the implantation of *smart* biomaterials that in their own right can induce a desired and specific morphogenetic response from the host tissues without the addition of exogenously applied bone morphogenetic and osteogenic proteins (BMPs/OPs). Members of the transforming growth factor-∃ (TGF-∃) superfamily of proteins are powerful inducers of bone formation.

Disks of four different types of biomaterials were prepared by the Council of Scientific and Industrial Research (CSIR) Materials and Technology (MATTEK) group, Pretoria, South Africa. The disks were 25mm in diameter and 3mm in thickness and had 69 concavities on one planar side and 25 on the other planar side. The depth of each individual concavity was equal to half the diameter of that particular concavity.

Phase pure hydroxyapatite (HA) with a calcium/phosphorus (Ca/P) molar ratio of 1.67 was prepared by a solid-state reaction between Merck tri-calcium phosphate (TCP) [Ca_3 (PO_4)$_2$] and Univar calcium hydroxide [$Ca(OH)_2$. Types 1 and 2 samples were prepared from hydroxyapatite powders Plasma Biotal, batch P120

(Type 1) and HAOM 21 (Type 2). Types 3 and 4 samples were prepared from degradable biphasic powders consisiting of a 37 mass percentage TCP mixture with 63 mass percent HA. Type 4 samples differed from the Type 3 samples in that large agglomerates of TCP and of HA were separately formed prior to pressing. These agglomerates were then mixed homogeneously and then pressed into discs that were sintered.

All the samples were sintered at 1020 ^{o}C for 1 hour using a ramp rate of 1.5 ^{o}C/minute. This was also a thorough sterilization treatment process. From the furnace the samples were immediately transferred in closed containers to a laminar flow cabinet where filtered air flowed over them. The samples were then transferred into envelopes of Sterilpeel that were immediately sealed in a thermal sealer, all the time untouched by hand. They were taken to the Bone Research Laboratory where they were autoclaved at 121^{o}C for 20 minutes.

The disks were implanted heterotopically in the *rectus abdominis* muscle of 6 baboons and harvested on days 30, 90 and 180 post-implantation. A total of 64 disks were implanted, 16 per animal per time period on days 30 and 90 post-implantation. For the 180 days time period, only Type 2 and Type 4 substrata were implanted, 8

disks per animal. Harvested tissues were subjected to alkaline phosphatase, histology, immunohistochemistry and Northern blot analyses to determine whether the spontaneous induction of bone that occurs only in the concavities is due to trapped BMPs/OPs from the circulation or site and local expression of BMPs/OPs within the concavities.

The alkaline phosphatase activity was generally low in tissues generated in concavities of the different substrata. The activity was relatively higher on 30 days compared to 90 days and was almost undetectable on 180 days. The activity expressed by type 1 samples on day 30 was significantly higher at 5% probability level compared to 180 days. The morphological and histological results of all substrata on 30 days revealed invasion of fibrovascular tissue and angiogenesis within the concavities. On day 90, there was evidence of spontaneous induction of bone formation in concavities of Types 2 and 4 but not in Types 1 and 3. On 180 days also there was induction of bone in concavities of Types 2 and 4. Bone was only observed within the concavities and never on planar surfaces between the concavities. The distribution of induced bone was variable in the concavities of the same substratum as measured histomorphometrically. BMP-3 and

OP-1 were immunolocalised at the interface of the substratum in concavities of Type 2 and Type 4.

Northern blot analyses of tissues generated within the concavities of the various substrata showed clear differences in the mRNA expression of the osteogenic markers including BMP-3, OP-1 and Collage Type IV. Type II collagen and TGFβ1 were however, not expressed in all the different time periods.

The results of this study suggest that the induction of bone within the concavities is due to the expression of BMP/OP family members within the concavities. Furthermore the results suggest that particle size also play an important role since bone formation was only only found in biomaterials with fine distribution of particles as compared to biomaterials with coarse particles. Further studies need to be carried out to give final insights into the spontaneous induction of bone formation within porous biomimetic matrices implanted extraskeletally in adult primates of the species *Papio ursinus*.

ACKNOWLEDGEMENTS

My sincere thanks go to:

My supervisor, Professor Ugo Ripamonti, for his guidance, input, mentorship and inspiration in the creation of this research project.

Dr Nathaniel Ramoshebi, for endless teaching, coaching and continued help during critical moments of this work.

Mrs June Teare and Mrs Louise Renton, for their continued help with the processing of the histological and immunological sections.

Dr Janet Patton and Mrs Jennefer Hesk, for their continued support.

Drs Wim Richter and the late DR Michael Thomas for their continued support through the execution of this thesis

The staff of the Central Animal Service and the Animal Unit of the University, for their assistance in the animal work.

My family and friends, for their support during the implementation of this work.

The Department of Orthopaedic Surgery, University of the Witwatersrand, Johannesburg, where I was registered as a student during the execution of this work.

This work is supported by grants of the South African Medical Research Council, the University of the Witwatersrand, Johannesburg and by *ad hoc* grants of the Bone Research Unit.

CONTENTS

	Page
Declaration	ii
Dedication	iii
Publications	iv
Abstract	vi
Acknowledgements	x
Contents	xii
List of figures	xviii
List of tables	xxiii
Abbreviations	xxiv

1.0	**INTRODUCTION**	**page**
1.1	Initiation of bone formation	1
1.2	Hydroxyapatite (HA) and bone formation	5
1.3	Calcium phosphates and bone formation	7
1.4	HA induced bone formation in different animal models	11
1.5	Intrinsic Osteoinductive biomaterials	15
1.6	Geometric induction of bone formation	19
1.7	The Transforming Growth Factor ß (TGF ß) Superfamily	21
1.8	Bone Morphogenetic Proteins (BMPs) /Osteogenic Proteins(OPs)	26
1.9	TGF ß and bone formation	28
1.10	BMPs/OPS and bone formation	34
1.11	Synergy between TGF-ßs and BMPs	38
1.12	Other Growth Factors	43
1.13	Carriers of bone formation	45

2.0 AIM 50

3.0 MATERIALS AND METHODS 51

3.1 Selection of animals 51

3.2 Biomaterials 52

3.3 Powders 52

3.4 Preparation of biomaterials 53

3.5 Type 1 samples 56

3.6 Type 2 samples 56

3.7 Type 3 samples 57

3.8 Type 4 samples 57

3.9 Implantation protocol 61

3.10 Tissue processing and analytical procedures

3.11 Alkaline phosphatase assay 63

3.11.1 Method 63

3.12 Protein Lowry assay 65

3.12.1 Method 65

3.13 Histology 65

3.13.1 Method 66

3.14 Immunolocalisation of BMP family members 67

3.14.1 Method 67

3.14.2 Antibodies 68

3.15 Northern Blot analysis 68

3.15.1 Preparation of total RNA 68

3.15.2 Method 68

3.16 Formaldehyde agarose gel electrophoresis 71

3.16.1 Method 71

3.17 Sample preparation and gel electrophoresis 71

3.17.1 Method 71

3.18 RNA transfer to membrane 72

3.18.1 Method 72

3.19 Probes and hybridisation 73

3.19.1 Probes 73

3.20 Amplification of constructs of *E. coli* 74

3.20.1 Method 74

3.21 Transformation of *E. coli* 76

3.21.1 Method 76

3.22 Preparation of plasmid DNA 77

3.22.1 Method 77

3.23 Preparation of probe labelled with 32PdCTP 77

3.23.1 Method 77

3.2.4 Hybridisation of probes and detection 78

3.24.1 Method 78

3.25 Signal quantitation 79

3.26 Quantitative analysis 80

3.27 mRNA analysis 80

3.28 Statistical analysis 81

4.0 RESULTS 82

4.1 Scanning Electron Microscope (SEM) characterisation 82

4.1.2 X-Ray Diffraction (XRD) 86

4.1.3 Fourier Transform Infra-Red (FTIR) Spectroscopy 91

4.1.4 Inductively Coupled Plasma mass Spectroscopy 95

4.2 Alkaline Phosphatase activity 96

4.2.1 30 days implantation 97

4.2.2 90 days implantation 97

4.2.3 180 days implantation 98

4.3 Histology and immunolocalisation 100

4.3.1 30 days implantation 101

4.3.2 90 days implantation 101

4.3.3 180 days implantation 101

4.4 Northern Blot Analyses 131

4.4.1 30 days 131

4.4.2 90 days 132

4.4.3 180 days 132

5.0 DISCUSSION 141

6.0 CONCLUDING STATEMENTS 154

7.0 REFERENCES 156

8.0 APPENDICES 194

LIST OF FIGURES

Figure 1: Photomicrograph of a hydroxyapatite (HA) disc with concavities on both planar surfaces.

Figure 1B: High power photomicrograph of a HA disk showing concavities

Figure 2: Die system used for creating concavities on the disks

Figure 3. Implantation protocol for the heterotopic model.

Figure 4: SEM (Scanning Electron Microscope) image of:

A: HA type 1

B: HA type 2

C: HA type 3

D: HA type 4

Figure 5: XRD (X-ray diffraction) image of:

A: Type 1 HA

B: Type 2 HA

C: Type 3 HA

D: Type 4 HA

Figure 6: FTIR (Fourier Transfom Infra-Red) image of:

A: HA type 1

B: HA type 2, 3 and 4 HA

Figure 7: Alkaline Phosphatase Activity of tissues in the concavities of:

A: Type 1, 2, 3, 4 HA at 30 days postimplantation

B: Type 1, 2, 3, 4 HA at 90 days postimplantation

C: Type 2 and 4 HA at 180 days posimplantation

Figure 8: Tissue morphogenesis in the concavities of tissues generated 30, postimplantation in HA (high power photomicrographs):

A: Type 1

B: Type 2

C: Type 3

D: Type 4

Figure 9: Tissue morphogenesis in the concavities of tissues generated 30 days postimplantation in HA (low power photomicrographs).

A: Type 1

B: Type 2

C: Type 3

D: Type 4

Figure 10: Tissue morphogenesis in the concavities of tissues generated 90 days postimplantation in HA (high power photomicrographs).

A: Type 1

B: Type 2

C: Type 3

D: Type 4

Figure 11: Tissue morphogenesis in the concavities of tissues generated 90 days postimplantation in HA (low power photomicrographs).

A: Type 1

B: Type 2

C: Type 3

D: Type 4

Figure 12: Surface geometry of tissues generated in the concavities of HA types 2 and 4 90 days postimplantation

Figure 13: Tissue morphogenesis in the concavities of tissues generated 180 days postimplantation in HA (high power photomicrographs).

A: Type 2

B: Type 4

Figure 14: Tissue morphogenesis in the concavities of tissues generated 180 days postimplantation in HA (low power photomicrographs).

A: Type 1

B: Type 2

Figure 15: The effect of surface geometry on of tissues generated in the concavities of hydroxyapatite Types 2 and 4 on day 180 post-implantation.

Figure 16: Immunolocalisation of BMP-3 and BMP-7/OP-1 in tissues generated within the concavities of the hydroxyapatite substratum on day 30 postimplantation.

A: Control of OP-1

B: Immunolocalisation of OP-1

C: Control of BMP-3

D: Immunolocalisation of BMP-3

Figure 17: Immunolocalisation of BMP-3 and BMP-7/OP-1 in tissues generated within the concavities of the hydroxyapatite substratum on day 90 postimplantation.

Figure 18. Northern analysis of mRNA expression of OP-1, BMP-3 and collagen type IV in specimens generated within the concavities of four different types of substrata

A: 30 days postimplantation

B: 90 days postimplantation

C: 180 days postimplantation.

LIST OF TABLES

Table 1. Summary of results generated from tissues harvested 30, 90 and 180 days postimplantation

Table 2. mRNA expression of OP-1, BMP-3, TGF-β1, Collagen type II and collagen type IV in specimens generated within the concavities of hydroxyapatite substrata Type 1 to 4 on 30, 90 and 180 days post-implantation.

ABBREVIATIONS USED IN THIS THESIS

TGF-β	transforming growth factor beta
BMP/OP	bone morphogenetic protein/osteogenic protein
SPHA	sintered porous hydroxyapatite
HA	hydroxyapatite
mRNA	messenger ribonucleic acid
cDNA	complementary deoxyribonucleic acid
PBS	phosphate buffered saline
r	recombinant
p	porcine
h	human
SSC	saline sodium citrate
DBM	demineralised bone matrix
ICBM	insoluble collagenous bone matrix

1.0 INTRODUCTION

1.1 Initiation of bone formation

Bone has a capacity to repair and regenerate. Lacroix (1945) observed that alcoholic extract of the rabbit long bone cartilagenous epiphyses promoted bone formation when implanted intramuscularly or subcutaneously. Based on this observation, the author hypothesised that in bone there may be substances that might initiate bone growth, which he named osteogenins. This was followed by the studies of Urist (1965) and Reddi and Huggins (1972) who first used *in vivo* assays to study bone-inductive properties of demineralised bone matrix and then stimulated many other groups to contribute to the growing knowledge of the molecular and cellular signals involved in endochondral bone formation

Bone tissue is a complex organ composed of differentiated cells called osteoblasts, which are derived from mesenchymal progenitor cells (Ohgushi *et al*., 1993). The major constituent of bone is calcium hydroxyapatite, which is composed of calcium phosphate laid into a framework of connective tissue (Yamashita *et al*., 1994). Bone also consists of trace elements (Driessens and Verbeeck, 1990).

The studies of Urist (1965) and Reddi and Huggins (1972) have led to the postulation of a bone morphogenetic protein/osteogenic protein (BMP/OP) complex in the bone matrix (Urist *et al*., 1984; Sampath *et al*., 1987). Intramuscular implantation and subcutaneous implantation of demineralised bone matrix (DBM) led to bone formation by induction in the recipient animals as reported by Urist (1965) and Reddi and Huggins (1972), respectively. To investigate whether the factor or factors responsible for bone formation in the demineralised bone matrix was the combined action of several factors present in bone, a separate protein, or a new unknown family of proteins, naturally-derived BMPs/OPs were isolated from the demineralised bone matrix and purified to provide information for amino acid sequences (Wang *et al*., 1988; Luyten *et al*., 1989). This work led to expression cloning and characterisation of the recombinant human BMPs/OPs (Wozney *et al*., 1988).

The purification and molecular cloning of the BMPs/OPs has set the stage for novel therapeutic approaches to correct congenital and acquired craniofacial and orthopaedic conditions (Ripamonti and Vukicevic, 1995). Furthermore, the purification of BMPs/OPs has led to the cellular and molecular dissection of bone development and regeneration.

The first sign that indicates imminent osteogenesis is the condensation of mesenchymal and mesodermal cells to form a primordium of bone. Bone has a considerable potential for repair and regeneration and the stages of fracture repair recapitulate the sequential developmental stages of embryonic endochondral bone development (Reddi, 1992; Wozney, 1992; Reddi, 1994). A cellular cascade that mimics embryonic endochondral bone development can be induced locally by implantation of demineralized bone matrix (DBM) in extra-skeletal sites (Urist, 1965; Reddi and Huggins, 1972; Reddi, 1981).

The cellular and biochemical events of this matrix-induced endochondral bone cascade have been well endorsed (Reddi and Huggins, 1972; Reddi, 1981). The developmental cascade of matrix-induced endochondral bone formation consists of chemotaxis and attachment of mesenchymal stem cells to the matrix, proliferation of mesenchymal progenitor cells followed by cartilage differentiation, which in turn is followed by calcification of the cartilage, chondrolysis and finally hematopoiesis in the newly formed ossicle (Reddi, 1981). These events are sequentially coordinated in a rigorous fashion by members of the transforming growth factor-beta (TGF-β) and bone morphogenetic proteins/osteogenic proteins (BMP/OP) families.

In rodents, the cascade of bone formation is as follows (Reddi 1981): Fibronectin deposition on the matrix, facilitating cell attachment, proliferation of mesenchymal cells follows, resulting in chondroblast differentiation; appearance of chondrogenic matrix as shown by sulphate incorporation into proteoglycans and appearance of chondrocytes. The beginning of angiogenesis and cartilage resorption or chondrolysis then follows. New bone formation in association with calcium incorporation occurs after differentiation of osteoblasts, followed by extensive bone remodeling with hematopoietic marrow formation as evidenced by iron incorporation.

Embryonic events give rise to five types of cells which are responsible for the production of the five mineralised tissues in the body. These are: osteoblasts producing bone, chondroblasts producing cartilage, odontoblats producing dentine, cementoblasts producing cementum and ameloblasts producing enamel (Urist, 1980). During development and adult life, osteoblasts and osteoclasts continuously replace old bone with new bone through the process of bone remodeling (reviewed by Parfitt, 1994). The cycles of bone deposition and resorption are tightly linked (Harris *et al.*, 1969) thereby maintaining skeletal integrity, bone mass and

shape. This concept postulates that bone resorption, which occurs in order to release calcium for homeostatic needs or to reshape bone structure to fit better its mechanical function, is followed by bone formation which under balanced conditions, restores the lost bone.

1.2 Hydroxyapatite and bone formation

Hydroxyapatite (HA) is an important biomaterial because of its affinity for BMPs/OPs which is employed for the chromatographic purification of BMPs/OPs extracted from the bone matrix and has been exploited for the construction of the delivery systems following BMPs/OPs' chromatographic adsorption onto porous hydroxyapatite (Ripamonti *et al*., 1993b).

Hydroxyapatite is desirable as a bone substitute because it is the prototype of human bone and teeth (Sasano *et al*., 1995) comprising 60-70% of the bone matrix and 98% of dental enamel (Jarcho, 1986). The desirability of alternatives to the currently available, usually metallic, uniformly dense and harder than bone implants has been the source of many intensive investigations in the research laboratories on biomaterials around the world. A

specified advantage of materials fabricated in a porous configuration is the potential for ingrowth of tissue such as to provide biological fixation of the hard tissue implants (Chiroff *et al*., 1975; Feldman and Estridge, 1984). Various techniques for the fabrication of materials have been devised. Extensive alterations of various hydroxyapatite porosities have been accomplished (Hulbert *et al*., 1970; Ripamonti *et al.,* 1999).

Denissen *et al*. (2000a) conducted experimental and clinical studies to evaluate the effect of highly biphosphonate-complexed hydroxyapatite implants on osteoconduction and repair in alveolar bone. They used porous hydroxyapatite implants pretreated with 10 (-2) M bisphosphonate solution and implanted in goats. The authors concluded that the study contributed to the understanding of the biological properties of hydroxyapatite implants as carriers for the bone-modulating agent biphosphonate. The study also suggested that normal osteoconduction and repair occurred in alveolar bone around the highly bisphosphonate-complexed hydroxyapatite implants (Denissen *et al*., 2000a).

Denissen *et al*. (2000b) performed another study to evaluate the effects of biphosphonate-complexed hydroxyapatite implants on osteoconduction and repair in rat tibiae. Indeed their results

suggested that normal osteoconduction and repair occurred in and around the highly bisphosphonate-complexed hydroxyapatite implants in rat tibiae; these results support the previous study.

Allumina substrata are also used in total joint replacement mainly because of their inertness, excellent biocompatibility and high wear resistance (Christel, 1992; Cooke, 1992; Heimke, 1990; Hulbert, 1990) although alumina does not bond to bone as well as HA. The problem of bonding between alumina and bone was solved by coating porous alumina substrata with HA (Takaoka *et al*., 1996). The HA-coated alumina has a high mechanical strength as well as bioactive properties. HA coating on other implants has been previously reported and it has been shown that HA coating stimulates bone formation (Cook *et al*., 1986; Cook *et al*., 1987; Dhert *et al*., 1991; Furlong, 1991; Geesink, *et al*., 1988; Soballe *et al*., 1989).

1.3 Calcium phosphates and bone formation

The calcium phosphate bioceramic materials are described as sintered polycrystalline solids whose structure is characterized by distinct individual crystals held together by grain boundary phases,

a typical result of the solid phase reaction during sintering (Osborn J F, 1985).

Tricalcium phosphate (TCP) is an important biomaterial that can be used as a bone graft substitute.TCP was reported to be comparable to hydroxyapatite in terms of biocompatibility and osteoconductivity in the presence of marrow cells (Ohgushi *et al*., 1990; Ohgushi *et al*., 1993). TCP is an important biomaterial because of its biodegradability. The concept that calcium phosphate biomaterials are safe and effective for a variety of clinical applications has been well documented (Metsger *et al*., 1982; De Groot, 1980; Jarcho, 1981). Two forms of calcium phosphate substrata, HA and TCP are the most commonly used. TCP, unlike hydroxyapatite, is not a natural component of bone mineral but is chemically similar to HA (Jarco, 1986).

Calcium phosphate biomaterials are the most biocompatible synthetic substances known for use in hard tissue implantations because they are devoid of local or synthetic toxicity, do not elicit inflammatory or foreign body reactions, can become functionally integrated with natural bone with no fibrous tissue encapsulation and can cause no alteration of normal bone mineralization processes (Jarcho, 1986). Moreover, another compelling feature

of calcium phosphate is their ability to become strongly bonded to living bone. This phenomenon of bonding has been observed and reported in many studies (Dessen *et al*., 1981; Jarcho, 1981; Jarcho, 1977; Kato *et al*., 1979; Ogiso, 1983; 1980; Tracy and Doremus, 1984). Probably the exceptional biocompatibility of these biomaterials is attributable to their being primarily composed of calcium and phosphate ions, the most common constituents of vertebrate hard tissue systems (Jarcho, 1986). Calcium phosphate biomaterials provide a physical matrix suitable for deposition of new bone and can display growth-guiding properties that cause bone to extend its growth into areas it would not otherwise occupy (Itatani and Marshall, 1984; McDavid *et al*., 1979, Pieench, 1982).

Calcium phosphate substrata have also demonstrated the ability to maintain bone bulk in areas where bone resorption normally takes place. Several investigators have noted that HA implants are able to prevent post extraction alveolar ridge resorption in much the same manner as do autogenous tooth roots (Jarcho, 1986). When placed either sub- or perigingivally in fresh extraction sockets of dogs, these implants become firmly ankylosed *via* the bone-bonding phenomenon while maintaining and increasing the height of surrounding bone relative to unimplanted control

extraction sites (Jarcho, 1986). Calcium phosphate substrata are also well tolerated by soft tissues, wherein they are usually surrounded by a quiescent fibrous tissue capsule (Jarcho, 1986). The factors governing bioresorbability of calcium phosphate biomaterials are not fully understood, but appear to include chemical composition and porosity of the particular form of calcium phosphate. It is thought that bioresorption can result from both chemical dissolution in biologic fluids and cell mediated processes such as phagocytosis (De Groot, 1983; 1980; Jarco, 1981). The surface area of calcium phosphate substratum is also important in determining bioresorption. High density biomaterials posses a much smaller surface area than porous ones and have thus a lesser resorbability.

The use of porous forms of calcium phosphate substrata offers several attractions conceptually. Despite the fact that porous implants are more easily carved than dense ones and also that the pores can provide a mechanical interlock leading to a firmer initial fixation of the implant during the immediate post operative phase, major and fundamental questions remain as to the suitability of porous implants for permanent implant applications. Porous implants have very little strength and depend on bone ingrowth to achieve a mechanically viable restoration.

Much experimental evidence attests to the ability of calcium phosphate biomaterials to bond to bone. Okumora *et al*. (1991); Fujiu and Ogino, (1984); Kitsugi *et al*., (1989). Hench et al. (1971) studied the hydroxyapatite-bone bonding mechanism at the interface between bone and glass. He found that the presence of crystals of hydroxyapatite on the surface of glass using scanning electro microscope (SEM), transmission electron microscope (TEM) and X-ray diffraction analysis. The results suggested the direct chemical bonding of hydroxyapatite crystals at the interface. Subsequently, many investigations of the interface between bone and bioactive hydroxyapatite have been performed in a variety of techniques. (Holland *et al*., 1985; Krajewski *et al*., 1988).

1.4 Hydroxyapatite-induced bone formation in different animal models

Studies using porous hydroxyapatite biomaterials have been carried out in different animal models. Ripamonti, (1996) used porous hydroxyapatite obtained after hydrothermal conversion of the calcium carbonate exoskeleton of coral to induce bone formation in the *rectus abdominis* of adult rabbits, dogs and baboons without addition of exogenous BMPs/OPs. The author reported minimal amount of bone in dogs and rabbits, and a

substantial amount of bone in the baboon (Ripamonti, 1996). In rats, implantation of hydroxyapatite both intramuscularly and subcutaneously does not result in bone formation (Ohgushi *et al*., 1989; Goshima *et al*., 1991; Yosghikawa *et al*., 1992; Ohgushi *et al*., 1993). Bone formation was also demonstrated within porous hydroxyapatite implanted intramuscularly in rabbits (Miller *et al*., 1991). Osteoinduction has also been observed in rabbit and rat models when the porous hydroxyapatite was combined with BMPs/OPs (Ripamonti *et al*., 1992a; Takaoka *et al*., 1988). Formation of bone has also been reported in dogs on implantation of porous hydroxyapatite in soft tissue sites (Yamasaki and Sakai, 1992). Arun *et al*. (2002) demonstrated osteoinduction upon implantation of porous hydroxyapatite in intramuscular and subcutaneous sites in sheep.

Kurashina *et al* (2002) reported ectopic osteogenesis with biphasic ceramics of hydroxyapatite and tricalcium phosphate in rabbits. The authors implanted porous calcium phosphate ceramics consisting of hydroxyapatite and tricalcium phosphate with different ratios intramuscularly in rabbits for six months. Their results showed bone formation in one type of ceramic while the other types showed some degree of degradation but not bone formation. They reported that the degradation rate of the

biomaterials may be one of the affecting factors in ceramic-induced osteogenesis. Further more, Yamasaki (1990) found bone formation induced by hydroxyapatite ceramic in the dogs' subcutis. Similar results were reported in different animal models such as rabbits, goats, pigs, dogs, monkeys, baboons and humans (Zhang *et al*. 1991; Vagervic, (1992); Toth, (1993); Klein, (1994); Green *et al*. (1995); Yang *et al*. (1996); Yuan *et al*. (1997); Sires *et al*. (1997); de Bruijn *et al*. (1999); Yuan *et al*. (2000).
Calcium phosphate ceramics have also been reported to be osteoinductive in muscles of dogs (Yuan *et al*., 2001).

Previous studies have shown that porous hydroxyapatite plays an important role as a cell substratum in BMP-induced heterotopic bone formation (Ono *et al*., 1992; Ono *et al*., 1995; Ono *et al*., 1996; Ravaglioli *et al*., 1992; Ripamonti *et al*., 1992a; Ripamonti *et al*., 1993b; Ripamonti *et al*., 1999; Ripamonti *et al*., 2001). An artificial cell substratum requires biochemical, physiochemical and geometric properties. The biochemical property involves mainly the molecules of the extracellular matrix, which bind to the adhesive receptor molecules of the cell surface. The physiochemical aspect is involved in the adsorption of cells on the substrate surfaces. These two properties have already been well documented. Geometry, which refers to the three dimensional

shape, porosity, particle size and geometrical configuration in the form of repetitive sequence of concavities, on the other hand is not yet well understood. The geometry of the substratum has been shown to profoundly influence the expression of the chondro-osteogenic phenotype *in vivo* although the mechanisms involved are not clearly understood (Reddi and Huggins, 1973; Ripamonti *et al*., 1992a; Sampath and Reddi, 1984; Ripamonti *et al*., 1999; Ripamonti, 2000c)

Jin *et al*. (2000) investigated the geometry of the BMPs/OPs carriers in bone formation in rats. They used three different types of hydroxyapatites, namely, porous particles, porous blocks and honeycomb-shaped hydroxyapatites. These carriers were compared in terms of their abilities to initiate osteogenesis when implanted subcutaneously with recombinant hBMP-2. Their results showed that direct bone formation occurred in porous and in block particles of hydroxyapatite while endochondral ossification occurred in honeycomb-shaped hydroxyapatite. Cartilage in the central zones and bone in the orifice zones of the tunnels of the honeycomb-shaped hydroxyapatite were observed at two weeks after which the cartilage disappeared and bone formation occurred throughout the inner surface of the tunnels of the hydroxyapatite, leaving space for capillaries within the tunnels. The authors

concluded that the geometry of the hydroxyapatite controls vascular capillary invasion and affects cell growth and differentiation and thus phenotype expression in the BMP-induced heterotopic bone and cartilage induction (Jin *et al.,* 2000).

Manipulation of the geometry and the surface characteristics of the substratum and incorporation of specific biological activities into biomaterials will result in predictable bone morphogenesis and growth for treatment of human bone defects. This phenomenon is defined as *geometric induction of bone formation* and will aid in achieving breakthroughs in tissue engineering of bone and related tissues for therapeutic osteogenesis in clinical contexts (Ripamonti *et al*., 1999; Ripamonti, 2000c).

1.5 Intrinsic osteoinductive biomaterials

The use of intrinsic osteoinductive biomaterials including porous hydroxyapatite (HA) has been documented (Ripamonti *et al*., 1992a; Ripamonti *et al*., 1993b; van Eeden and Ripamonti, 1994; Ripamonti *et al*., 1999; Ripamonti *et al*., 2000a Ripamonti *et al*., 20001). Further experiments were conducted by Ripamonti and co-workers to create and study biomaterials that in their own right, when implanted heterotopically in recipient animals, can induce specific morphogenetic responses from the host tissue without the

addition of exogenously applied BMPs/OPs, *i.e.*, biomaterials with intrinsic osteoinductive activity (Ripamonti *et al.*, 1999).

The optimal induction of bone formation is dependent on the combined action of BMPs/OPs and the insoluble substratum that is complementary. The preparation of composites of osteoconductive biomaterials with BMPs/OPs results in the formulation of osteoinductive biomaterials (Ripamonti and Duneas, 1996; Ripamonti *et al.*, 1999). This concept is of great significance for future therapeutic applications. The acid test for osteoinductivity is the histological evidence of bone formation by induction in extraskeletal heterotopic sites of animals.

Ideal biomaterials for tissue engineering of bone should be non immunogenic, carvable, and amenable to contouring for optimal adaptation to the various shapes of bone defects, providing mechanical support when needed (Ripamonti and Duneas, 1996). In addition to initiating optimal osteogenesis with relatively low doses of hBMPs/OPs, ideal biomaterials should also promote rapid vascular and mesenchymal cell invasion to be brought into contact with BMPs/OPs previously adsorbed onto the carrier (Ripamonti and Duneas, 1996). It should also have the ability to remodel and resorb. Materials made of calcium phosphate

apatites have to date been the most useful synthetic biomaterials for bone replacement therapies (Jarcho, 1981; Hench, and Wilson, 1984). They are all capable of osteoconductivity and osteointegration to varying degrees depending on preparation and specific chemical composition.

Several studies have been performed that establish that some porous hydroxyapatite obtained from the calcium carbonate exoskeleton of corals can induce bone differentiation in direct contact with the hydroxyapatite substratum when implanted extraskeletally in adult baboons (Ripamonti, 1990; Ripamonti *et al*., 1993a; Ripamonti, 1996, van Eeden and Ripamonti, 1994). In these experiments in heterotopic sites of baboons, bone formation was only limited to porous hydroxyapatites in block configuration as opposed to identical porous hydroxyapatite in granular and particulate configuration.

It is important to differentiate between an osteoconductive and an osteoinductive biomaterial. The former does not posses inherent osteoinductivity *per se*, but is capable of guiding and directing bone growth at its interface and achieving osteointegration after orthotopic implantation (Ripamonti and Duneas, 1996; Ripamonti *et al*., 1999). The latter bears osteoinductivity and its

discriminatory bioaction is osteogenesis (Ripamonti and Duneas, 1996). The generation of bone by the implantation of biomaterials that can induce desired and specific responses from the host tissues without addition of exogenously applied BMPs/OPs is an exciting and novel concept of bone tissue engineering (Ripamonti *et al.*, 1999).

The use of biocompatible and bioactive materials for drug delivery and tissue engineering has been well documented (Hoffman 1995; Ito *et al.*, 1997; Williams, 1997; Graham.1998; Ripamonti *et al.*, 1999; Wang *et al*, 1999; Galaev and Mattiason, 1999; Langer, 2000). These biomaterials have the ability to control biological functions by responding to physical, chemical or biological stimuli (Hoffman, 1995). This concept has been highlighted for tissue engineering of bone by the heterotopic induction of bone (Ripamonti *et al.*, 1999) and osteoconduction by porous hydroxyapatite in experimental animals (Chang *et al.*, 2000). The mechanism behind osteogenesis in these bone induction studies appears to be greatly dependent on the nature and the structure of the substratum (van Eeden and Ripamonti, 1994; Tsuruga *et al.*, 1997; Kuboki *et al.*, 1995; 1998; Murata *et al.*, 1998; Ripamonti *et al.*, 1999; Kurioka *et al.*, 1999; Jin *et al.*, 2000).

The general background for undertaking such studies is the aim to develop biomimetic biomaterials that are specifically designed to enable endogenously produced molecular signals to adsorb onto the implanted matrix or to intrinsically activate their genes (Ripamonti *et al*., 1999; Ripamonti, 2000c; Ripamonti *et al*., 2001) by the implantation of these structurally correct matrices in sites where bone induction is required. The adaptable character of these biomaterials makes them more practical and more cost effective in their application than devices requiring the combination of both carriers and growth factors (Ripamonti *et al*., 2001).

1.6 Geometric induction of bone formation

The effects of matrices on cell differentiation were first demonstrated by Reddi and Huggins (1973). They showed that the matrices of open and dead-end tube structures had different effects on osteogenesis and chondrogenesis. The dead-end tubes induced chondrogenesis while the open-end tubes induced osteogenesis. The authors suggested that the result was due to the higher vasculature in the open tube and that the higher oxygen and nutrient supply favored osteogenesis while the lesser vasculature in the other tube led only to chondrogenesis (Reddi and Huggins, 1972).

The critical role of the geometry of the substratum in the regulation of cell growth and endochondral bone differentiation has been reported previously using different geometric configurations of collagenous matrix indicating that the endochondral sequence can be greatly altered by the geometry of the inductor (Reddi and Huggins, 1973; Reddi, 1974; Sampath and Reddi, 1984).

Ripamonti *et al*. (1992a) reported that the geometry of the substratum had a profound influence on bone induction in rodents. The authors delivered BMPs/OPs using non-resorbable porous hydroxyapatite in granular and disc configurations. The expression of the osteogenic phenotype was exclusively observed in porous hydroxyapatite in disc configuration as opposed to granular hydroxyapatite with identical pore dimensions even in the presence of exogenously-applied BMPs/OPs (Ripamonti *et al*., 1992a). van Eeden and Ripamonti later reported the effects of the geometry of the carrier on bone formation by comparing porous hydroxyapatite in block and granular forms with different pore sizes (200 and 500 µm) (van Eeden and Ripamonti, 1994). In this study there was higher efficacy of bone induction in the block configuration and no bone in the granular form.

Monolithic discs of sintered hydroxyapatite with concavities of 800 and 1600μm diameter on both planar surfaces were implanted in the *rectus abdominis* of adult baboons (*Papio ursinus*) to investigate the geometric influence on bone formation (Ripamonti, *et al*., 1999). Spontaneous initiation of bone proved to be regulated by the geometry of the substratum i.e. the concavities. This supports a novel concept in tissue engineering of bone, that is, substrata with osteoinductive geometric configurations, since bone morphogenesis and the generation of marrow depends exclusively on the geometry of the HA substratum (Ripamonti *et al*., 1999).

1.7 The TGF-ß superfamily

The TGF-ß superfamily comprises a large group of structurally related signalling proteins that are secreted as dimers and then cleaved after an Arg-X-X-X-Arg site to release biologically active carboxy-terminal domains containing seven highly conserved cysteine residues (Kingsley, 1994). The group consists of BMPs (Wozney *et al*., 1988; Özkaynak *et al*., 1990; Celeste *et al*., 1990); activins and inhibins (Mason *et al*., 1985; Forage *et al*., 1986; Mayo *et al*., 1986; Schwall *et al*., 1988), the 60 A (Wharton *et al*., 1991) the Müllerian inhibitory substance (MIS) (Cate *et al*., 1996), the *dpp* gene products of *Drosophila melanogaster* (Padget *et al*.,

1987; Ferguson and Anderson, 1992); the vegetal Vg-1 gene products of *Xenopus Laevis* (Weeks and Melton, 1987); the Vg-1 related analogue of murine Vgr-1 (Lyons *et al*, 1989); the more distantly related growth and differentiating factors (GDFs) (Lee, 1990; Lee, 1991; McPherron and Lee, 1993; Jones *et al*., 1992; Cunningham *et al*., 1995), the cartilage derived morphogenetic proteins (CDMPs) (Chang *et al*., 1994) and finally, the TGF-ßs themselves (Derynck *et al*., 1985; Roberts and Sporn, 1990).

TGF-βs are biologically active peptides whose unique feature is to induce anchorage-dependent, non-neoplastic cells to lose contact inhibition and to undergo anchorage independent growth, a property that can be quantitated by measuring the formation of colonies of cells in soft agar (De Larco and Torado, 1978; Roberts, *et al*., 1980; Roberts *et al*., 1981). TGF-βs were identified in human platelets by Assoian *et al*. (1983) as composed of a 25 kDa polypeptide made up of two 12.5 kDa subunits held together by disulphide linkage.

TGF-βs are released from the cell in inactive complexes that require activation (Centrella *et al*., 1994). To become biologically active, they have to be dissociated from the latent complex (Gentry *et al*., 1987). The TGF-β family comprises 5 closely

related proteins called TGF-β 1 to –5 (Roberts and Sporn, 1990) of which 1 to –3 are mammalian, 4, now known as a new molecule called ebaf/lefty-A (Kothapalli *et al*., 1997) was identified in chicken and the isoform -5 in *Xenopus laevis*. Like BMPs/OPs the amino acid carboxyl terminal domain of the TGF-βs is highly conserved between species (Roberts *et al*., 1991).

Active TGF-β contains 9 cystein residues, seven of which are conserved within members of the family. TGF-β1 is identical in man, monkey, cow and chicken. TGF-β 2 is 71% homologous to TGF-β1 and the other TGF-βs share homology in the range of 64% to 83% with TGF-β1 (Roberts *et al*., 1991). The mature region of TGF-β3 has an approximately 80% identity to the mature regions of TGF-β1 and TGF-β2. The precursor regions of the first three isoforms share 27% sequence identity (ten Djike *et al*., 1988; Derynck *et al*., 1988). The first three isoforms have been found also in human tissues. Wataya-Kaneda, *et al*. (1994) used immunohistochemistry to show that TGF-β2 localisation was mainly in the intercellular space of all the layers of the epidermis and weakly in the cytoplasm. TGF-β3 was present in the subepidermal area of the dermis and TGF-β1 was not observed either in the dermis or epidermis. These results suggest that TGF-β2 and -3 may play a crucial role in the regulation of the human

skin function in an epithelial autocrine or mesenchymal -epithelial interaction manner.

Members of the TGF-β family have diverse biological activities and play critical roles in the migration, proliferation and differentiation of a variety of cells during embryogenesis (Heine *et al*., 1987; Pelton *et al*., 1990), repair and regeneration as well as maintenance of tissues during post-fetal life (Roberts and Sporn, 1990; Derynck, 1994; Kingsley; 1994). TGF-βs were reported to play important roles in epithelial-mesenchymal interactions in that they enhance the differentiation of epithelial and mesenchymal cells (Vukicevic *et al*., 1996). Lehnet and Akhust (1988); Pelton *et al*. (1989; 1990); Millan *et al*. (1991); Schmidt *et al*. (1991) reported the temporal and spatial expression of TGF-β isoforms in various developing tissues undergoing epithelial and mesenchymal interactions such as kidney, heart, hair, palate, lung, skin, whisker follicles, teeth and mammary glands. Moreover, TGF-β1 is abundantly found in connective tissue, cartilage and bone as well as in tissues derived from neural crest mesenchyme (Heine *et al*., 1987).

TGF-β2 has been found in early facial mesenchyme and in various epithelial cells (Pelton *et al*., 1989). Heine *et al*. (1987)

also reported the localisation of TGF-β2 during mesenchyme and mesoderm remodeling. TGF-β2 was localized during the formation of digits from limb buds, palate formation and heart valves formation. de Bortolli *et al*. (1995) reported the role of TGF-β isoforms in epithelial maturation of the developing rat fetal lung. Immunofluorescence showed localisation of TGF-β 1,-2, and –3 in rat fetal lung fibroblasts.

TGF-β1 knockout mice die in *utero* and the remainders give in to uncontrolled inflammation after birth (Kulkarni *et al*., 1993). Letterio and Bottinger (1998) reported the role of TGF-β isoforms in the regulation of the immune system. Their results showed evidence for altered development, activation and function of various immune populations in knockout mice. TGF-βs increase the cytokine-dependence of T cells for survival (Sillet *et al*., 2001). Clark and Coker (1998) demonstrated the role of TGF-βs in homeostatic and pathogenic processes and suggested that TGF-βs may play an important role in the diagnosis and treatment of various diseases characterized by inflammation and fibrosis. Furthermore, TGF-β has been reported to promote virus replication in infected monocytes and peripheral blood mononuclear cells under certain *in vitro* conditions (Lotz and Seth, 1993).

1.8 Bone morphogenetic proteins (BMPs)

Bone has a capacity to repair and regenerate. Lacroix (1945) observed that alcoholic extract of the rabbit long bone cartilagenous epiphyses promoted bone formation when implanted intramuscularly or subcutaneously. Based on this observation, the author hypothesised that in bone there may be substances that might initiate bone growth, which he named osteogenins. This was followed by the studies of Urist (1965) and Reddi and Huggins (1972) who first used *in vivo* assays to study the bone-inductive properties of demineralised bone matrix and then stimulated many other groups to contribute to the growing knowledge of the molecular and cellular signals involved in endochondral bone formation.

The studies of Urist (1965) and Reddi and Huggins (1972) have led to the postulation of a bone morphogenetic protein/osteogenic protein (BMP/OP) complex in the bone matrix (Urist *et al*., 1984; Sampath *et al*., 1987). Intramuscular or subcutaneous implantation of demineralised bone matrix (DBM) led to bone formation by induction in the recipient animals as reported by Urist (1965) and Reddi and Huggins (1972), respectively. To investigate whether the factor or factors responsible for bone formation in the demineralised bone matrix was the combined action of several

proteins present in bone, a separate protein, or a new unknown family of proteins, naturally-derived BMPs/OPs were isolated from demineralised bone matrix and purified to provide information for amino acid sequences (Wang *et al*., 1988; Luyten *et al*., 1989). This work led to expression cloning and characterisation of the recombinant human BMPs/OPs (Wozney *et al*., 1988).

The purification and molecular cloning of the BMPs/OPs has set the stage for novel therapeutic approaches to correct congenital and acquired craniofacial and orthopaedic conditions (Ripamonti and Vukicevic, 1995). Furthermore, the purification of BMPs/OPs has led to the cellular and molecular dissection of bone development and regeneration.

BMPs/OPs have the ability to singly induce *de novo* endochondral bone formation when implanted in heterotopic sites of experimental animals (Reddi, 1992; Wozney, 1992; Reddi, 1994). On the basis of characteristics that include amino acid sequences in the carboxyl terminal region and their tertiary structure, the BMPs/OPs are grouped as a family within the transforming growth factor beta (TGF-β) superfamily (Wozney *et al*., 1988; Reddi, 1992; Wozney, 1992; Centrella, 1994). BMP-1 is the only BMP/OP that is not a member of the TGF-β superfamily (Kessler, 1996;

Reddi, 1996). It is a procollagen C-proteinase, functioning *in vivo* for the proper assembly of collagen within the extracellular matrix (Kessler, 1996; Reddi, 1996).

To initiate the biochemical and morphological sequences required for tissue engineering of bone, three key components are needed: a soluble osteoinductive signal, a suitable insoluble substratum that acts as a delivery system and scaffold for new bone to form and responding mesenchymal cells capable of differentiation into bone cells (Reddi, 1994; Ripamonti and Duneas, 1996; Ripamonti and Reddi, 1997).

The ability of BMPs/OPs to induce bone in heterotopic sites is a characteristic that has attracted the strong attention of scientists in the orthopedic, craniofacial and dental fields in anticipation of its clinical applications. To achieve the clinical applications of BMPs/OPs, optimal carriers must be investigated and developed.

1.9 TGF-ß and bone formation

Since their first detection in skeletal tissues, TGF-β family members have been investigated as potential regulators of bone cell activities. Target cells include cells that participate in various stages of bone formation and they may induce primary and

secondary effects on bone resorbing osteoclasts (Centrella *et al*., 1994). Several lines of evidence have indicated that the secreted proteins of the TGF-β superfamily are involved in the local and systemic regulation of tissue morphogenesis, including skeletogenesis, osteogenesis, cementogenesis and nephrogenesis (Wozney *et al*., 1988; Reddi, 1994; 1997; 1998; Ripamonti and Vukicevic, 1995; Vukicevic *et al*., 1996; 1998; Duneas *et al*., 1998; Ripamonti and Reddi, 1997).

When TGF-β is injected directly to calvariae or to overlying periosteal tissues, the bone mass increases in mice and rats (Noda and Camilliere, 1989; Marcelli *et al*., 1990). Marcelli *et al*. (1990) showed that repeated injections of rhTGF-β1 into the subcutaneous tissue overlying the calvaria of neonatal mice resulted in a marked increase in the periosteal thickness and cellularity and stimulation of newly mineralised bone without a chondrogenic phase. Beck *et al*. (1991) reported that topical application of TGF-β1 to cartilage in full thickness wounds on rabbit ears rapidly induces healing and bone formation. Later studies using the rabbit calvarial model showed that defects treated with hTGF-β1 were characterized by an increase in parameters of bone formation up to 49 days (Beck *et al*., 1993). However, when implanted into calvarial defects of the primate

Papio ursinus, hTGF-β1 promotes histologically and histomorphometrically limited chondro-osteogenesis and confined only to defect margins as evaluated on day 30 post implantation (Ripamonti *et al*., 1996c).

TGF-β1 also plays important roles during injury. Upon platelet degranulation at the injury site, TGF-β1 is released into the surrounding tissue and a complex sequence of events that promote healing is then initiated. Systemic injection of TGF-β2 leads to generalized increase in osteoblastic activity (Rosen *et al*., 1994). Systemic administration of TGF-β2 also prevents impaired bone formation and osteopenia induced by unloading in rats (Machwate *et al*., 1995). Ripamonti *et al*. (1997) and Duneas *et al*. (1998) demonstrated that recombinant human and platelet-derived TGF-β1 induces endochondral bone formation in heterotopic sites of the baboon (*Papio ursinus*). It was further demonstrated that hTGF-β1 interacts synergistically with hOP-1 to induce massive ossicles in the *rectus abdominis* of primates as evaluated by key parameters of bone formation on days 14 and 30 postimplantation (Ripamonti *et al*., 1997). In 2000, Ripamonti and co-workers reported the heterotopic induction of endochondral bone formation by hTGF-β2 in the baboon (*Papio ursinus*) (Ripamonti *et al*., 2000a). They showed that hTGF-β2 induces

endochondral bone formation 30 days postimplantation in heterotopic intramuscular sites using insoluble collagenous bone matrix as well as sintered porous hydroxyapatite as carriers.

In rodents however, TGF-β1 induces only granulation tissue with potentially marked fibrosis (Roberts *et al*., 1986; Shinozaki *et al*., 1997). The finding that TGF-β1 is an inducer of endochondral bone formation in the primate raises important questions about the specificity and possible redundancy of proteins involved in bone formation and the evolutionary conservation of related proteins from phylogenetically distinct species (Ripamonti *et al*., 1997; Duneas *et al*., 1998; Ripamonti *et al*., 2000a). TGF-β1 however, has been reported to show limited bone induction in orthotopic sites of the baboon (Ripamonti *et al*., 1996c) suggesting that the bone inductive activity may be site and tissue specific (Ripamonti *et al*., 1997; Duneas *et al*., 1998; Ripamonti, 2000; Ripamonti *et al*., 2001).

TGF-βs regulate a variety of osteoblast activities related to bone formation (Centrella *et al*., 1994). TGF-β2 functions as a local positive regulator of bone remodelling. Alterations in TGF-β2 by bone cells or in their responsiveness to TGF-β2 may contribute to the pathogenesis of metabolic bone disease (Erdebacher and

Derynck, 1996). TGF-βs also induce matrix protein synthesis in most tissues, more especially in bone. TGF-β isoforms have also been reported to enhance collagen production and collagen mRNA levels (Raghu *et al*., 1989). Fine *et al*. (1990) further investigated the effect of TGF-βs on collagen and reported that TGF-β isoforms increase the amount of collagen type I mRNA in human embryonic and lung fibroblasts. Further more, TGF-β isoforms increases the proliferative effect of epidermal growth factor (Fine *et al*., 1990).

To date, TGF-βs, naturally-derived or recombinantly produced, fail to induce bone formation in rodents, showing instead a fibrovascular response (Roberts *et al*., 1986; Sampath *et al*., 1987; Hammonds *et al*., 1991). Studies were performed in the subcutaneous space of rodents that confirmed that the heterotopic implantation of TGF-β1 and -2 combined with insoluble collagenous bone matrix or in conjunction with hydroxyapatite granular carriers, results in the induction of a fibrogenic response without any sign of cartilage or bone formation (Roberts *et al*., 1986; Sampath *et al*., 1987; Hammonds *et al*., 1991; Shinozaki *et al*., 1997; Matsaba *et al*., 2001). Furthermore, it was demonstrated that when used in subcutaneous sites, TGF-βs 1 and -2 have been implicated in the genesis of cutaneous scarring due to

increased monocyte and macrophage infiltration and fibronectin and collagen types I and III deposition (Shah *et al*., 1995).

However, in marked contrast to studies in rodents, TGF-βs-1 and -2 induce vigorous endochondral bone formation in heterotopic sites of adult non-human primates (Ripamonti *et al*., 1997; Duneas *et al*., 1998; Ripamonti *et al*., 2000; Ripamonti *et al*., 2001). Ripamonti *et al*. (2000a) showed for the first time that hTGF-β2 induces endochondral bone formation in heterotopic sites in adult baboons (*Papio ursinus*). The same study also demonstrated that TGF-β2 does not require only the insoluble collagenous bone matrix as carrier, since bone was initiated even when TGF-β2 was combined with sintered porous hydroxyapatites. One important feature about TGF-βs is that the bone inductive activity in primates is site specific, with extensive endochondral bone induction in heterotopic sites but limited in orthotopic sites (Ripamonti *et al*., 1996c; Duneas *et al*., 1998; Ripamonti *et al*., 2000; Ripamonti *et al*., 2001). The site and tissue specificity of bone induction by hTGF-β2 is not carrier related since equal results were obtained when sintered hydroxyapatites were used as carrier and implanted in orthotopic and heterotopic sites (Ripamonti *et al*., 2000).

1.10 BMPs/OPs and bone formation

Naturally-derived BMPs/OPs were the first proteins to be tested applying the bone induction principle for the repair of bony defects in primate models including humans. *In vivo* studies of BMPs/OPs have made it possible to extend the knowledge of their morphogenetic potential from rodents to primates. Studies with primates are a prerequisite for the exploration of potential therapeutic applications for the regeneration of bone in man. The first experiments in humans were reported by Johnson and co-workers, (1988). Upon the treatment of refractory tibial and femoral non-unions using various doses of naturally-derived BMPs/OPs, results showed union with BMPs/OPs supplementation in patients who had undergone unsuccessful multiple surgical grafting attempts (Johnson *et al*., 1988). In very recent experiments, naturally-derived BMPs/OPs have been implanted in craniofacial defects in man and the biopsy specimens from the operated sites examined 90 days after BMPs/OPs implantation. The results showed bone formation by induction (Ferretti and Ripamonti, 2002).

The efficacy of naturally-derived BMPs delivered by both hydroxyapatites and collagenous substrata was demonstrated in the calvarial model of the adult baboon (*Papio ursinus*) and

heterotopically in the *rectus abdominis* by Ripamonti *et al*. (1992c); Ripamonti *et al*. (1993a); Ripamonti *et al*. (1993b); Ripamonti *et al*. (2001). Naturally derived BMP/OP fractions were shown to completely regenerate calvarial defects in adult baboons 90 days post implantation (Ripamonti *et al*. 1992a; Ripamonti *et al*., 1993a). In 1994, Ripamonti *et al*. reported that naturally-derived BMPs/OPs also play important roles in regenerating periodontal ligament, cementum and alveolar bone in surgically created periodontal defects in *Papio ursinus* (Ripamonti *et al*., 1994). High doses of recombinant human OP-1 (hOP-1), when used with collagenous matrix as carrier, induces massive bone differentiation 30 days after implantation in calvarial defects (Ripamonti and Reddi, 1995; Ripamonti *et al*., 1996b). In addition, the pleiotropic function of BMPs/OPs has been shown by OP-1, BMP-2 and BMP-4 inducing also dentinogenesis (Rutherford *et al*., 1993; Nakashima *et al*., 1994).

Osteogenic protein-1 (OP-1), also known as BMP-7, has been evaluated extensively in preclinical studies in critical size defects in rabbits, canine, sheep, and non-human primate models (Cook *et al*., 1994a; Cook *et al*., 1994b; Cook *et al*., 1995; Cook and Rueger, 1996; Ripamonti *et al*., 1996a; Ripamonti *et al*., 1997, Ripamonti *et al*., 2000b; Grauer *et al*., 2001). In each of the above

studies, hOP-1 was associated with a high degree of success, comparable in frequency and completeness of repair with that seen with bone autografts. More importantly, all new bone induced by osteogenic molecules, including hOP-1, is the same as the autogenous bone, and this bone continues to remodel in the same manner as is normal for the particular skeletal site and its biomechanical environment (Friedlaender *et al*., 2001).

Takahashi *et al*. (1999) reported the use of porous hydroxyapatite graft containing human bone morphogenic protein-2 (hBMP-2) for cervical fusion in a caprine model. Their results showed that the addition of hBMP-2 to a porous hydroxyapatite graft enhances the rate of anterior cervical fusion. hBMP-2 has also been reported to enhance tendon healing in dogs (Rodeo *et al*., 1999). Their results showed accelerated healing in the sites where hBMP-2 was administered. Friedlaender *et al*. (2001) reported the safety and efficacy of hOP-1 in the treatment of tibial nonunions. They concluded that hOP-1, implanted with insoluble collagenous matrix as carrier, is a safe and effective treatment for tibial nonunions in clinical contexts. Moreover, their study provided clinical and radiographic results comparable with those achieved with bone autograft, without donor site morbidity (Friedlaender *et al*. 2001). hBMP-2 has also been shown to play critical roles in

the healing of rat segmental femoral defects (Lee *et al*., 1994) and sheep segmental osteoperiosteal femoral defects (Gerhart *et al*., 1993).

In a rabbit ulna defect model, hOP-1 delivered by collagenous matrix was used to treat 1.5-cm segmental osteoperiosteal defects as evaluated 8 weeks after treatment (Cook *et al*., 1994). In an equivalent 8 week model, 2 cm rabbit ulna defects were treated with different doses of hBMP-2 delivered by D, L-lactide-co-glycoside as carrier and there was a dose dependent response in bone regeneration. The newly formed bone was biomechanically of comparable strength with unoperated control ulnae (Bostrom *et al*., 1996).

In African green monkeys, hOP-1 delivered by collagenous matrix as carrier was used to treat surgically created 2 cm osteoperiosteal defects in the distal tibiae and the ulnae. Radiographic and histologic evaluation at 20 weeks revealed that all hOP-1 treated sites underwent new bone formation (Cook *et al*., 1995). In a canine posterior segmental spinal fusion model, treatment with hBMP-2 delivered by D, L-lactide-co- glycolide resulted in equivalent spinal fusion rates as determined by

biomechanical testing when compared with autogenous grafts. The accumulated data from the above mentioned experiments and others have made it possible for both hOP-1 and hBMP-2 to proceed into the next step of clinical trials for both orthopedic and craniofacial applications. At the time of writing this thesis, the Food and Drug Administration (FDA) had not as yet approved hOP-1 for human orthopedic use. Yet, hOP-1 has been cleared in Europe and also in Australia. There are still challenges and more studies that need to be carried out to explore insights to the mechanistic events that take place in the regeneration and engineering of bone which may help to approach therapeutic tissue regeneration in molecular terms.

1.11 Synergy between TGF-βs and BMPs/OPs

Synergistic interactions amongst different classes of growth factors and morphogens could be a general principle deployed in embryonic development and in postnatal life as shown by experiments using different subclasses of growth factors and morphogens (Rameshwar *et al*., 1977; Ripamonti *et al*., 1997; Duneas *et al*., 1998; Sekiya *et al*., 1999).

Previous studies have shown that TGF-βs when applied singly fail to induce bone formation in rodents (Roberts *et al*., 1986;

Sampath *et al*., 1987; Hammonds *et al*., 1991). Demonstration of therapeutic mosaicism in tissue engineering requires ample testing of doses and ratios of recombinant morphogen combinations (Ripamonti *et al*., 2000). It has been demonstrated that hOP-1 and recombinantly produced and platelet derived TGF-β1 interact synergistically to architecturally configure large ossicles both heterotopically in the *rectus abdominis* and orthotopically in calvarial defects of adult primates (Ripamonti *et al*., 1997; Duneas *et al*., 1998).

Ripamonti *et al*. (1997) and Duneas *et al*. (1998) showed that addition of comparatively low amounts of hTGF-β1 and pTGF-β1, respectively to hOP-1 resulted in synergistically increased parameters of bone formation 30 and 90 days post implantation in calvarial defects and heterotopically in the *rectus abdominis*. Ripamonti *et al*. (1997) reported that addition of hTGF-β1 to hOP-1 led to a synergistic induction of bone formation 15 days post implantation in the adult primate. The binary applications resulted in the morphogenesis of cartilage highly reminiscent of *de novo* embryonic growth plates, indicating that the memory of developmental events in the embryo can be re-deployed post-natally by the application of synergistic molecular combinations (Ripamonti *et al*., 1997).

The addition of TGF-β to hOP-1 influences tissue induction, directing development of events towards a more chondrogenic phenotype. Si *et al*. (1998) reported a synergistic interaction between TGF-β and BMP-2 in a hydroxyapatite bovine bone implanted heterotopically in mice. Matsaba *et al*. (2001) reported that TGF-β1, which singly does not induce bone formation in rodents, synergizes with hOP-1 to induce endochondral bone formation in rats as well as increasing the level of alkaline phosphatase and calcium temporally and dose dependently.

Angiogenesis is a prerequisite for bone formation and it is a critical morphogenetic event invading the cartilage anlage to initiate osteogenesis (Foidart and Reddi, 1980; Reddi and Kuettner, 1998). Enhanced vascularisation may hence be part of the mechanism whereby hOP-1 and TGF-β1 synergise in heterotopic bone induction. Ramoshebi and Ripamonti (2000), reported that in the chorioallantoic membrane (CAM) assay, hOP-1 is singly angiogenic and that this angiogenic activity is synergistically enhanced by the simultaneous application of pTGF-β1 resulting in a highly intense overall angiogenic response. These results further indicated an additional instance of a positive interaction between OP-1 and TGF-β1.

Bentz *et al*. (1989; 1991) reported in rodent experiments that the combination of naturally-derived BMP fractions (BMP-2 and -3) with bovine bone-derived TGF-β2 increased the ratio of cartilage to bone. Ogawa *et al*. (1992) also reported the enhancement of bone formation caused by the interaction of TGF-βs with naturally-derived fractions containing BMPs 2 and -3. Their results demonstrated that implants containing combinations of naturally sourced TGF-β2 and BMP fractions resulted in increased chondrogenesis when compared to BMPs/OPs alone in rodents. The results were dose dependent for TGF-β2 and increases in cartilage were noted at higher concentrations of the morphogen. The combination of the morphogens also increased alkaline phosphatase activity 8 fold when compared to BMP alone.

In 1993, Kibblewhite and colleagues reported what may be a form of indirect synergy between BMPs and TGF-β1 in a rabbit craniofacial on lay model (Kibblewhite *et al*., 1993). The results showed that when TGF-β1 is added to demineralised bone matrix, it induces significantly higher amounts of bone and greater resorption of the implanted matrix when compared to demineralised bone matrix alone (Kibblewhite *et al*,. 1993). The authors' results demonstrate the potential of TGF-β1 in

accelerating osteoinduction. The reported TGF-β1 inductive behavior could have been influenced by the BMPs/OPs present in the demineralised bone matrix.

Cunningham *et al*. (1992) also investigated synergy between BMPs/OPs and TGF-βs. The authors suggested that BMPs/OPs may have early effects in bone induction by stimulating the chemotaxis of monocytes to the area. Once attracted, the monocytes are stimulated to produce chemotactic and mitogenic cytokines and growth factors including TGF-βs as shown by Northern blot analyses. Basic FGF (bFGF) has also been reported to accelerate actin expression in animal hemisphere cells when combined with TGF-β1 (Kimelman and Kirschner,1987). Synergy between bFGF and TGF-β1 has also been reported by Ramoshebi and Ripamonti (2000) in the CAM assay.

There may be several mechanisms by which TGF-β synergizes with BMPs/OPs. As suggested previously for a combination of bovine-derived TGF-β2 and BMP fractions (Bentz *et al*., 1989; 1991) TGF-β may act as a chemotactic and mitogenic factor for responding precursor cells for subsequent induction by BMPs/OPs. Also, possibly by simultaneous shift and redistribution in receptor binding profiles for TGF-β1 which are regulated by

hOP-1 (Centrella *et al*., 1995). Mundy (1995) suggested that while BMPs/OPs act at an earlier control point in the osteoblast lineage, TGF-β may regulate the latter steps in the bone and cartilage lineages.

1.12 Other growth factors

Advances in molecular cloning techniques have resulted in the expression of additional gene-related products of the BMP and TGF-β families. These include the CDMPs (Chang *et al*., 1994), GDFs (Lee, 1990; Jones et al., 1992; Mcpherron and Lee, 1993), the recombinant *drosophila* gene products *decapentaplegic* (*dpp*) and 60 A, vegetal-1 gene products of *Xenopus laevis*, MIS (Cate *et al*., 1986) and the hormones activins and inhibins (Mason *et al*., 1985; Schwall *et al*., 1988; Cate *et al*., 1986; Padgett *et al*., 1987; Weeks and Melton, 1987; Lyons *et al*., 1989; Ripamonti and Vukicevic, 1995). Importantly, it was reported that the recombinant drosophila genes, *dpp* and 60A are inducers of endochondral bone formation in mammals (Sampath *et al*., 1993).

It has also been reported that CDMP-1 and -2 are most closely related to BMP-5, -6, and -7 (OP-1) (Chang *et al*., 1994). In contrast to the other members of the BMP/OP family, expression of CDMP-1 and -2 is predominantly in the cartilaginous tissue,

hence the name, and particularly in condensing mesenchyme of developing limbs (Chang *et al*., 1994). The equivalent of CDMP-1 in the mouse is GDF-5 and is linked to a mouse disorder characterized by a distinct shortening of the limbs without other tissue abnormalities, a mutation called brachypodism, suggesting that GDF-5 may be required for proper development of the limbs (Storm *et al*., 1994). The types of mutations observed in brachypodism mice were found to be effective null mutations for the gene encoding GDF-5/CDMP-1. Hotten *et al*. (1996) showed that hGDF-5 is capable of inducing chondrogenesis *in vivo* and *in vitro* in rat limb bud cells. Moreover, hGDF-5 has been shown to stimulate mesenchyme aggregation and chondrogenesis in rat limb bud cells *in vitro*, and also partially purified hGDF-5 induces cartilage and bone formation in muscular tissues of rodents *in vivo* (Hotten *et al*., 1996). GDF-10, a new member of the BMP family highly related to BMP-3, is strongly expressed in neonatal and adult calvariae, with lower expression in the femur, which is of endochondral origin unlike the calvaria which is of intramembranous origin (Cunningham *et al*., 1995). This observation suggests a site-specific regulatory role of different TGF-ß family members in various sites of the skeleton and underscores the therapeutic importance of site targeting with

exogenous applications of specific morphogens (Ripamonti *et al*., 1997; 1998; Ripamonti and Duneas, 1998).

Another group of growth factors, fibroblast growth factors (FGFs) have also been identified (Mundy, 1996; Reardon *et al*., 1994; Rousseau *et al*., 1994). The role of FGF and other growth factors in the regulation of angiogenesis in *vivo* has been well documented (Schreiber *et al*., 1986; Hayek *et al*., 1987; Sprugel *et al*., 1987; Cao *et al*., 1996; Fajardo *et al*., 1996). Other major bone cell mitogens whose receptors are frequently expressed in bone cells are platelet-derived growth factors (PDGFs) (Graves *et al*., 1984).

1.13 Carriers for bone formation

Several carriers for bone formation have been investigated indicating that the carrier is critical for bone induction to occur. BMP-induced chondro-osteogenesis in heterotopic tissues was originally discovered by Urist (1965) upon implantation of DBM. One interesting aspect of BMP/OP-induced chondro-osteogenesis is that, to induce *in vivo* cartilage or bone formation, purified or recombinant BMPs/OPs require a carrier to act as a delivery system (Reddi, 1994a; Ripamonti and Duneas, 1996; Reddi, 1994b; Ripamonti and Duneas 1998). The most widely used

carrier of BMPs/OPs is the insoluble collagenous bone matrix, which is the demineralised guanidinium extracted and inactive residue of the bone matrix. The osteoinductive nature of the demineralised bone matrix can be abolished by dissociative extraction resulting in two components: a soluble protein extract and an insoluble residue, which is the insoluble collagenous bone matrix (ICBM) (Sampath and Reddi, 1981). Reconstitution of the two components restores the osteoinductive activity. Sampath and Reddi, (1981) also showed that the factors responsible for osteoinductivity reside in the solubilised component and when reconstituted with an appropriate carrier, the osteoinductivity can be restored. This operational reconstitution was a hallmark in the field of bone induction since it allowed the identification of the proteins responsible for the osteoinductive activity as well as the focusing on carrier matrices as delivery systems.

Itoh *et al*. (2000) investigated the biocompatibility and osteoconductivity of a novel hydroxyapatite/collagen (HAP/Col) composite biomaterial as well as its ability to act as a BMP/OP carrier. The authors reported that based on their findings, HAP/Col-composite has a high osteoconductive activity and is also able to induce bone remodelling. Furthermore they suggested that HAP/Col-composite has characteristics similar to natural bone

because it was able to induce the development of osteogenic cells and bone remodelling units. In cases where the HAP/Col-implants are grafted at sites where weight bearing is needed from the early postoperative days, treatment with hBMP-2 at a specific dose is useful to promote callus formation and to shorten the time needed for bone union (Itoh *et al*., 2000).

BMPs/OPs, when reconstituted with ICBM, induce endochondral bone formation. Moreover, Sasano *et al*. (1993) showed that, other carriers such as a fibrous collagen membrane, when used with BMPs/OPs can induce direct bone formation independent of the cartilage phase. Kuboki *et al*. (1995) also showed that BMPs/OPs singly induce direct, *i.e*., intramembranous osteogenesis when porous particles of hydroxyapatite are used as carrier, while on the other hand, fibre glass membranes, when used as a carrier only induces chondrogenesis. The authors concluded that vasculature is the crucial factor that determines osteogenesis or chondrogenesis. Kuboki *et al*. (1998) reported that fibrous collagen membrane carrier does not only induce bone, but also regenerates cementum and periodontal defects in the cat canine and monkey molar, respectively. Miki *et al*. (2000) reported complete regeneration of bone with bone marrow four weeks after implantation of freeze dried poly glycolic acid-co-lactic acid

(PGLA) with hBMP-2 in rodents. The authors suggested that the FD-PGLA/HA/hBMP-2 composite could also be an optimum bone substitute with osteoinductive potential and could function as an alternative bone graft material for autogenous bone in humans.

Previous studies revealed that there are cartilage-directing carriers such as fibrous glass membranes (Kuboki *et al*., 1995) and bone-directing carriers such as porous particles of hydroxyapatite and titanium mesh (Kuboki *et al*., 1998). It has also been shown that porous hydroxyapatites acted as ideal delivery systems for BMPs/OPs, providing evidence that the osteogenic activity of BMPs/OPs could be restored and delivered by an insoluble substratum other than the collagenous matrix (Ripamonti *et al*., 1992a; Ripamonti *et al*., 1992c and Ripamonti *et al*., 1993b). Ripamonti and co-authors have shown in a number of experiments that the implantation of specific porous hydroxyapatites in the *rectus abdominis* of primates resulted in the morphogenesis of bone 60 and 90 days after implantation even without the exogenous application of BMPs/OPs (Ripamonti, 1990; Ripamonti *et al*., 1991b; Ripamonti *et al*., 1993b; Ripamonti, 1996). Bone formation may be the result of adsorption of endogenously produced or circulating BMPs/OPs onto the substratum and induction of bone as a secondary response

(Ripamonti *et al*., 1991b; Ripamonti *et al*., 1993a; Ripamonti *et al*., 1993b; Ripamonti *et al*., 1999).

As previously reported, spontaneous bone formation occurs within the concavities of hydroxyapatite (Ripamonti *et al*., 1999. Immunolocalisation patterns of BMP-3 and OP-1 were observed in the concavities at the hydroxyapatite interface with the invading fibrovascular tissue (Ripamonti *et al*., 1999; Ripamonti, 2000c). The question remains:

Are BMPs/OPs present within the concavities **locally** produced to initiate bone formation within the concavities of the substratum, or rather **secreted** onto the hydroxyapatite by invading capillaries with associated mesenchymal cells and later initiating bone formation as a secondary response?

It is against this background that the present study was conducted to investigate the two possibilities.

2.0 AIM

To investigate whether BMPs/OPs present within the concavities are **locally** produced to initiate bone formation within the concavities of the substratum, or rather **secreted** onto the hydroxyapatite by invading capillaries with associated mesenchymal cells and later initiating bone formation as a secondary response.

3.0 MATERIALS AND METHODS

3.1 Selection of animals

Six clinically healthy adult Chacma baboons (*Papio ursinus*) were selected from the primate colony of the University of the Witwatersrand, Johannesburg. Criteria for selection were normal hematological and biochemical profiles (Melton and Melton, 1982) and skeletal maturity, confirmed by radiographic evidence of closure of the distal epiphyseal plate of the radius and ulna. Following standard quarantine procedures, the animals were housed individually in suspended wire-mesh cages in the primate unit of the Central Animal Service of the University. Animals were kept under slight negative pressure (-25 kPa) with controlled ventilation, at 22^{o}C and humidity at ±40%, and controlled photoperiod (lights on 06h00 to 18h00). The diet of the baboons consisted of a balanced protein-fat-carbohydrate diet with vitamins (thiamine, riboflavin and nicotinic acid) and mineral supplements (Calcium: Phosphate (Ca:P) = 1.2:1), and a soft dietary intake of sweet potatoes, pumpkins and oranges mixed in a ratio of 3:1 with a protein-vitamin-mineral dietary supplement (Dreyer and Du Bruyn, 1968). The baboons had access to tap water *ad libitum.* The research protocol was approved by the Animal Ethics Screening Committee of the University (AESC number: 00/106/5).

3.2 Biomaterials

Four different types of substrate materials were prepared in the form of discs (20mm diameter X 3mm thickness) with a series of concavities on both planar surfaces (Figs. 1A and 1B). The discs, with specific geometries were constructed by the Council of Scientific and Industrial Research (CSIR), Materials and Technology group (MATTEK), Pretoria, South Africa. In this study the term geometry refers to concavities of different dimensions, which act as microenvironment for induction of bone.

3.3 Powders

Four different types of powders containing hydroxyapatite (HA) were used for the uni-axially pressing of sample discs. The samples were in the form of discs of 3mm thickness and 20mm diameter. Pressing was done at 20 MPA in a piston and die arrangement (Fig. 2) using a polymeric pressing binder. The pistons that were used for pressing had embedded hemispheres of different diameters and depths on both planar surfaces.

The resulting discs therefore had hemispherical indentations on the surfaces with the depth of half the diameter of the indentations. The same HA starting powder that was used in type 2 biomaterials was also used in types 3 and 4. The major

differences between the implants were particle size and distribution of the starting powders. as opposed to a highly crystalline, coarsened (>1 microns) hydroxyapatite powder (Type 2), or a fine distribution (<100 microns) of TCP in hydroxyapatite matrix (Type 3) as opposed to discreet (100-300 microns) zones of TCP in hydroxyapatite matrix (Type 4) both produced from highly crystalline coarsened powders

3.4 Preparation of biomaterials

Phase pure HA with a calcium/phosphorus (Ca/P) molar ratio of 1.67 was prepared by a solid-state reaction between Merck tri-calcium phosphate (TCP) [Ca_3 (PO_4)$_2$] and Univar calcium hydroxide [$Ca(OH)_2$] according to the chemical reaction:

$$\mathbf{3Ca_3(PO_4)_2 + Ca(OH)_2 = Ca_{10}(PO_4)_6(OH)_2}$$

The specification of the foodstuff grade TCP was: Cl (chloride) <0.1%, F (fluoride) <0.005%, (SO4) sulphate <0.5%, As<0.0002%, Fe (iron) <0.04% and the total of all heavy metals <0.003%. Less than 0.1% was insoluble in hydrochloric acid. The calcium hydroxide had a stated assay of 95-100% with carbonate <5%. The stated As contents was below 0.0003%, with copper (Cu) <0.001%, Fe< 0.1% and the total of all heavy metals <0.002%.

All samples were air-fired. The elements mentioned were in accordance to ASTM Standard F1185-88 which is for ceramic hydroxyapatite intended for surgical implants with a total heavy metal limit as 50ppm. The stated purities of the chemicals are within these limits. Indivisual samples were not analysed, but the material from which the samples were made, was analysed.

Aqueous suspensions of the starting materials (HA) were mixed in a Silverson High shear high-speed mixer for 15 minutes and then gelled with a suitable gelling agent (Rohm and Haas Duramax D-3007) to prevent separation during drying. The material was dried at 120^{o}C for 12 hours. The dry-soft cake was crushed and screened below 300 micron. The loosely packed powder was reacted in covered alumina crucibles at 1000^{o} C for 18 hours to yield hydroxyapatite as verified by Scanning Electron Microscopy (SEM), X-Ray powder Diffraction (XRD) and Fourier Transform Infra-Red Spectroscopy (FTIR) and it was ball-milled to a powder with a median particle size of approximately 1 micron (Thomas *et al*., 1999; Richter *et al*., 1999).

The discs were pressed from powder in the DIE system using two pistons with embedded steel balls on their faces (Fig. 2) - one piston from each side. Since the balls pressed into the powder

only half way (being halfway into the steel piston) the depths of the concavities were half the diameter of the concavities. One side of the disc had 25 concavities of the same diameter and the other side had 69 (smaller) concavities of the same diameter, different from the previous side (Figure 1). The size of the concavities was varied on both sites of the discs to determine the range of diameters suitable for induction. The diameters and depths of the different concavities will be discussed in detail in the following subsections of the implanted different biomaterials

The final preparation of the samples was the sintering step at 1020 ^{o}C for 1 hour using a ramp rate of 1.5 ^{o}C/minute. This was also a thorough sterilization treatment process, which resulted in any remnants of any organic material, living or dead, being vaporized. From the furnace the samples were immediately transferred in closed containers to a laminar flow cabinet where filtered air flowed over it. The samples were then transferred into envelopes of Sterilpeel that were immediately sealed in a thermal sealer - all the time untouched by hand. They were taken to the Bone Research Laboratory where they were autoclaved at 121^{o}C for 20 minutes. On the microstructural level, the substrata presented a surface with high open microporosity and with specific surface area in excess of 1.5m^{2} /g.

3.5 Type 1 samples

A commercially available hydroxyapatite powder (from Plasma Biotal, batch P120) which consisted of relatively fine particles (1 micron) of hydroxyapatite was mixed with a pressing binder for pressing Type 1 samples.

The samples were sintered to yield discs of 20mm in diameter and 3mm thick. One side of the disk had concavities of 1.8 mm in diameter and a depth of 0.9mm. The other side had concavities of 0.9 mm diameter and 0.45mm depth. These samples had a microporosity (bulk material) of 39%. Type 1 samples were the only samples pressed using a commercial powder.

3.6 Type 2 Samples

Hydroxyapatite powder (HAOM 21) was pressed similar to the Type 1 samples.

The starting powder consisted of a highly crystalline, coarsened (>1 microns) hydroxyapatite powder. The discs had a microporosity (bulk material) of 40%. Concavities had diameters of 1.9mm on one side with a depth of 0.8mm, and 1.0mm on the other side with a depth of 0.5mm.

3.7 Type 3 Samples

The same hydroxyapatite starting powder that was used in type 2 samples was mixed at the micron level with a fine distribution (<100 microns) of tri-calcium phosphate powder to yield a homogeneous powder consisting of 37 mass percent TCP and 63 mass percent HA. The powder was pressed into discs having hemispherically indented surfaces. The concavities had a diameter of 1.9 mm on one side with a depth of 0.8mm and 1.0mm on the other side with a depth of 0.5mm. The samples had a microporosity (bulk material) of 38%.

3.8 Type 4 Samples

The same HA starting powder that was used in type 2 and 3 was used with discreet (100-300 microns) zones of TCP both produced from highly crystalline coarsened powders. Samples consisted of a 37 mass percentage TCP mixture with 63 mass percent HA. Type 4 samples therefore differed from the Type 3 samples in that large agglomerates of TCP and of HA were separately formed prior to pressing. These agglomerates were then mixed homogeneously and then pressed into discs that were sintered. The microporosity (bulk material) of type 4 samples was 37%. The diameters of the concavities were 1.9mm and 1.0mm while the depth was 0.8mm and 0.5mm respectively.

Figure 1A: Photomicrograph of a hydroxyapatite disc with concavities on both planar surfaces.



Figure 1B:

Photomicrograph of a hydroxyapatite disc showing concavities

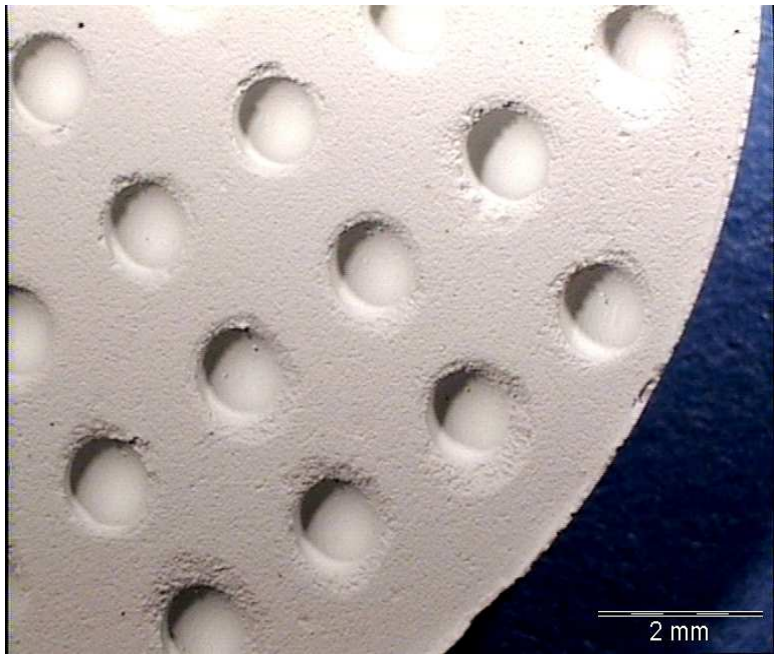


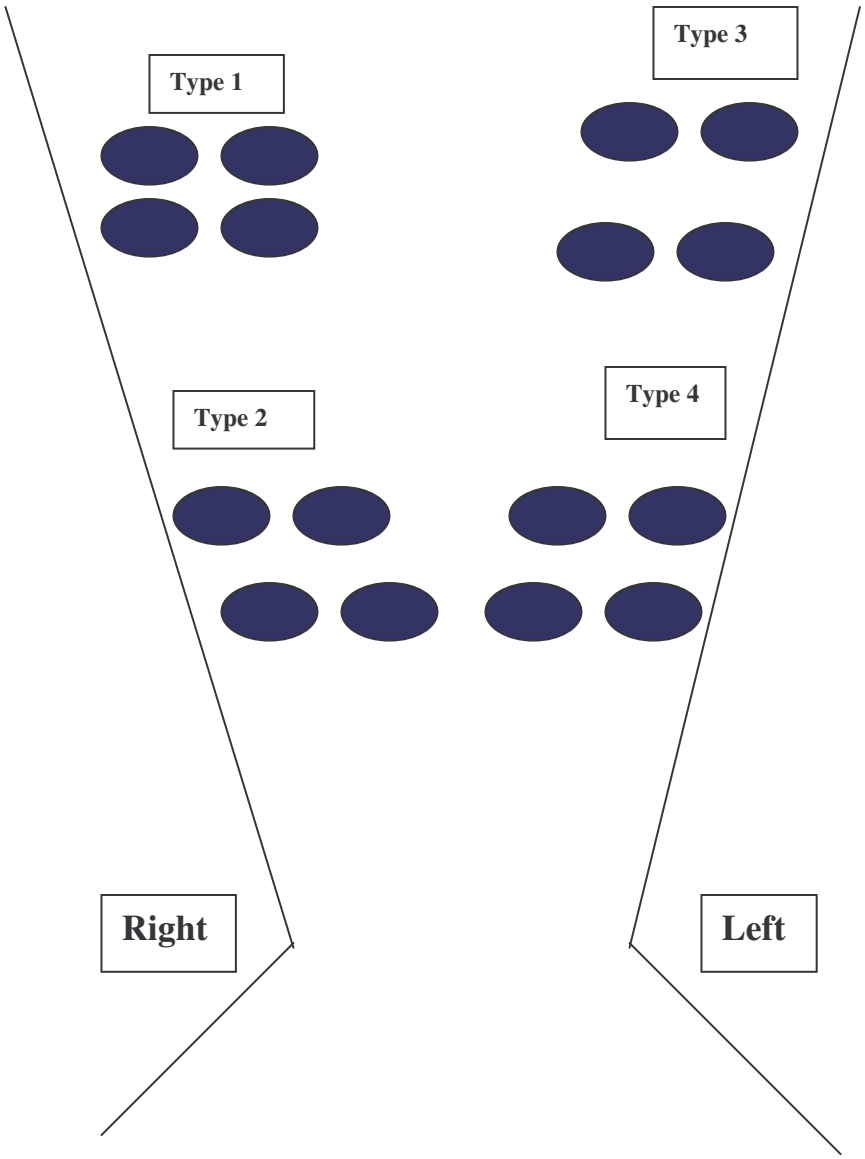
Figure 2. Die system used to create concavities on the samples



3.9 Implantation Protocol

Before implantation in the baboon, the samples were sterilized in an autoclave at 121^{o} C on dry cycle for 20 minutes. The heterotopic model of tissue morphogenesis by osteoinductive and osteoconductive biomaterials in the adult baboon has been described in detail (Ripamonti, 1992; Ripamonti *et al*., 1992a; Ripamonti *et al*., 1993b; Ripamonti, 1996). In four animals, a total of 64 discs were implanted bilaterally in intramuscular pouches to be harvested on day 30 and 90. Four discs were implanted per pouch created in the *rectus abdominis* muscle*,* 16 implants per animal, as shown in Fig. 3. 180 days post-implantation in the additional two animals, only Types 2 and 4 were implanted, 8 implants per animal. The total number of implants for the study was 80. All discs were implanted in the same relative position with the larger concavities facing ventrally.

Figure 3. Implantation protocol for the heterotopic model:



3.10 Tissue processing and analytical procedures

Anaesthetized animals were euthanased with an intravenous overdose of sodium pentobarbitone, 2 animals on day 30, 2 animals on day 90 and 2 animals on day 180. Implants were harvested, freed of adhered soft tissues and then subjected to histological and immunohistochemical analyses (Ripamonti *et al*., 1999). For biochemical and Northern Blot analyses, the tissues grown on both planar surfaces and within the concavities of the substratum were peeled off the disc and pooled for each type of sample.

3.11 Alkaline Phosphatase assay

Refer to Appendix 1 for the list of reagents.

3.11.1 Method:

Harvested tissues were homogenised in 2 ml of homogenising buffer. After centrifugation the alkaline phosphatase activity of the supernatant was used as index of bone formation by induction (Reddi and Huggins, 1972; Ripamonti *et al*., 1997; Duneas *et al*., 1998, Matsaba et al., 2002).

The supernatant was transferred into a new tube and used for the assay. One ml of substrate solution and 1 ml of buffer solution were added to clean test tubes which were then placed in a 37^{o}C water bath to equilibrate temperature. Blanks were prepared by adding 2 ml of base solution to tubes containing substrate and buffer solutions. The sample assay was then added to all tubes and the reaction was left for 30 minutes after which it was stopped with 2 ml of the base solution.

The alkaline phosphatase activity was detected by the appearance of a yellow coloured reaction that resulted from the enzymatic conversion of the substrate, para-nitrophenyl phosphate (PNPP) at pH 9.3. The absorbance of the samples was determined by spectrophotometer at 400 nm. Alkaline phosphatase was determined as units of activity per mg protein. One unit of alkaline phosphatase activity is defined as that which generates 1 µg of PNPP in 30 minutes at 37^{o}C. This unit of activity was calculated based on the extinction coefficient (ε) value of PNPP, which is 218.58. The amount of solubilised protein was determined by the Lowry assay (Lowry, 1951).

3.12 Protein Lowry Assay

Refer to Appendix 2 for reagents

3.12.1 Method:

Standard solutions were prepared with appropriate volumes (20, 40, 60 and 80 µl) of the BSA stock. To standards and sample tubes, distilled water was added to give a final volume of 400 µl. Blanks were prepared with distilled water without sample assay. To all tubes, 2 ml of copper reagent were added and the reaction was allowed to proceed for 30 minutes after which 200 µl of phenol reagent was added and contents vortexed. The reaction was allowed to proceed for another 30 minutes and the absorbance of the samples was determined at 750 nm by using standard values to obtain a standard curve, and the protein in the sample read from the curve.

3.13 Histology

Harvested tissues were fixed in 10% formalin (pH 7.4) and demineralised in formic acid-hydrochloric acid solution. After dehydrating in ascending grades of ethanol, tissues were

impregnated with nitrocellulose, cleared in chloroform and impregnated with paraffin wax under vacuum and embedded in paraffin wax. Sections were cut at 4 µm and stained using a modified Goldner's Trichome method outlined below (Ripamonti *et al*., 1997; Duneas *et al*., 1998; Ripamonti *et al*., 1999; Ripamonti, 2000c; Ripamonti *et al*., 2000a).

Refer to Appendix 3 for reagents

3.13.1 Method (modified Goldner's Trichome):

The difference between the original Goldner's stain and the modified method is the counterstaing. The original method counterstains with a green stain while the modified method counterstains with a blue stain so everything that is green representing mineralized bone in the original method will appear blue in the modified method. The blue stain representing mineralised bone was chosen for photographic purposes. Bone is differentiated from the dense connective tissue and any other tissue that make the blue stain by the fact that bone has osteocytes; this is a characteristic feature that all the other tissues in the study do not have. Morphologically, bone stains blue on decalcified sections (with modified Goldner's Trichome) as matrix

with lacunae filled by osteocytic cells and often has osteoblastic cells facing the connective tissue matrix highly vascularised.

Sections were stained in stable iron haematoxylin for 20 minutes, fuschin ponceau for 45 minutes, differentiated in Orange G for 20 minutes then stained in methyl blue for 10 minutes. In between the stains, sections were washed in running tap water, differentiated in acid alcohol and immersed in 1% acetic acid. The sections were then dehydrated in series of alcohol and mounted with entellan (Merck, Germany).

3.14 Immunolocalisation of TGF-β family members

Additional sections were cut at 5 μm, mounted on incubated silanized slides, and used for immunohistochemical staining of OP-1 and BMP-3 markers of bone formation.

Refer to Appendix 4 for reagents

3.14.1 Method:

Pre-stained sections were rehydrated in series of ethanols and decolourised in 1% acid alcohol, washed in water and placed in buffer. Slides were then placed in hydrogen peroxide and rinsed again in buffer. Horse serum, primary antibody, and secondary antibody were added followed by 3, 3-diamino benzidine (DAB)

(Sigma-Aldrich, Germany) then rinsed in tap water. The control samples were prepared without the primary antibody, which was replaced by buffer. The control was run for all samples. The nuclei was stained with Carazzi's Haematoxylin, dehydrated and mounted with entellan (Merk, Germany).

3.14.2 Antibodies

All antibodies were bought from Santa Cruz Biotechnology, Inc. Whitehead Scientific (Pty) LTD, Brackenfell, South Africa.

OP-1: An affinity-purified goat polyclonal antibody raised against a peptide mapping at the amino terminus of the OP-1 of human origin.

BMP-3: An affinity-purified goat polyclonal antibody raised against a peptide mapping at the amino terminus of the BMP-3 precursor of human origin.

3.15 Northern Blot Analysis

3.15.1 Preparation of total RNA

Refer to Appendix 5 for reagents

3.15.2 Method:

Pooled tissues harvested from the concavities weighing between 100 and 200 mg from replicate specimens were used for Northern analyses. These tissues were peeled off the surface of the concavities. All glassware was baked at 250^{o}C overnight and plastic ware autoclaved at 121^{o}C for 20 minutes in the presence of 0.1% DEPC (ICN Biochemicals Inc. OHIO). All solutions were prepared in deionised distilled water treated with DEPC. Sample tissues were snap-frozen in liquid nitrogen and stored at -70^{o}C.

Samples were crushed to a fine powder with a heat-sterilized mortar and pestle pre-cooled to -70^{o}C. Crushed samples were homogenised on ice in Tri- Pure isolation reagent (Boehringer Mannheim Biochemicals), 1 ml per 100 mg of tissue, with an IKA Ultra-Turrax T025 tissue homogeniser at 20000 rpm (Janke and Kunkel, Staifen, Germany). Following homogenisation, samples were centrifuged at 4000 rpm in a Heraeus megafuge at room temperature for 10 minutes. The supernatant was aliquoted into 2 ml Eppendorf tubes and the pellet was discarded. Chloroform (0.2 ml/ 100 ml of the supernatant) was added and the tubes were shaken for 15 seconds and left at room temperature for 15minutes, then centrifuged at 13000 rpm at 4^{o}C for 20 minutes to separate the phases.

The upper layer that contained the RNA was transferred to a new tube and 0.5 ml of 100% isopropanol was added for 1ml of aqueous layer. The tubes were capped and inverted several times to mix, then incubated at room temperature for 15 minutes to allow the RNA to precipitate. The tubes were spun in a microfuge at 13000 rpm at 4^{o}C for 20 minutes to pelletise the RNA. The supernatant was discarded and the pellet was washed with 75% ethanol to reduce the salt concentration. The tubes were vortexed briefly until the pellet floated, and spun to settle the pellet. The ethanol was decanted and the pellets were dried for 5 minutes under vacuum. The pellets were resuspended in 30µl of lauryl sarcosine/EDTA solution.

The concentration of the RNA was determined spectrophotometrically at 260 nm by employing an extinction coefficient of 1 representing a concentration of 40 µg/ml. The quality of the RNA was judged by the A260/A280 ratio of absorbance of the sample; the scrutiny of the quality of ribosomal RNA bands visualised on agarose gels and by the quality of gamma actin signals on Northern blots.

3.16 Formaldehyde Agarose Gel Electrophoresis

Refer to Appendix 6 for reagents

3.16.1 Method:

A 2% stock agarose (electrophoresis grade) gel was made in 0.1% DEPC treated water and autoclaved. The appropriate volume of the gel was melted in the microwave oven, mixed with a volume of concentrated electrophoresis buffer to give a 1x concentration in the final preparation and with formaldehyde to a final gel concentration of 1% agarose.

3.17 Sample preparation and gel electrophoresis

Refer to Appendix 7 for reagents

3.17.1 Method

Before electrophoresis, samples of RNA containing 5 and 20µg of RNA were denatured at 65^{o}C in appropriate volumes of formamide, formaldehyde and 5X electrophoresis buffer. Samples were then mixed with gel loading buffer and electrophoresis was started at 5V/cm until the dye had reached 2/3 of the gel length. The gel was stained with ethidium bromide (500 ng/ml in 0.1M ammonium acetate) for 1 hour and then destained for 16 hours

with changes of DEPC treated water. The gel was then photographed on ultra violet illumination using a Polaroid camera.

3.18 RNA transfer to membrane

Refer to Appendix 8 for reagents

3.18.1 Method:

A 20X concentrate of SSC was prepared by adding 175.3g of NaCl and 88.2g of tri-sodium citrate to 1 litre of DEPC treated water, adjusting the pH to 7.0. The solution was sterilized by autoclaving at 121^{o}C for 20 minutes. RNA was transferred to a nylon membrane (Hybond N^{+}, Amersham) by capillary blotting using an apparatus specific for the purpose (Life Science Technologies, UK). The transfer was allowed to proceed for 48 hours in the presence of 20X SSC as described *(Sambrook et al., 1989*). The membrane was baked at 80^{o}C under vacuum to effect the crosslinking of RNA to the membrane.

3.19 Probes and hybridization

3.19.1 probes:

Type II collagen: this is a 2.2 kb fragment of the gene, coding from amino acid 343 of the triple helix to 70 amino acids inside the C-propeptide (Baldwin *et al.,* 1989).

Type IV collagen-alpha 2 cDNA: this is most of the collagenous domain (Hostikka and *Trygvasson.,* 1988).

OP-1 cDNA: comprises a 679 bp fragment harboured within pÖ320 (Helder *et al.,* 1995) and covers amino acids 63 to 262 of the pro-region and the first 25 amino acids of the mature polypeptide.

cDNA for TGF-ß$_1$ (*pRK5-ß1E*): contains the unmodified wild type TGF-ß$_1$ precursor (Derynck *et al.,* 1985).

cDNA BMP-3: contains a 1508 bp insert including the full coding region of hBMP-3 (Wozney *et al.,* 1988).

cDNAs for gamma actin and collagens were gifts of Professor de Wet, University of the Witwatersrand, Johannesburg.

cDNA for OP-1 was a gift from Dr David Rueger, Stryker Biotech, Boston, MA, USA.

cDNA for BMP-3 was a gift from Professor A. Hari Reddi, formely at John Hopkins University, Maryland, USA.

Type II collagen cDNA was a 2.2 kb fragment of the gene, coding from amino acid 343 of the triple helix to 70 amino acids inside the C-propeptide (Baldwin *et al.,* 1989).

cDNA for TGF-$ß_1$: (pRK5-ß1E) contains the unmodified wild type TGF-$ß_1$ precursor (Derrynck *et al.,* 1985). cDNAs for OP-1 and TGF-ß1 were gifts from Professor S. Vukicevic, University of Zagreb, Croatia.

3.20 Amplification of Constructs of *E. coli*

Refer to appendix 9 for reagents

3.20.1 Method:

Escherichia coli strain XL1Blue, a gift from W. de Wet, department of Medical Biochemistry, University of the Witwatersrand, was used as a vector for transformation. An overnight culture was prepared in LB medium (0.5% bacto yeast, 1% NaCl, 1% bactotryptone (Life technologies, UK) in deionised water which was autoclaved at 121^{o}C for 20 minutes on liquid cycle and cooled to room temperature. Bacteria were then grown for 16 hours on

LB-agar (Sigma Aldrich, Germany) plates. The bacteria were made competent by the $CaCl_2$ method (Cohen *et al.,* 1972).

Briefly, a single bacterial colony was picked from the LB agar plate and inoculated into 10 ml of LB medium, incubated at 37^{o}C with vigorous aeration overnight. One ml of the overnight incubation was transferred to 100 ml of LB medium in a 1 litre flask and incubated at 37^{o}C with vigorous aeration until the OD_{600} was approximately 0.4. The cells were transferred to a sterile ice-cold 50 ml falcon tube, cooled by placing on ice for 10 minutes after and were recovered by centrifugation at 4000 rpm for 5 minutes at 4^{o}C. The medium was decanted and the pellet was resuspended in 10 ml ice-cold 0.1 M $CaCl_2$ by gentle shaking and stored on ice for 30 minutes. The cells were recovered by centrifugation again at 4000 rpm for 5 minutes at 4^{o}C. The pellet was resuspended in 2 ml of ice-cold $CaCl_2$ (0.1 M) for each 50ml of original culture, mixed with glycerol (0.15 ml glycerol: 0.85 ml cells) snap-frozen in liquid nitrogen and stored at -70^{o}C until use.

3.21 Transformation of *E.coli*

Refer to Appendix 10 for reagents

3.21.1 Method:

Using a chilled sterile pipette tip, 200 µl of the bacterial suspension was transferred to a sterile Eppendorf tube. Super coiled plasmid DNA (100 ng) was added to the tube, mixed and stored on ice for 30 minutes. A control was made with competent bacteria that received no plasmid. The cells were transferred to a water bath at 42^{o}C for 90 seconds, and back to ice for 2 minutes. LB medium (800 µl) was added to the mixture and incubated at 37^{o}C with gentle aeration for 45 minutes to allow the bacteria to express the antibiotic resistance marker encoded by the plasmid. 100 µl of the transformed competent cells was transferred on to 90 mm LB agar plates containing the appropriate antibiotic and, using a sterile bent glass rod, the transformed cells were spread over the surface of the agar plate. The plates were inverted and incubated at 37^{o}C overnight.

3.22 Preparation of plasmid DNA

Refer to Appendix 11 for reagents

3.22.1 Method:

A High Pure Plasmid Kit (Boehringer Mannheim) was used for this purpose. Plasmid DNA was isolated from *E.coli* (XL1 Blue) by lysing the bacterial cells according to the alkaline lysis method (Birnboim and Dolly, 1979). An overnight culture of transformed bacterial cells was grown in 4 ml of LB at 37^{o}C. Cells were collected by centrifugation in the Heraeus megafuge. The cells were lysed and bacterial RNA was removed by the addition of RNAse A supplied with the kit. The lysate was neutralised and adjusted to high salt binding conditions after which chromosomal DNA was precipitated and the supernatant, which contained the plasmid was purified from the salts, proteins and other cellular impurities and eluted in 10 mM Tris-HCl buffer.

3.23 Preparation of probe Labelled with ^{32}P dCTP

Refer to Appendix 12 for reagents

3.23.1 Method:

The vector DNA was treated with suitable restriction enzymes to cleave the inserts. Restriction digests of plasmid vectors and molecular weight markers were run on 1% agarose gel in TBE

buffer at 5 volts per centimetre. The DNA was visualised by ultraviolet (UV) transillumination of the gel.

The inserts were identified according to molecular weight. The DNA concentration was then determined by spectrophotometric analysis of the sample absorbance at a wavelength of 260 nm, where an absorbance of 1 unit represents a DNA concentration of 50µg/ml. DNA (25 ng) was labelled with alpha- ^{32}P dCTP using a random prime labelling kit (DNA megaprime labelling kit RPN 1606, Amersham Life Science). A DNA purification kit (QIAquick, White Head Scientific) was used to remove unincorporated label and the purified probe was used for hybridization.

3.24 Hybridisation of probes and detection

Refer to Appendix 13 for reagents

3.24.1 Method

Conical propylene tubes of 50 ml capacity were used for the hybridization procedure that was carried out in a hybridization oven (Hybaid Corporation, UK). The probe was mixed with 100 µl of sonicated fish sperm DNA (10 mg/ml) and boiled for 2 minutes to denature the DNA. A hybridization solution (QuikHYB, White Head Scientific) supplied commercially for this purpose was used to prehybridize membranes first at 37^{o}C for 10 minutes, then at

68°C for 20 minutes. Probe was added and hybridization was allowed to continue for 2 hours at 68°C except for type IV collagen detection, which was carried out at 72°C because of the non-specific binding of the probe to GC rich sequences of ribosomal RNA at lower temperatures.

Membranes were washed twice for 15 minutes at room temperature with 150 ml of 2X SSC, 0.1% SDS, followed by another wash at 68°C with 0.1X SSC, 0.1% SDS. The blot for type IV collagen was washed at 72°C to achieve a higher stringency. Membranes were dried on blotting paper and covered with a Saran Wrap. Autoradiography was performed with Kodak Biomax MS film at -70°C for given time periods, ranging between 16 hours to 5 days. Films were developed and processed.

3.25 Signal quantitation

The signal intensity for each lane was quantitated by scanning densitometry (Gel Documentation and Analysis system, Syngene, U.K) and normalized against values obtained for the gamma actin signal. Values were adjusted to relative densitometric units and presented as percentages of gamma actin signals (Matsaba *et al*., 2001; Ripamonti *et al*., 2000a).

3.26 Quantitative analyses

The histological sections of 90 and 180 days were analyzed to quantitate the percentage area of the newly formed bone in relation to the total surface area of the concavity. The sections were analyzed under a research microscope (Provis X70, Olympus Optical Co. Japan) projected to a computer. The analysis was achieved with the support of a computer software (Flexible Image Processing System ® ver. 2.15, CSIR, South Africa) installed in a Pentium computer with a colour monitor (Ripamonti *et al*., 1996a, Ripamonti *et al*., 1997; Ramoshebi and Ripamonti, 2000). The area of bone in mm^2 that had formed in the concavities was measured in relation to the total surface area of the concavity and presented in the form of percentage using a mathematical formular:

% of bone=area of bone/total area of the concavityX100.

3.27 mRNA analysis

The signal intensity for each lane was quantitated by scanning densitometry (Gel Documentation and Analysis system, Syngene, U.K) and normalized against values obtained for the gamma actin signal. Values were adjusted to relative densitometric units and presented as percentages of gamma actin signals in the form of

bar graphs (Ripamonti *et al*., 2000a; Matsaba *et al*., 2001). The signal intensities for the three different time periods were compared visually based on the percentage values obtained for the signal intensities and recorded in the form of a table as follows: +++ high expression, ++ moderate expression, + low expression, - no expression (Table 1).

3.28 Statistical analysis

The data were analyzed with the Graph Pad Prism^{TM} version 2.0 (San Diego USA). An Analysis of Variance procedure (ANOVA) was performed. Comparison of the mean values was obtained using the Bonferroni's Multiple Comparison Test procedure on the dependent variables that were included in the analysis. The critical level of statistical significance chosen was $P < 0.05$.

4.0 RESULTS

4.1 Characterisation:

4.1.1SEM

Figure 4A: A SEM image of the HA used for Type I sample, showing the microporosity

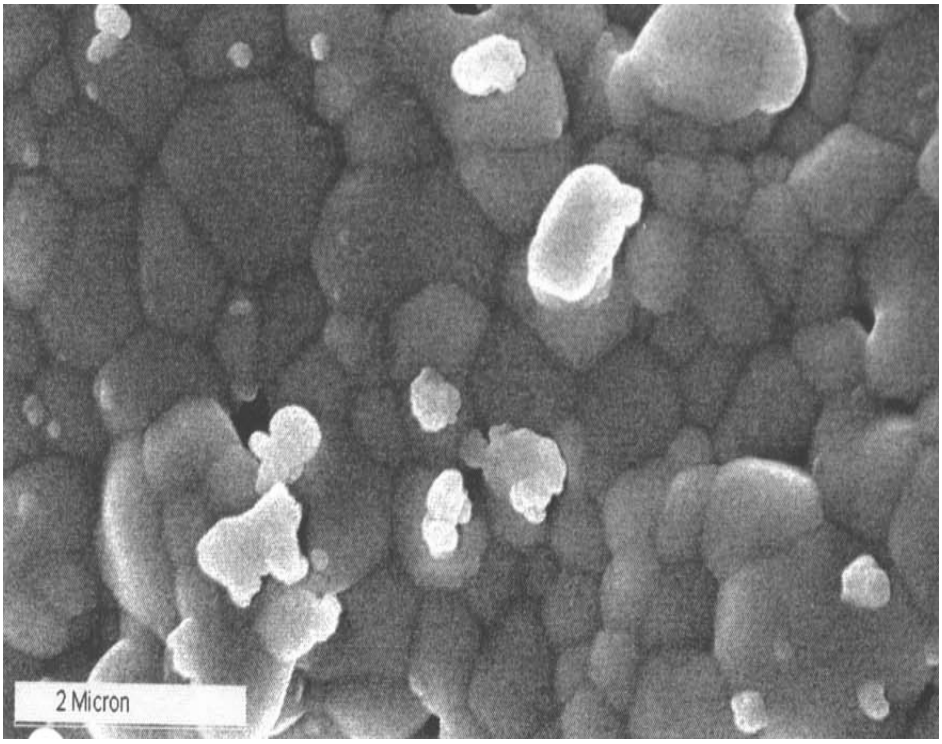


Figure 4B. A SEM image of the HA used as Type II sample, the same HA was used for type III and IV samples. The microporosity can be seen.

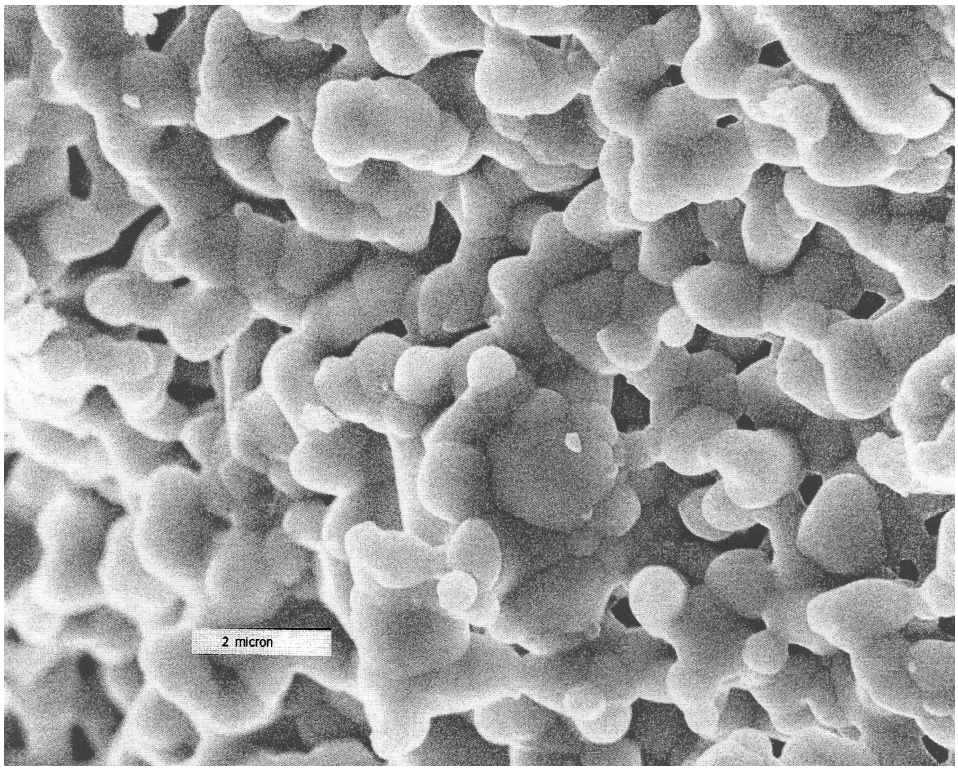


Figure 4C. A SEM image of the HA/TCP used as Type III sample, showing the microporosity

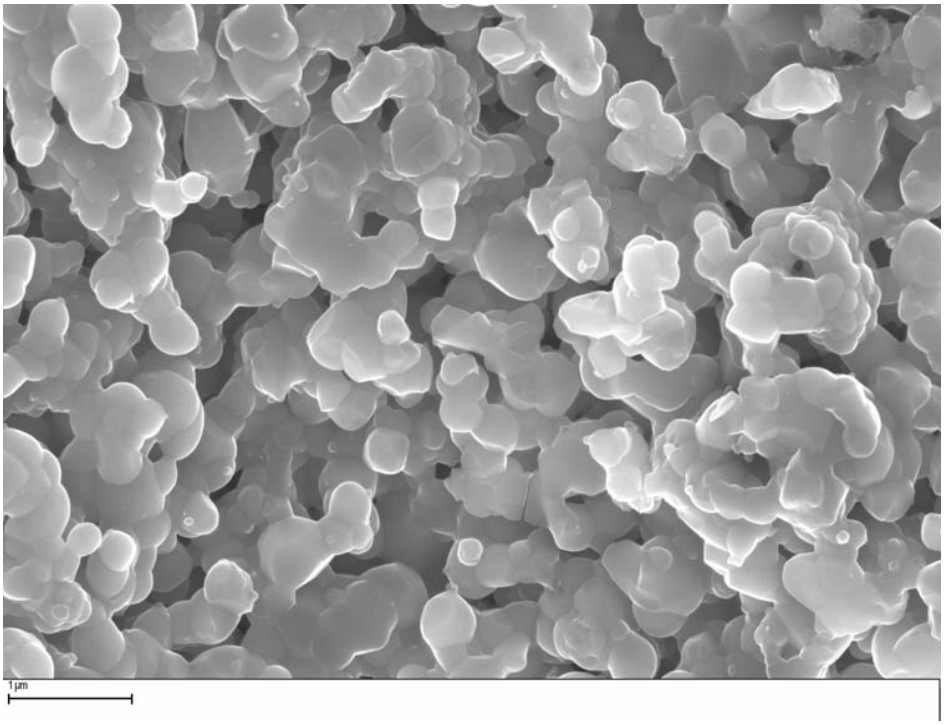


Figure 4 D: A SEM image of the HA/TCP used as Type IV showing the microporosity

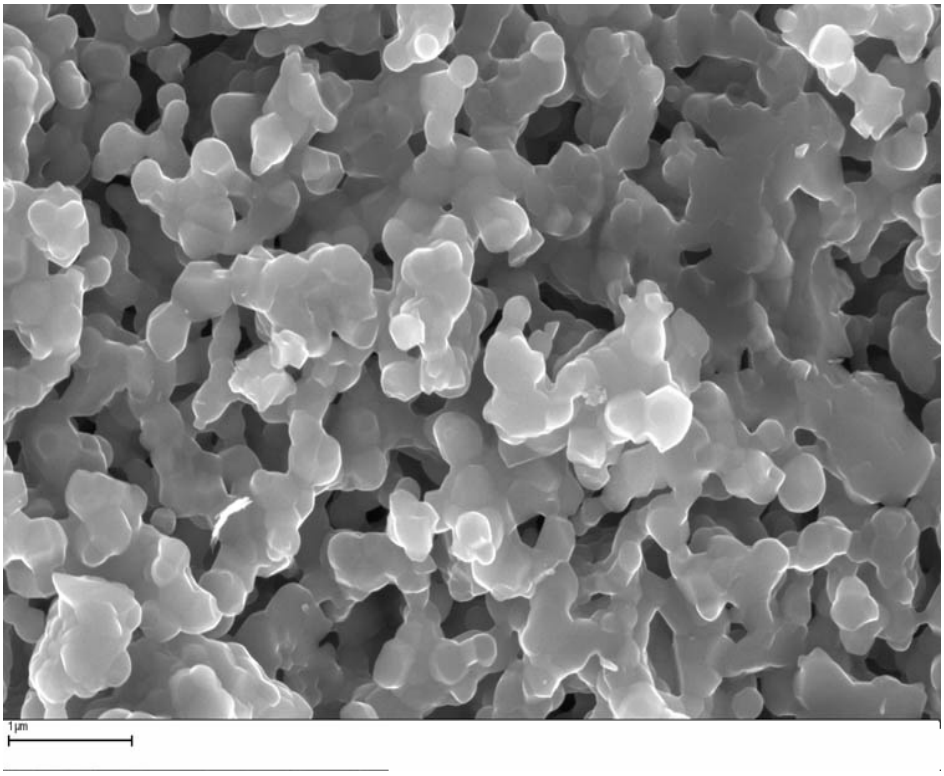


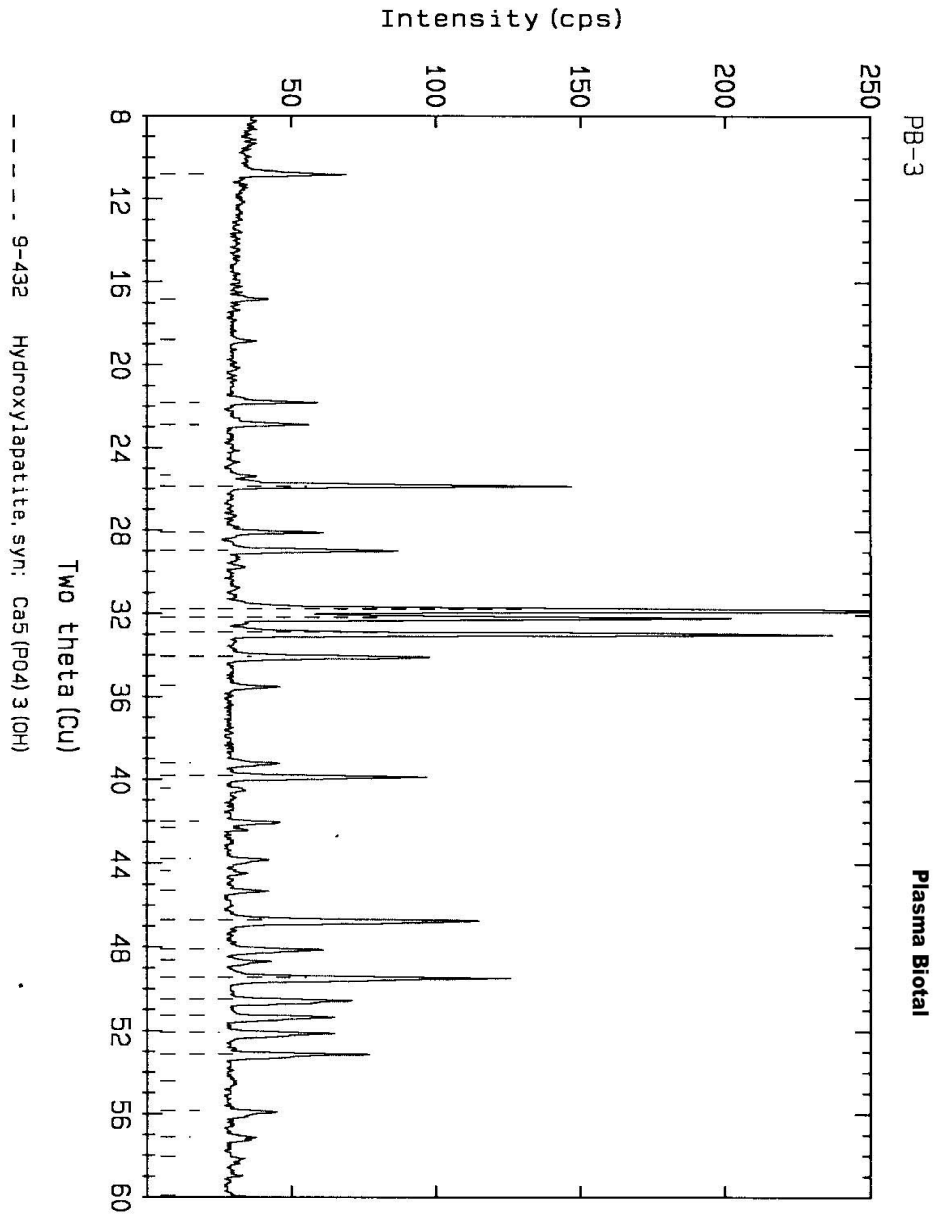
Figure 5.

4.1.2 XRD

Specimens of the implant were subjected to XRD analysis on a Phillips PW 1830 generator operating at 45kV and 20 mA. Copper K_{alpha1} radiation with a wavelength of 1,5406 A^0 was used. The sample was scanned at a stepsize of 0,02 degrees 2-theta and step time of 1 second. Phase identification was done through comparison of the diffractogram with standard data from the ICDD.

The results are shown below. No significant quantity of any phase other than hydroxyapatite was noted.

A. XRD pattern of the Plasma Biotal material that was used as Type I material. The pattern shows it to be single phase.



B. XRD of the HA material used as Type II showing it is single phase material. This powder was also used as the HA component in Types III and IV samples.

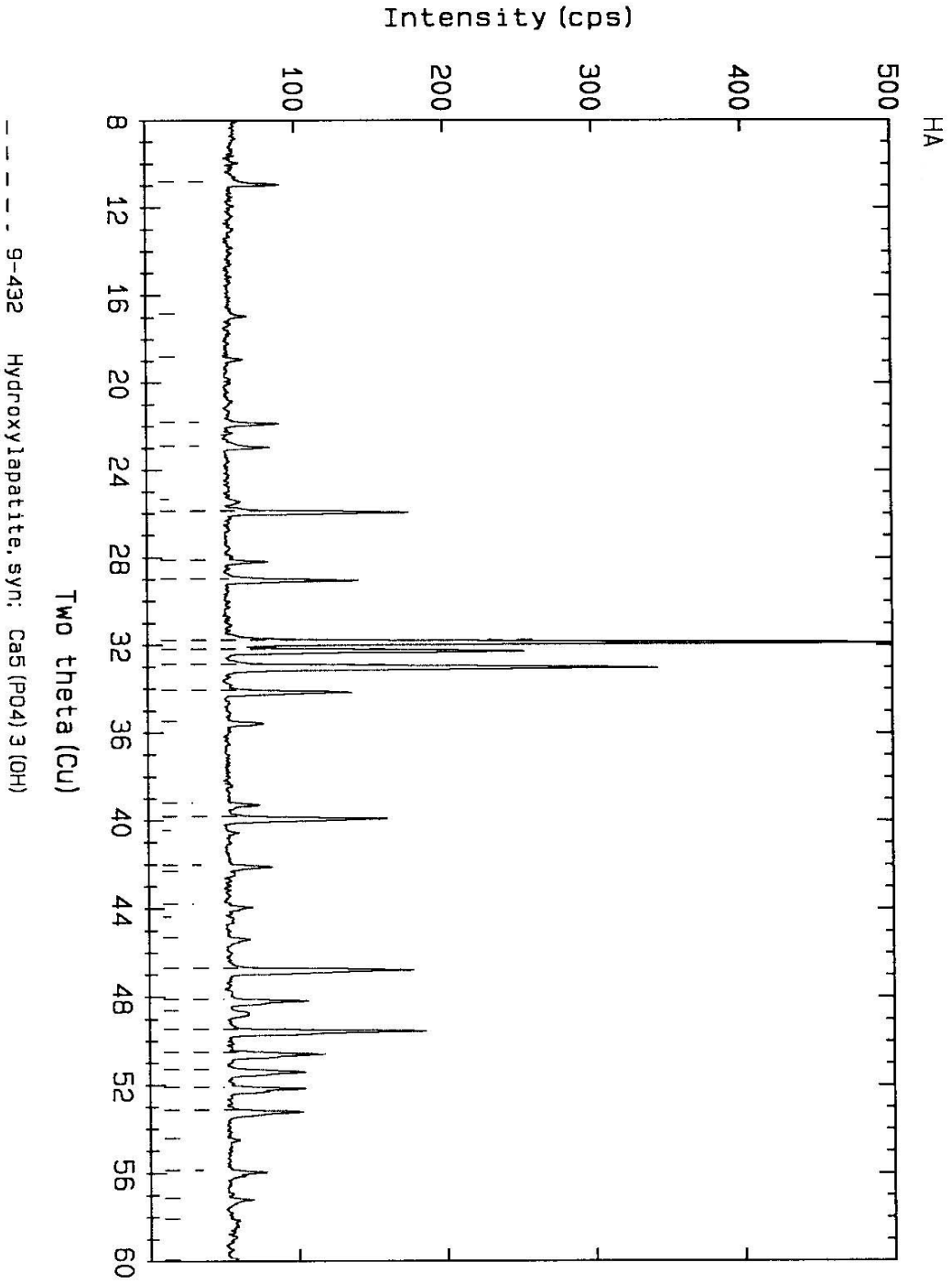


Figure 5C. XRD spectrum for type III materials showing the presence of HA and TCP that made up the sample.

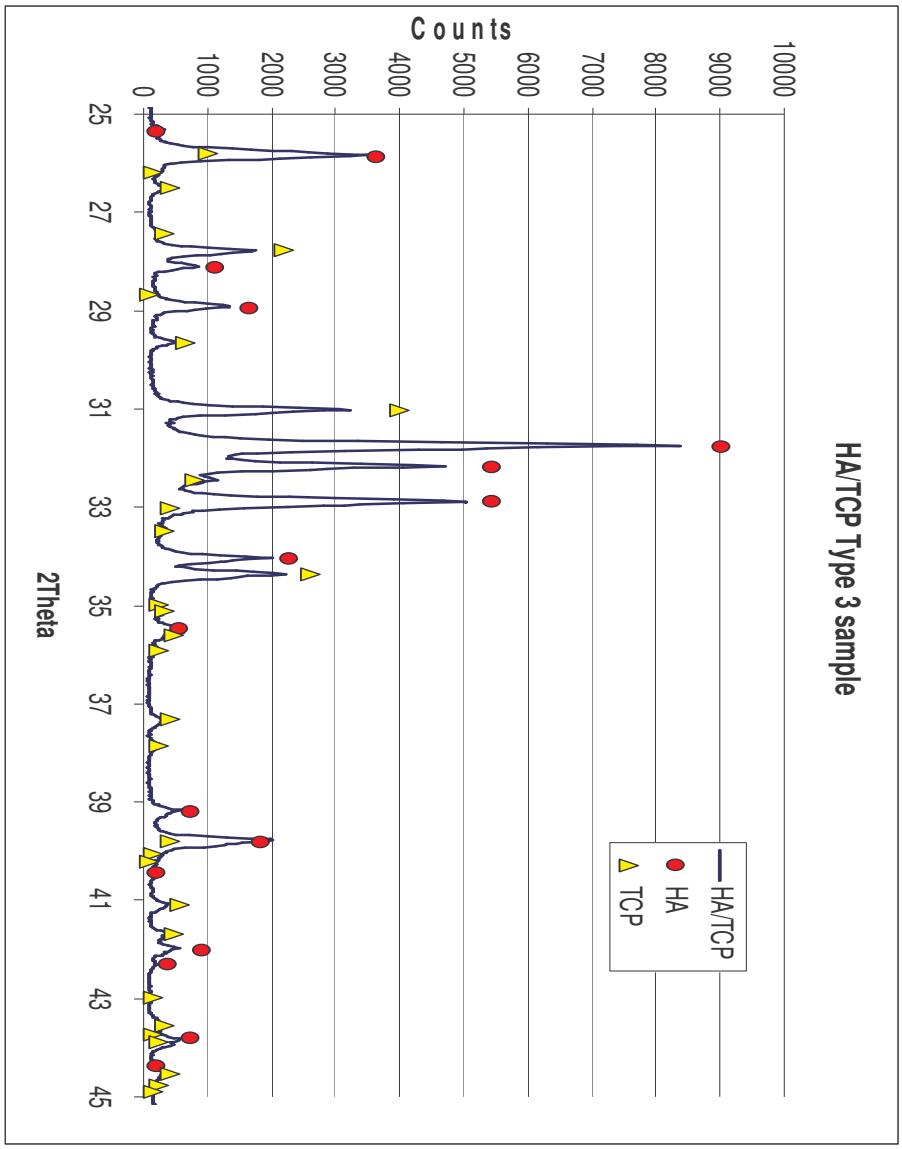


Figure 5D. XRD spectrum for type IV materials showing the presence of HA and TCP that made up the sample.

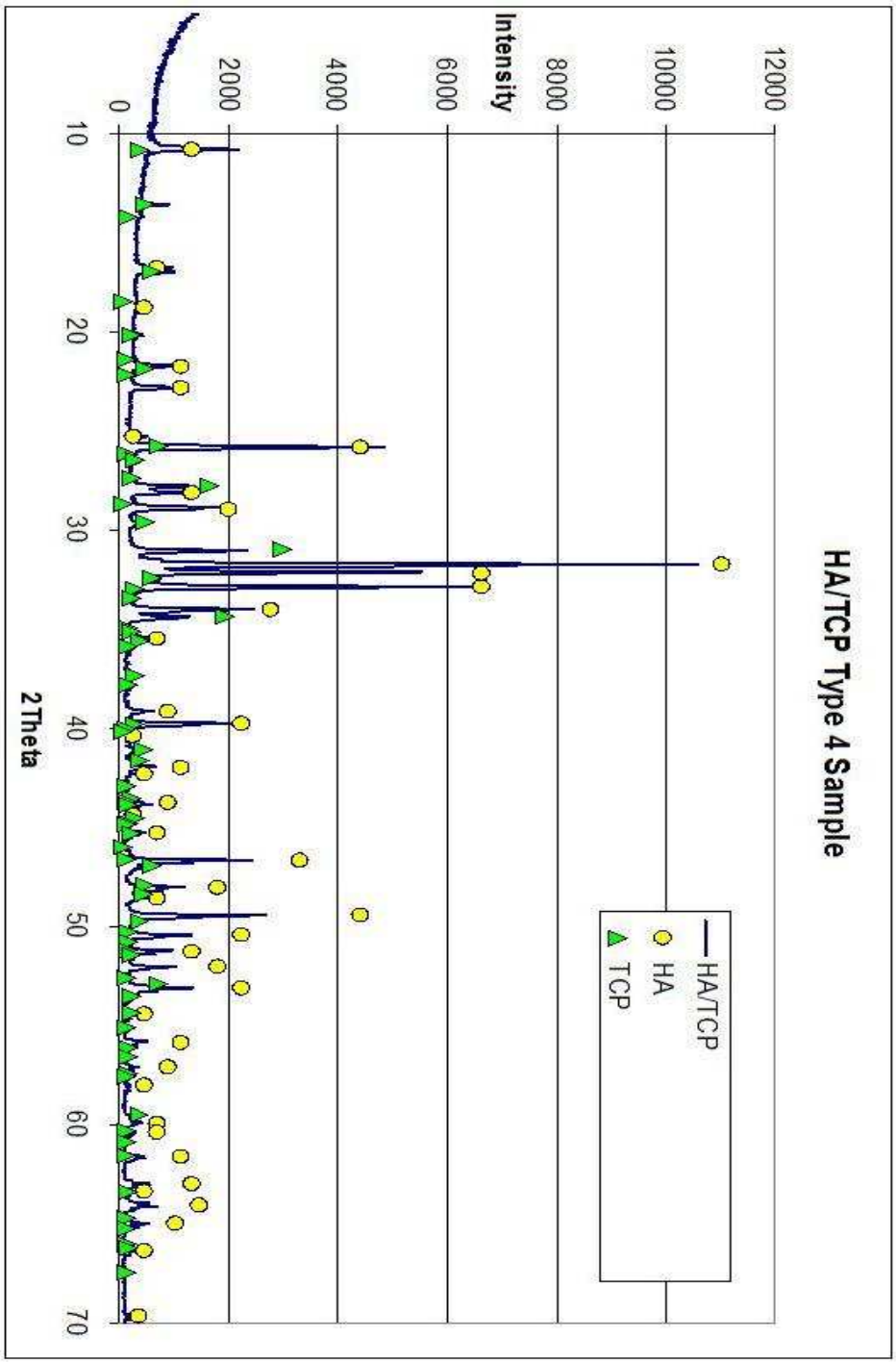
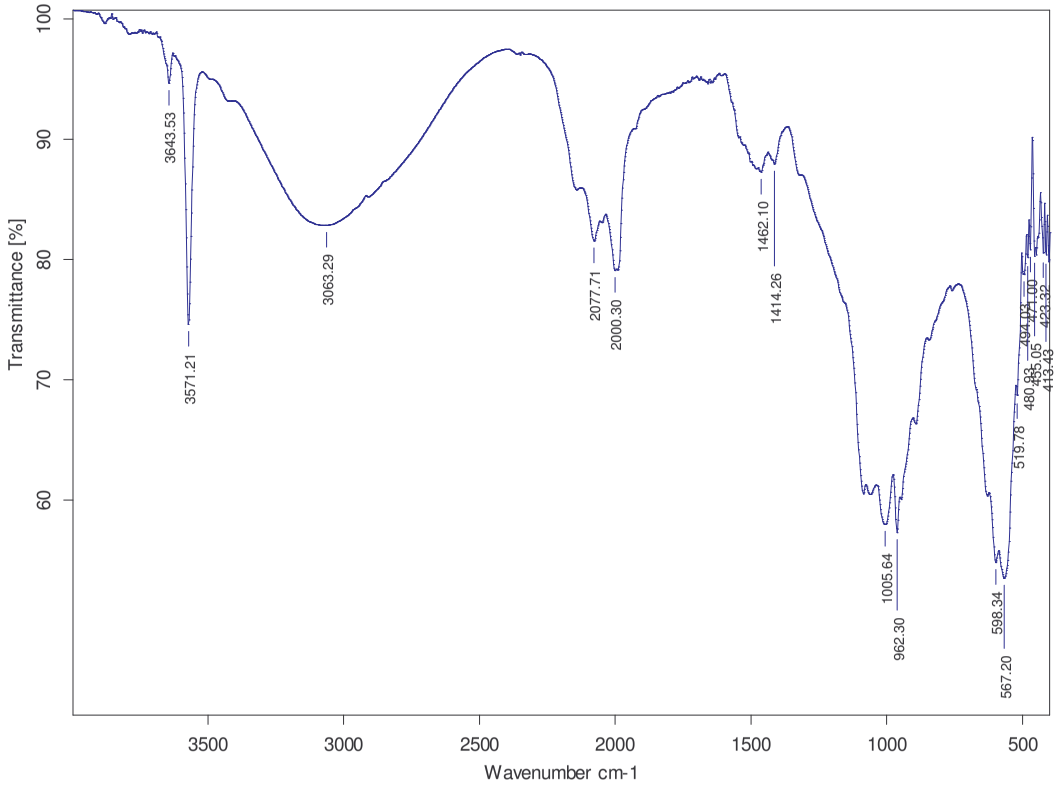


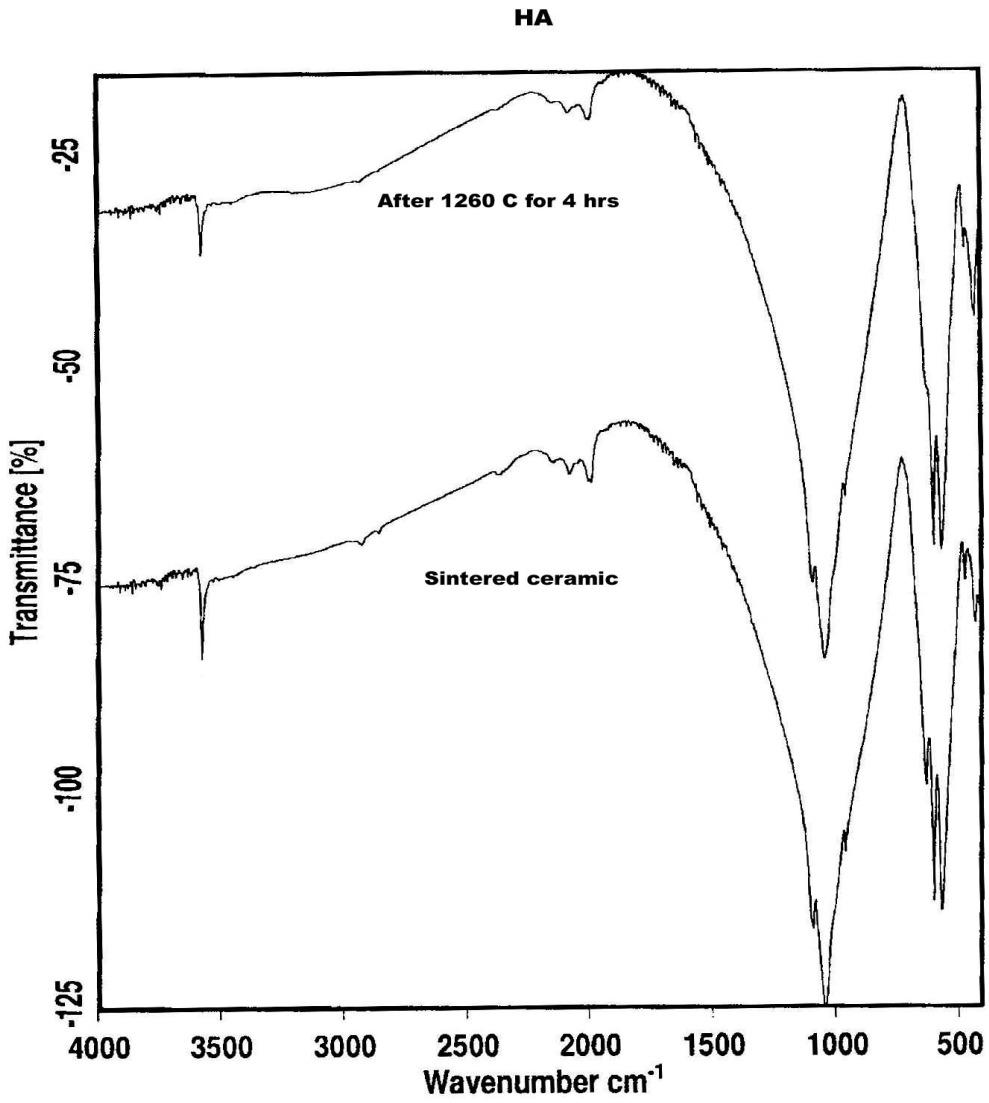
Figure 6

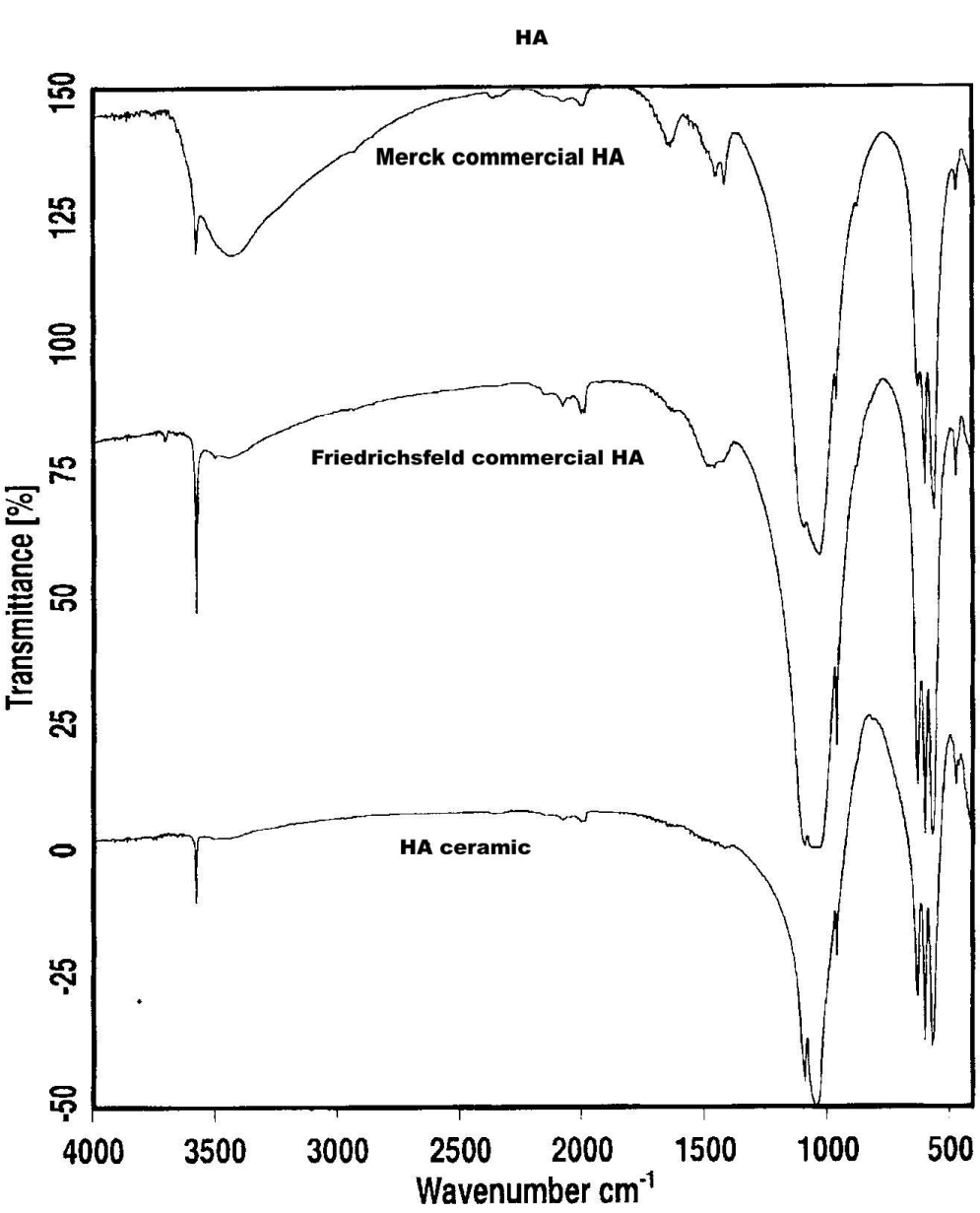
4.1.3 FTIR

A. FTIR of Plasma Biotal

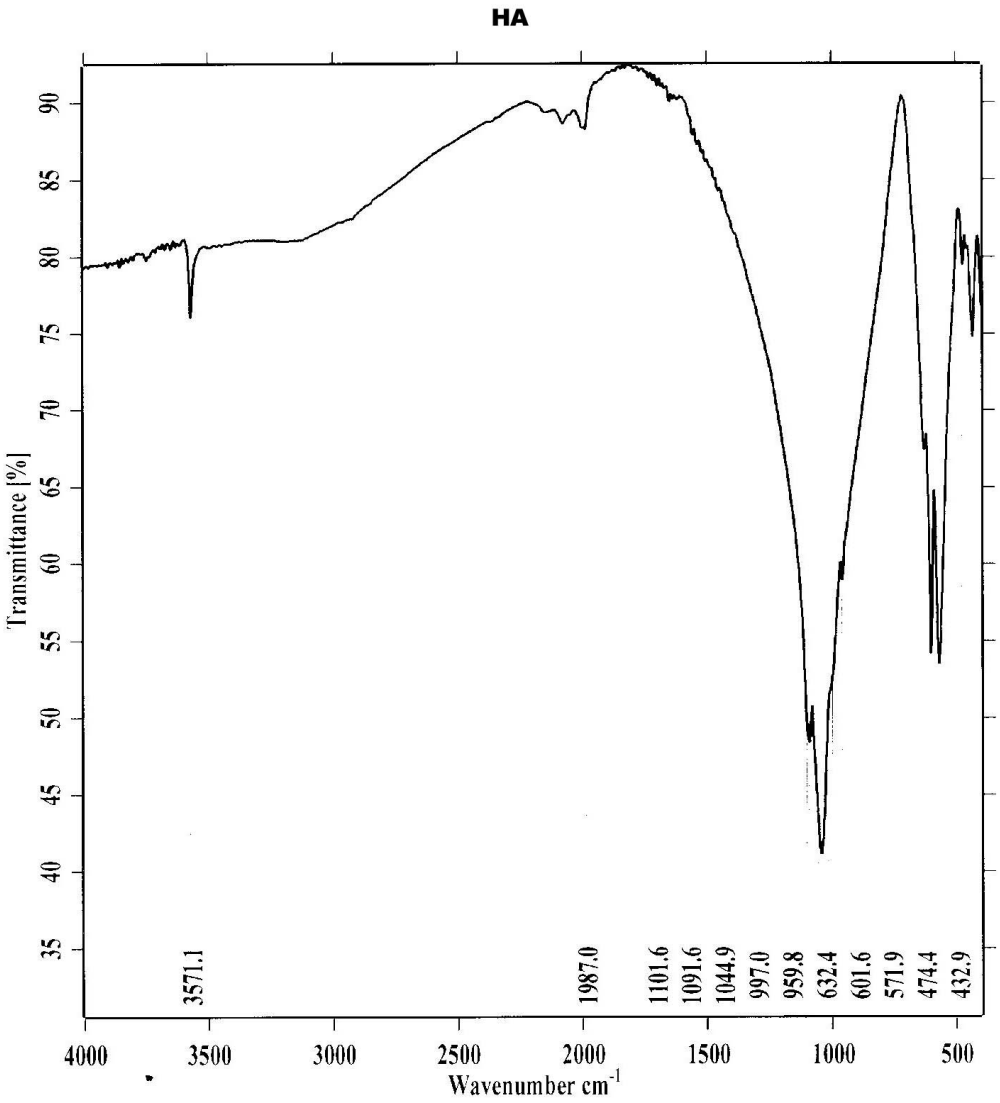


B. FTIR spectrum of the Type II HA material that was also used as the HA component in Types III and IV. The observed band at 3571 cm^{-1} is indicative that the OH groups are intact.





C. FTIR spectrum of type II material. The lower spectrum is that of the material as used in the ceramics for types II, III and IV ceramics. The top spectrum is that of the material after it has been exposed to a temperature of 1 240C for 3 hours to ascertain its stability under these conditions. The spectra show that the material was essentially unchanged and would not readily degrade under the sintering conditions used in the present study.



D. The FTIR spectrum of the Type II material (previous page lower –figure 6 C) in comparison with that of the commercial Merck HA material (top figure 6C) and Friedrichsfeld HA material (previous page figure 6 C middle). The absorbance bands in these three materials are essentially the same.

4.1.4 Inductively Coupled Plasma – Mass Spectroscopy

Hydroxyapatite-based implants are required to meet a specification for maximum levels of heavy metals according to the American Society for Testing Materials (ASTM) F 1185 - 88. This specification is for ceramic hydroxyapatite intended for surgical implants. A semi-quantitative laser ablation high resolution ICP-MS analysis of two implant samples was conducted. The results indicated that As, cadmium (Cd) and lead (Pb) are below the ASTM specifications. Traces of Hg were detected but in concentrations also below the ASTM specification.

4.2 ALKALINE PHOSPHATASE ACTIVITY

At the end of each time period (30, 90 and 180 days) tissues were harvested and analyzed for osteoinduction through alkaline phosphatase activity, histology, immunohistochemistry and gene expression.

4.2.1 Alkaline Phosphatase activity

The harvested tissue included connective tissue on the planar surfaces.

Tissues were homogenized on ice in 2ml of homogenizing buffer (appendix 1) in sterile elkay tubes (AEC Amersham). The alkaline phosphatase activity of the supernatant after homogenization of specimens was determined with 0.1M p-nitrophenyl phosphate as a substrate at pH 9.3 and 37^{o} C for 30 minutes. Under the assay conditions 1 unit of enzyme liberates 1 µmol of p-nitrophenol. Alkaline phosphatase is expressed as units of activity per microgram protein (Reddi and Huggins, 1972, Matsaba *et al*., 2001). Values are means ±standard error of mean (SEM).

4.2.2 30 days implantation

The activity of alkaline phosphatase was generally low in tissues generated by all four types of substrata. There were relatively small differences in the level of alkaline phosphatase expressed and there were no significant differences (Fig. 4 A). Generally, alkaline phosphatase activity was relatively higher on day 30 as compared to day 90 and was almost non-detectable on day 180 (Fig. 4 A-C). Alkaline phosphatase activity expressed by Type 1 was significantly higher at 5% probability level between 30 days and 180 days. The minimum amount of alkaline phosphatase activity was x units per milligram protein while the maximum was x units per milligram protein. There was no significant difference between the expressions of alkaline phosphatase within the four samples.

4.2.3 90 days implantation

The alkaline activity was relatively low in all the four types of substrata. Type 2 showed the highest expression compared to Types 1, 3 and 4 and this difference was significant at 5 % probability level. Type 2 expression reached maximum of 0.27

units per milligram protein (Fig. 4 B). Types 1 and 4 were relatively similar and Type 3 was a bit higher though there was no significant difference.

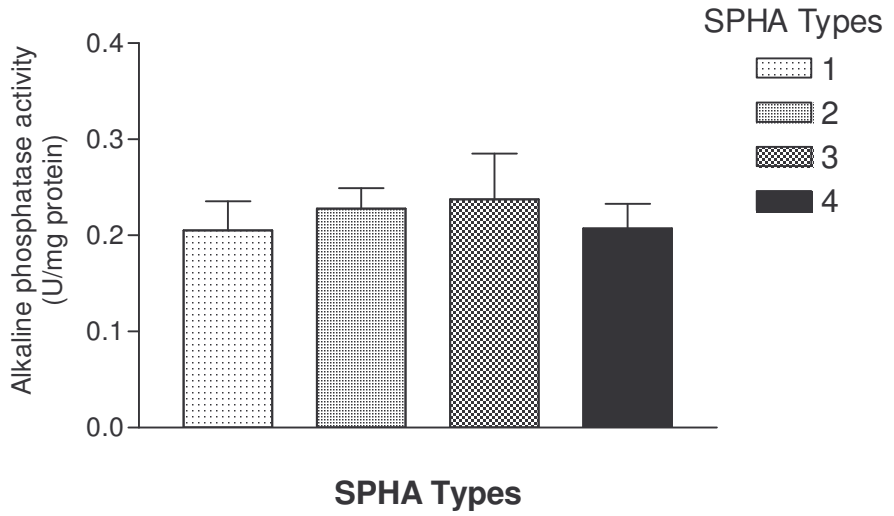
4.2.4 180 days implantation

Only Type 2 and Type 4 samples were implanted for this time period.

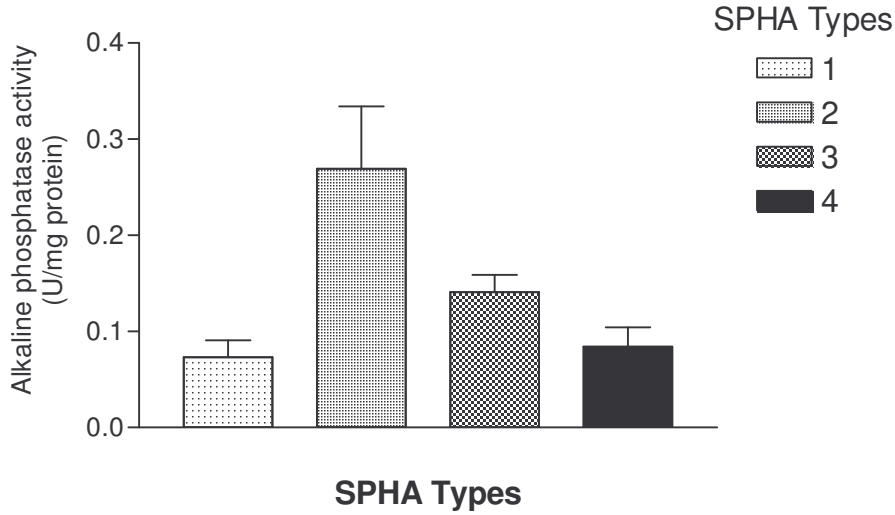
The alkaline phosphatase activity was relatively low in both Type 2 and 4.

Figure 7. The effect of surface geometry on alkaline phosphatase activity of tissues generated in the concavities of substrata Types 1, 2, 3 and 4. Values are means ±SEM. N=6. A: 30 days, B: 90 days, C: 180 days

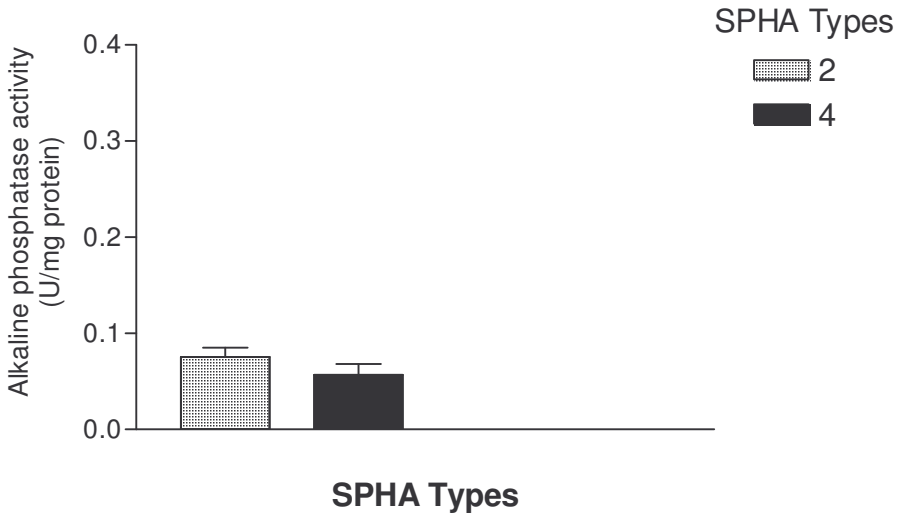
A. 30 days



B. 90 days



C. 180 days



4.3. Histology and Immunolocalisation

Harvested tissue for histology was trimmed of adhering muscle but included connective tissue on the planar surfaces. The morphological hallmarks employed to identify bone tissue were as follows: With the modified Goldner's Trichome stain used in this study, bone tissue stains blue on decalcified sections as matrix with lacunae filled by osteocytic cells and often, but not always, has osteoblastic cells facing the connective tissue matrix highly vascularised. The only difference between the original Goldner's stain and the modified one is the counterstaining. The original method counterstains with a green stain while the modified method counterstains with a blue stain so everything that is green representing mineralized bone in the original method will appear blue in the modified method.

4.3.1 30 days implantation

Histological analysis revealed condensation of fibrovascular tissue and collagenic material, which predates bone formation within the concavities of the substratum and morphogenetic events including angiogenesis, a prerequisite of bone formation in all four Types of substrata. These morphological events occured solely within the concavities and not on the planar sites in between concavities. (Fig. 5a; A-D).

Immunohistochemistry showed localisation of OP-1 and BMP-3 in Types 2 and 4 substrata. (Fig. 6 B and C). This localisation of BMPs/OPs was observed only within the concavities and not on the planar surfaces.

4.3.2 90 days implantation

Morphological and histological examination revealed that bone differentiation was exclusively initiated in the concavities of Type 2 and Type 4 substrata reaching 58.6% in Type 2 and 28.2% in Type 4 (Fig. 5b; B and D and Fig. 8 A). Types 1 and 3 showed vascular tissue invasion within the concavities of the substratum (Fig. 5b; A and C).

4.3.3 180 days implantation

Histological results revealed the spontaneous initiation of bone formation and vascular invasion within the concavities of both substrata Types 2 and 4 (Fig. 5c; A and B). The newly formed bone reached 23% and 10 % of newly formed bone area in relation to the total area in mm^2 of the concavities of Type 2 and Type 4 (Fig. 8 B), respectively as measured with the support of a computer software (Flexible Image Processing System ® ver. 2.15, CSIR, South Africa) installed in a Pentium computer with a colour monitor (Ripamonti *et al*., 1996a, Ripamonti *et al*., 1997; Ramoshebi and Ripamonti, 2000).

Figure 8. Tissue morphogenesis in concavities of the four types of substrata on day 30 postimplantation

30 days

High power photomicrographs (A-D)

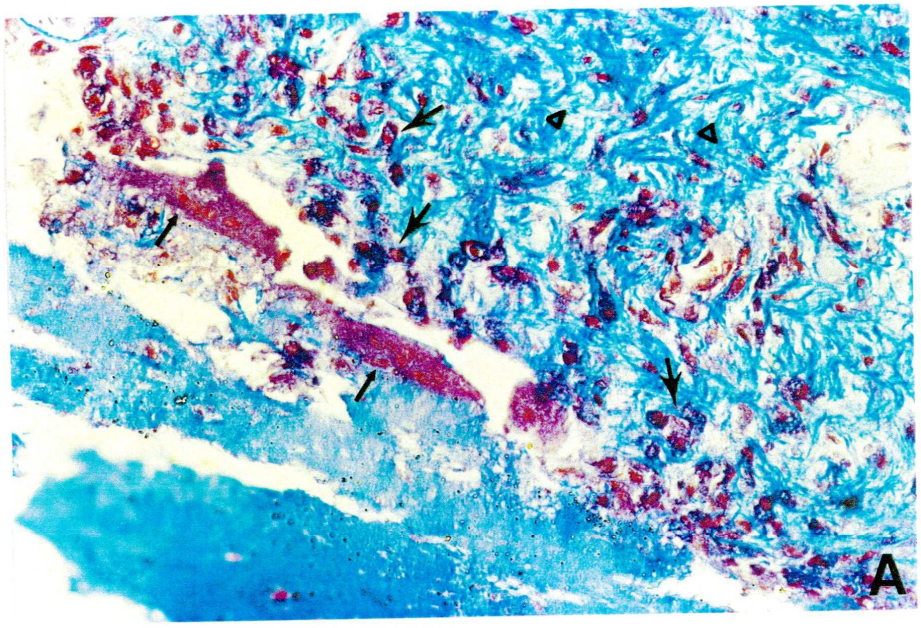
A: Type 1; B: Type 2; C: Type 3; D: Type 4.

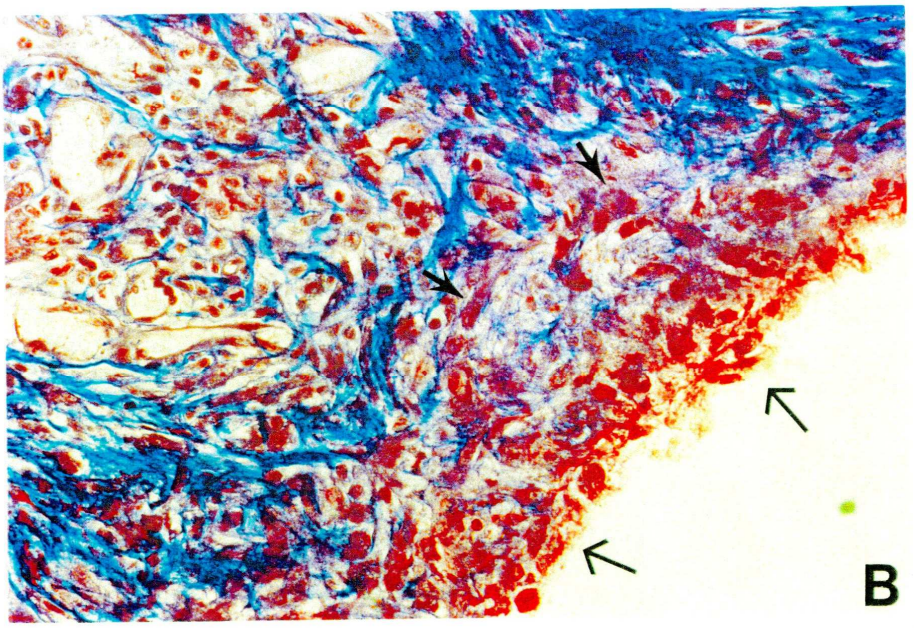
A: Vascular invasion and capillary evidence in close contact with the substratum interface (pointy arrows). Mesenchymal tissue condensation within the substratum in blue (open arrow heads) and giant multinucleated cells (straight arrows) attached to the substratum. Original magnification: X101

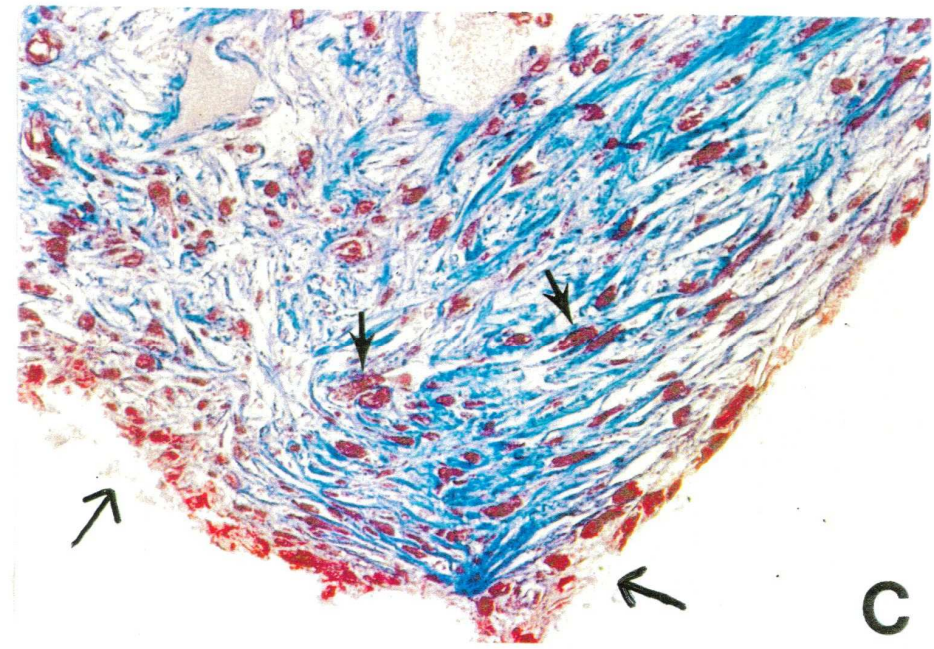
B: Capillary sprouting (pointy arrows) within the network of collagen fibers in blue. Substratum interface (long arrows) Original magnification: X101

C: Vascular invasion within collagen (pointy arrows). Substratum resorption (long arrows). Original magnification: X50

D:Resorption of the substratum (long arrow). Densely packed collagen condensation (open arrow heads) and vascular invasion (pointy arrow). Original magnification: X50


A


B


C

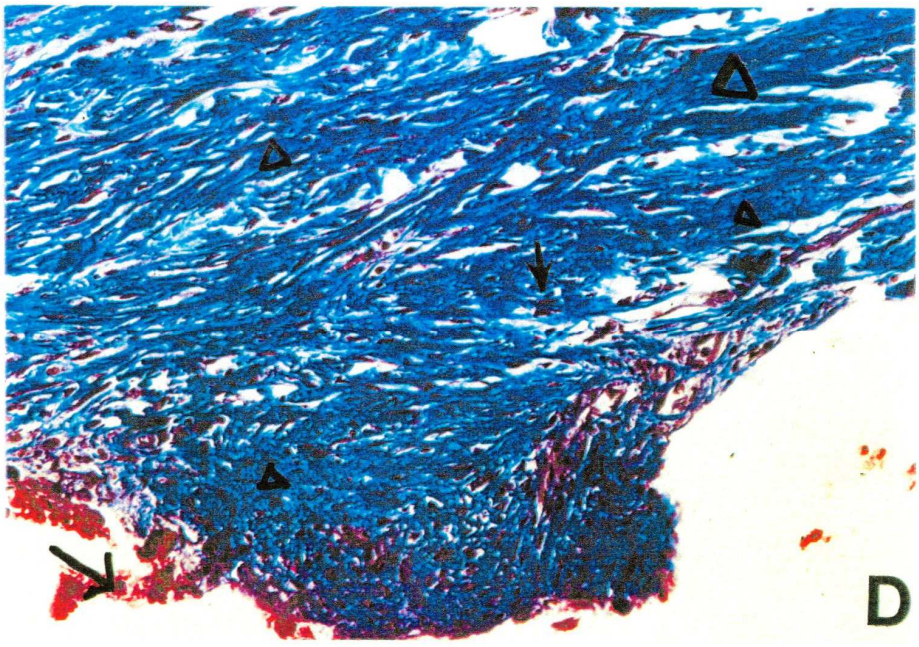
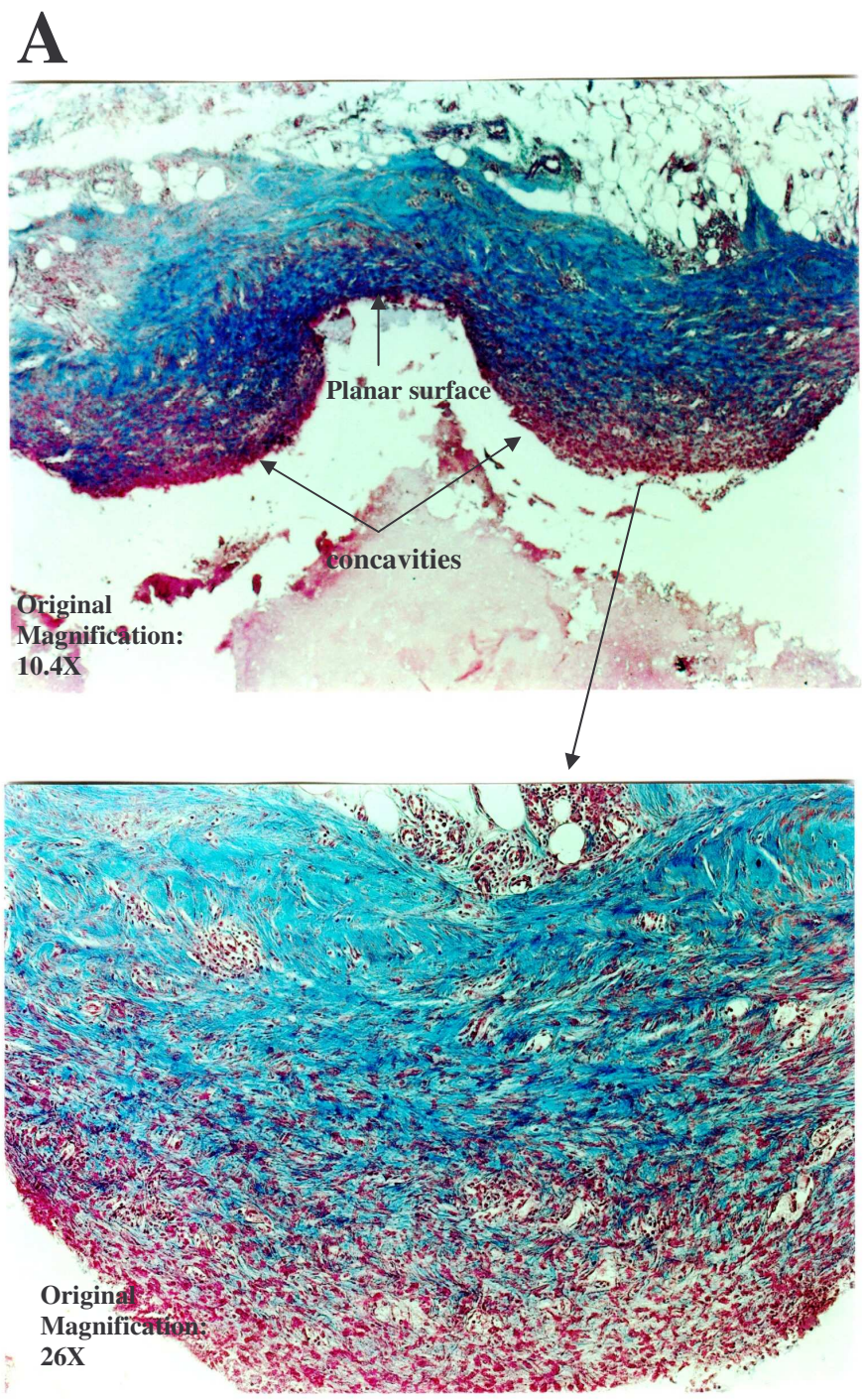
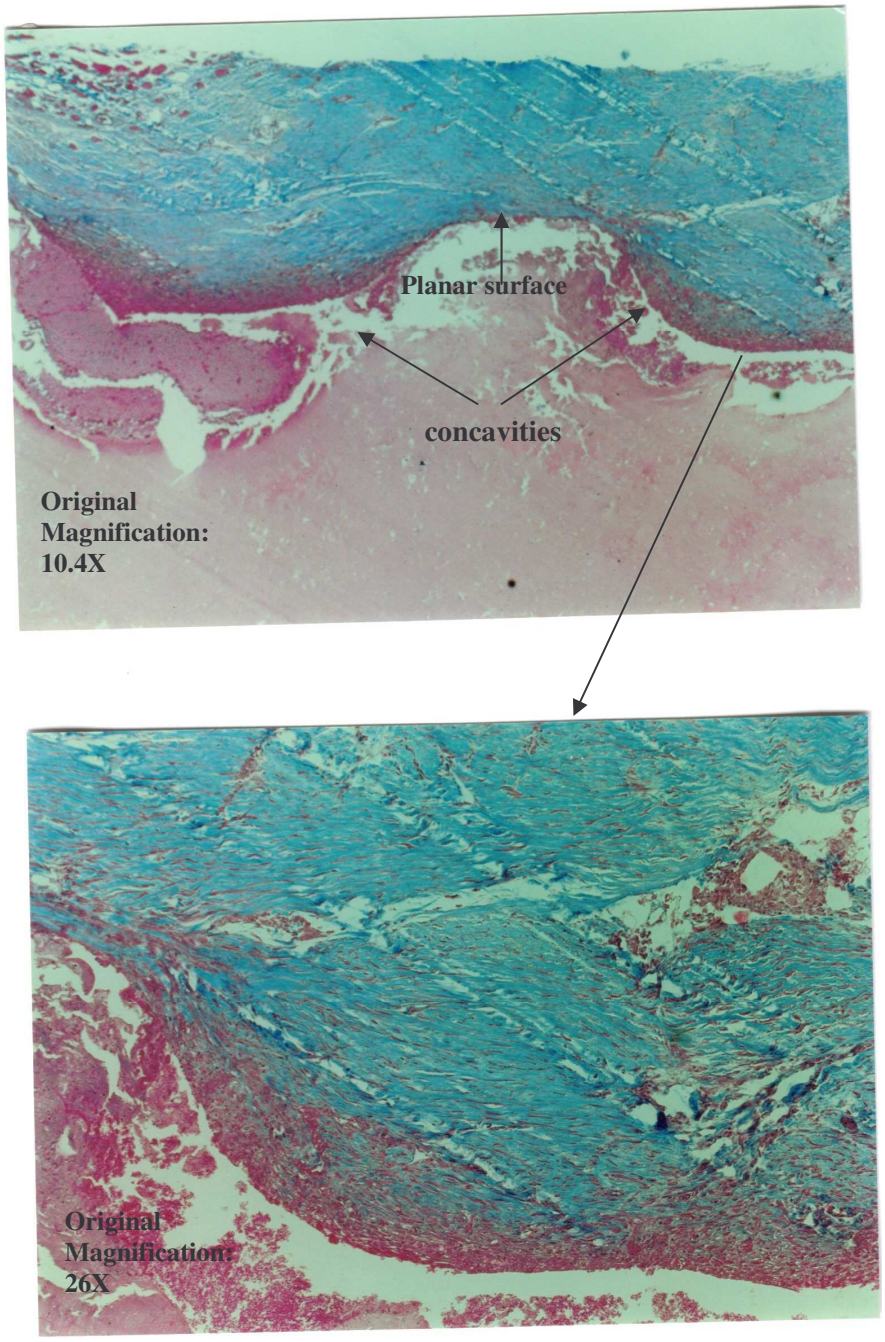

D

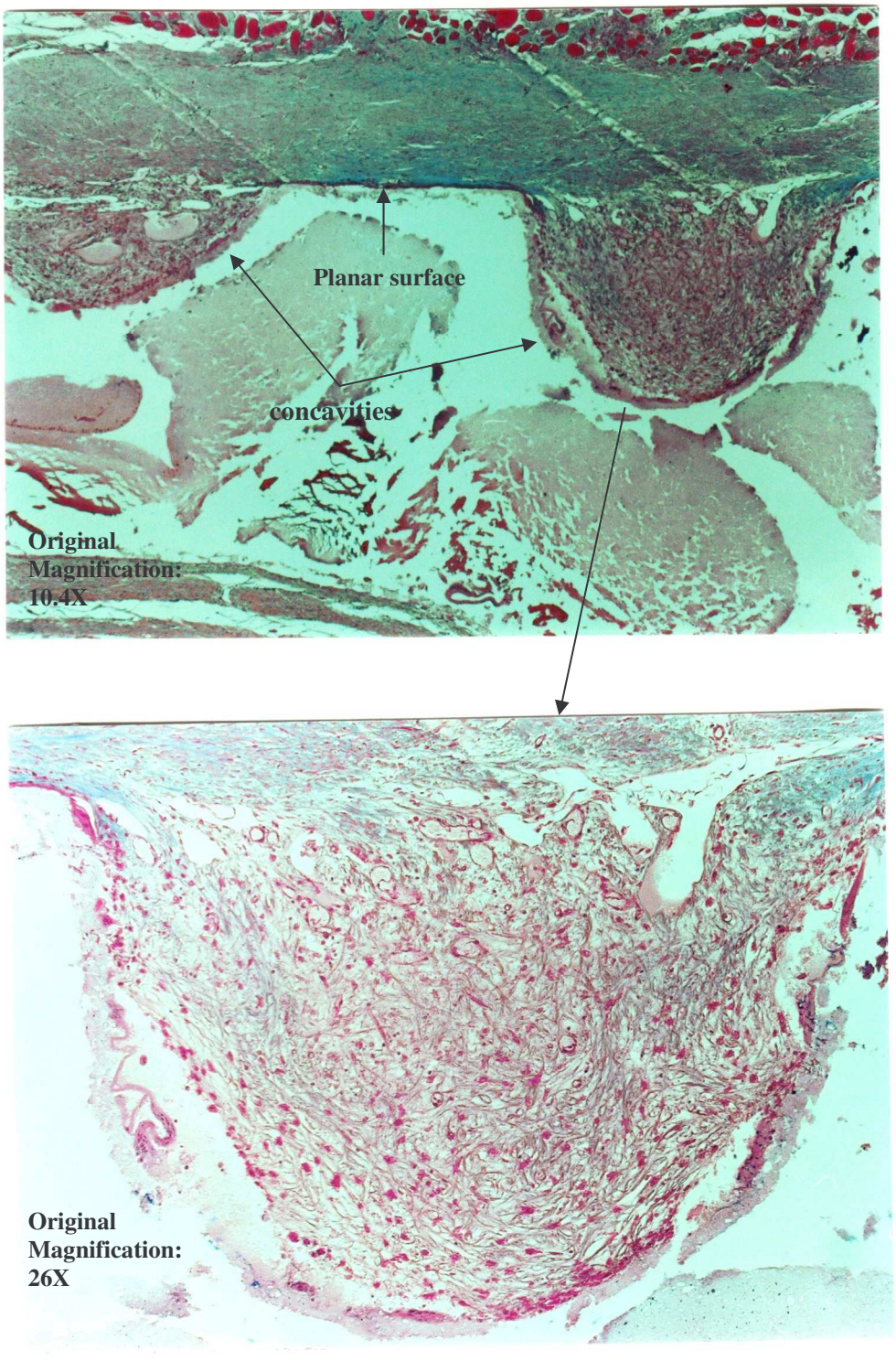
Figure 9. Low power photomicrographs showing vascular invasion within the concavities as compared to the planar surfaces in between concavities (A-D).



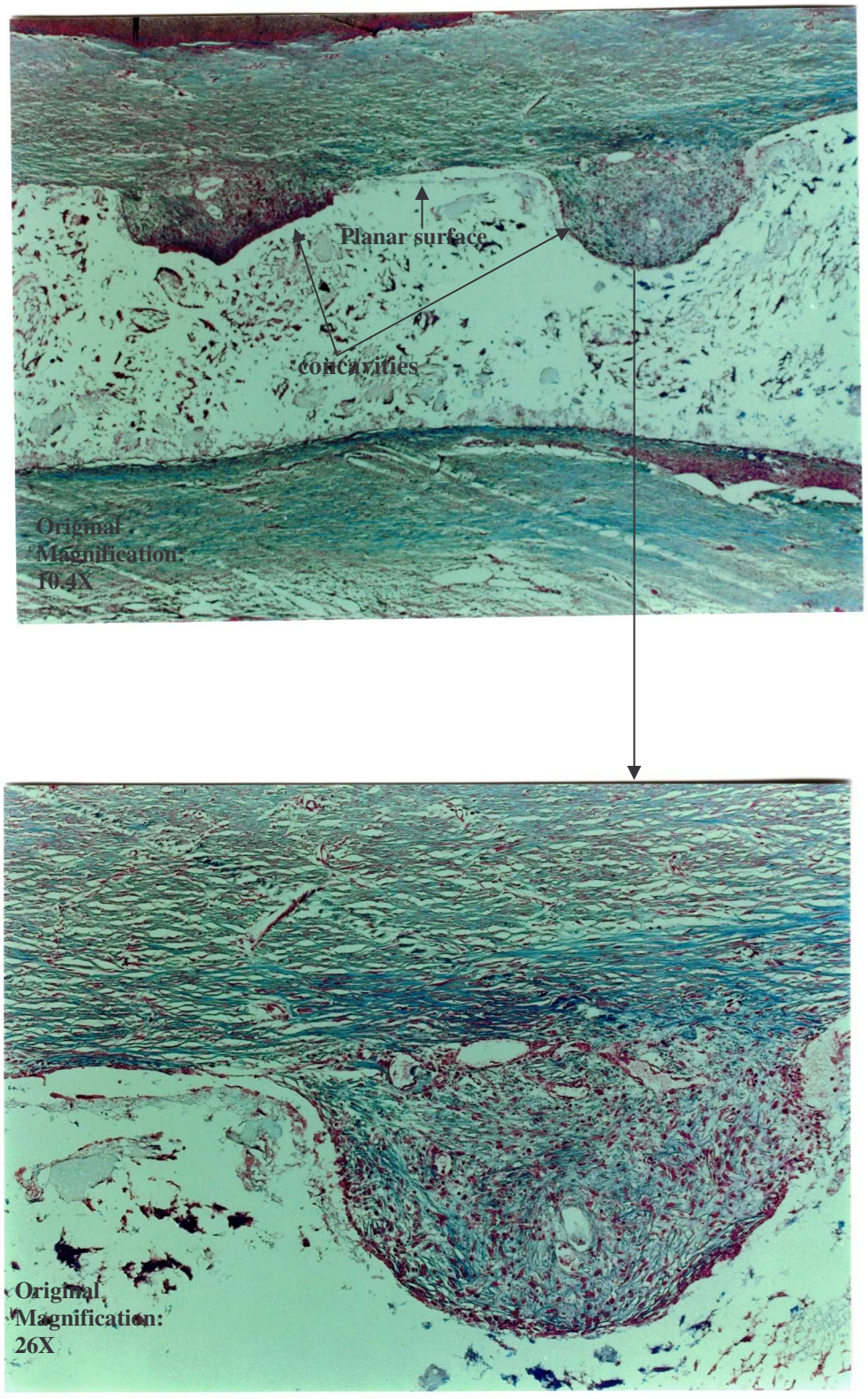
B


Planar surface
concavities
Original
Magnification:
10.4X
Original
Magnification:
26X

C


Planar surface
concavities
Original
Magnification:
10.4X
Original
Magnification:
26X

D


Planar surface
concavities
Original Magnification: 10.4X
Original Magnification: 26X

90 days

Tissue morphogenesis and spontaneous induction of bone in concavities of the substratum on day 90 after heterotopic implantation.

Figure 10. High power photomicrographs

A: Type 1: Pronounced vascular invasion (pointy arrows) within collagen fibers. Artefactural separation of soft tissue (small arrows).

Original magnification X101

B: Type 2: Newly formed bone (arrow heads) covered by osteoblastic cells (curved arrows). Osteocityc cells within the newly formed bone (straight arrows)

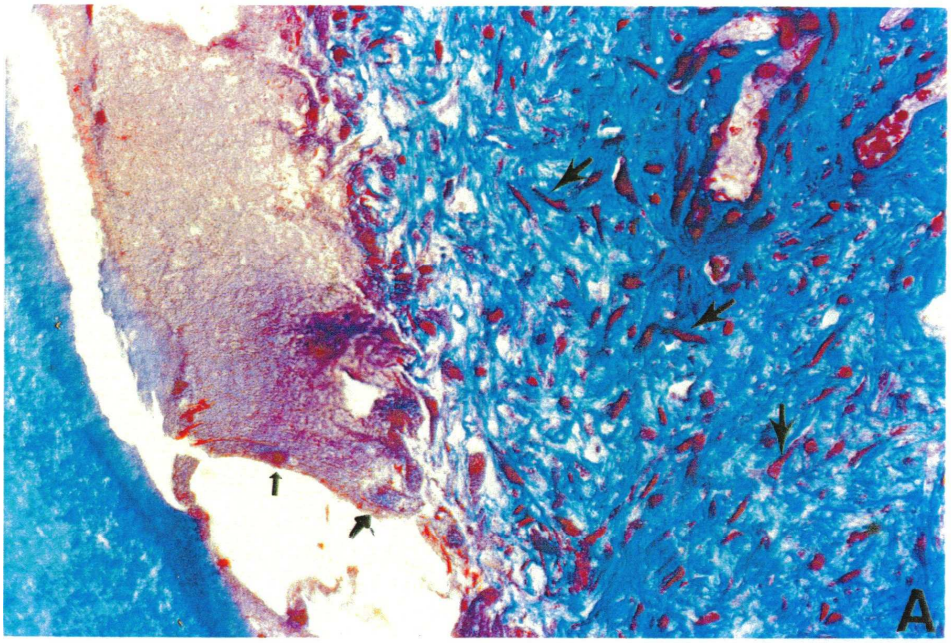
Original magnification X101

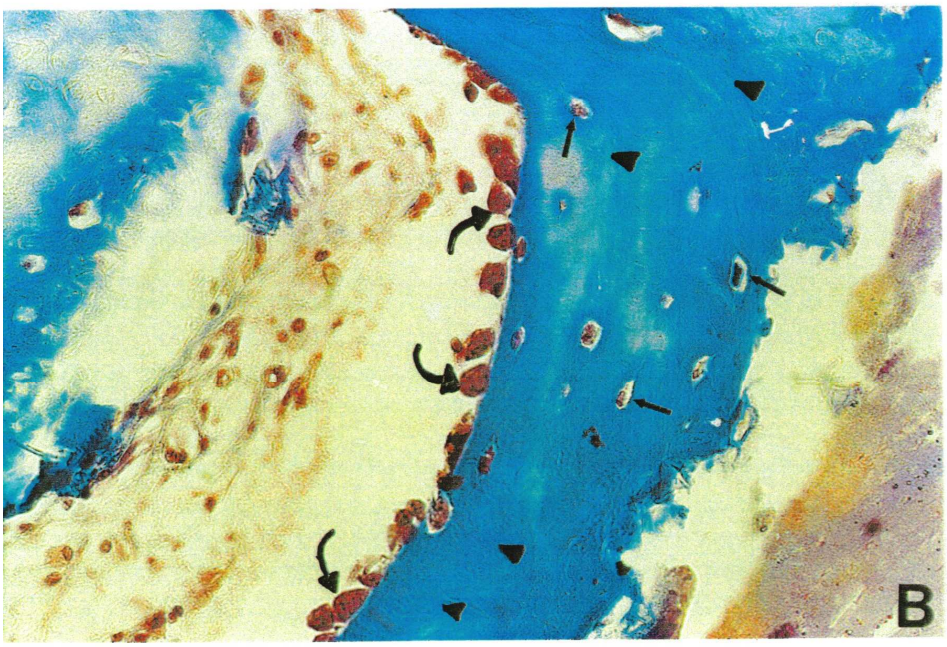
C: Type 3: Vascular invasion (pointy arrows) within collagen (in blue)

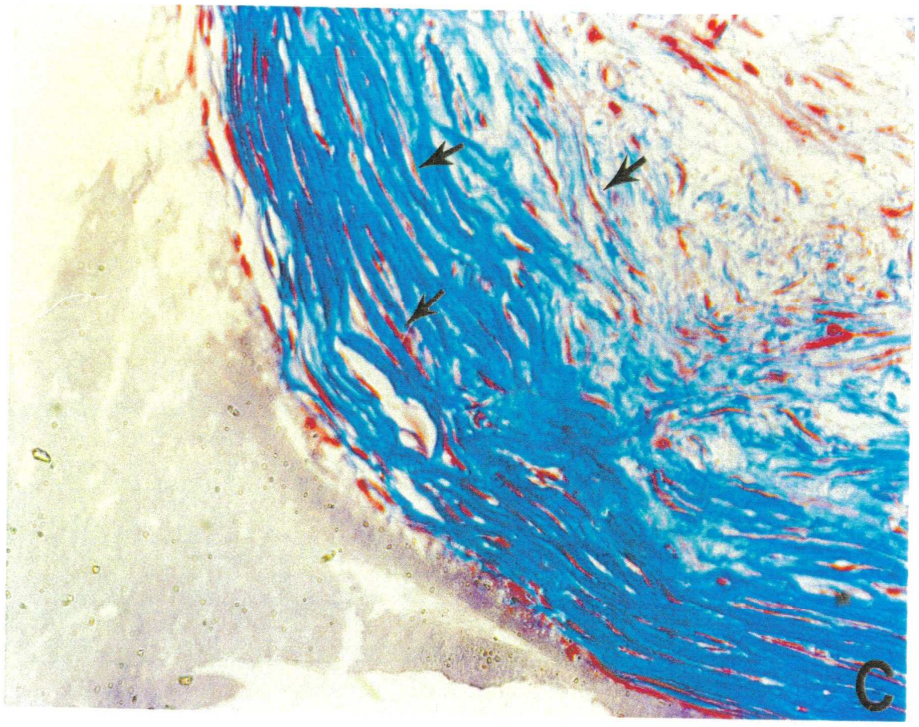
Original magnification X101

D: Type 4: Bone induction (arrow heads) in close attachment to substratum and covered by osteoblastic cells (curved arrows)

Original magnification X101


A


B


C

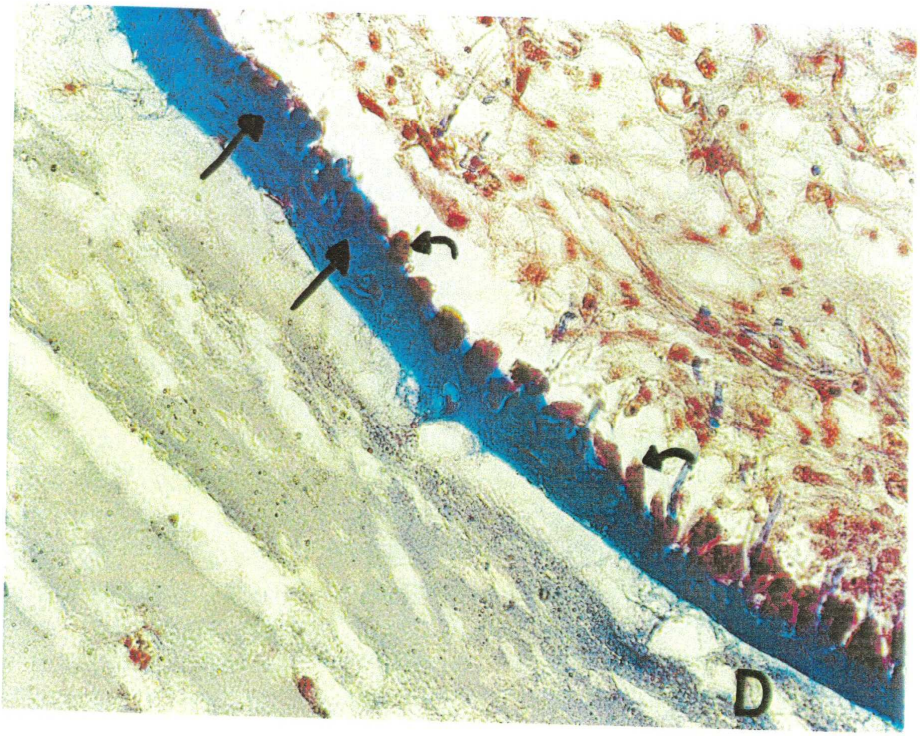
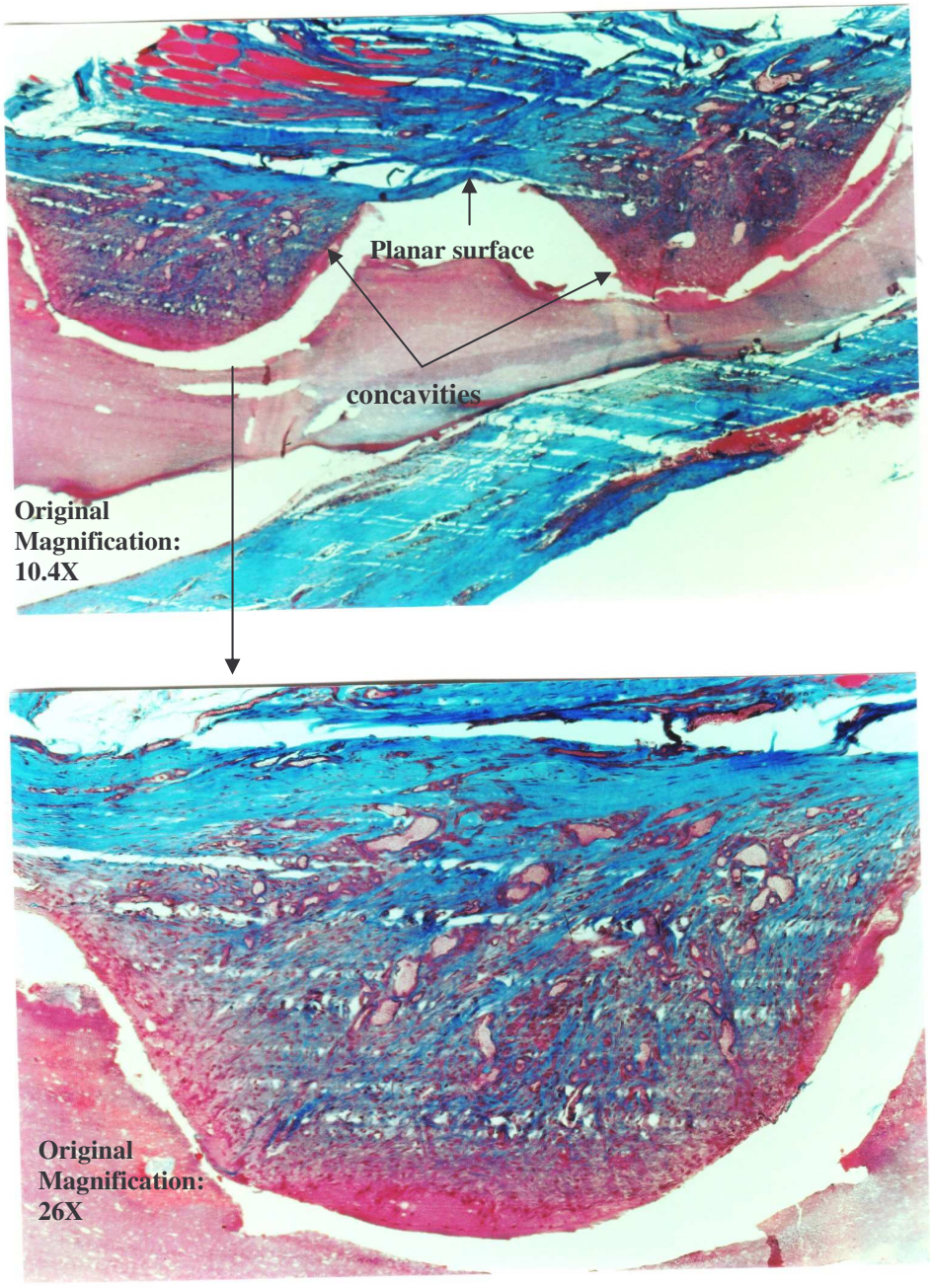
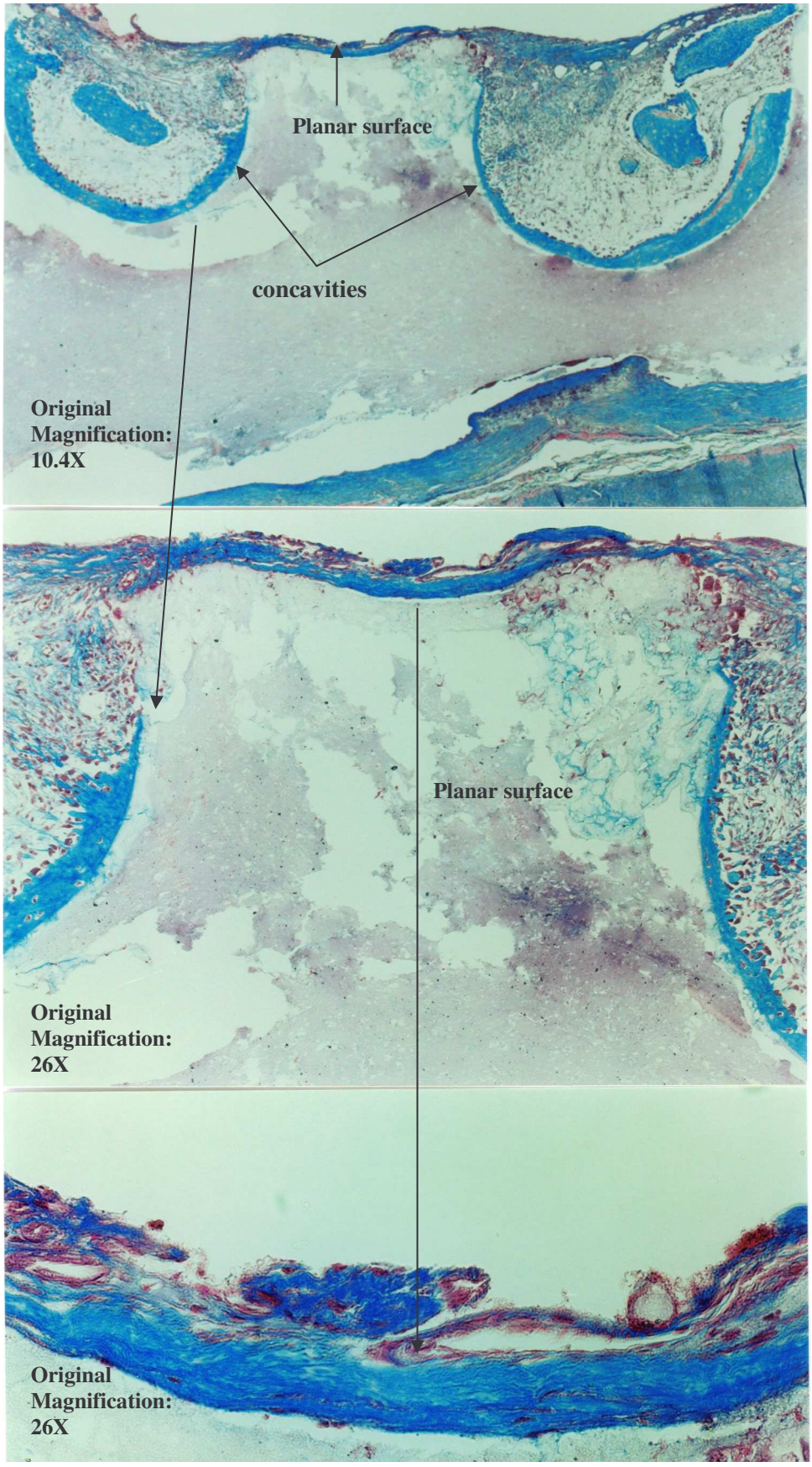

D

Figure 11:Low power photomicrographs of Types 1-4 (A-D) successively showing vascular invasion (A and C) within the concavities and newly formed bone (B and D) within the concavities

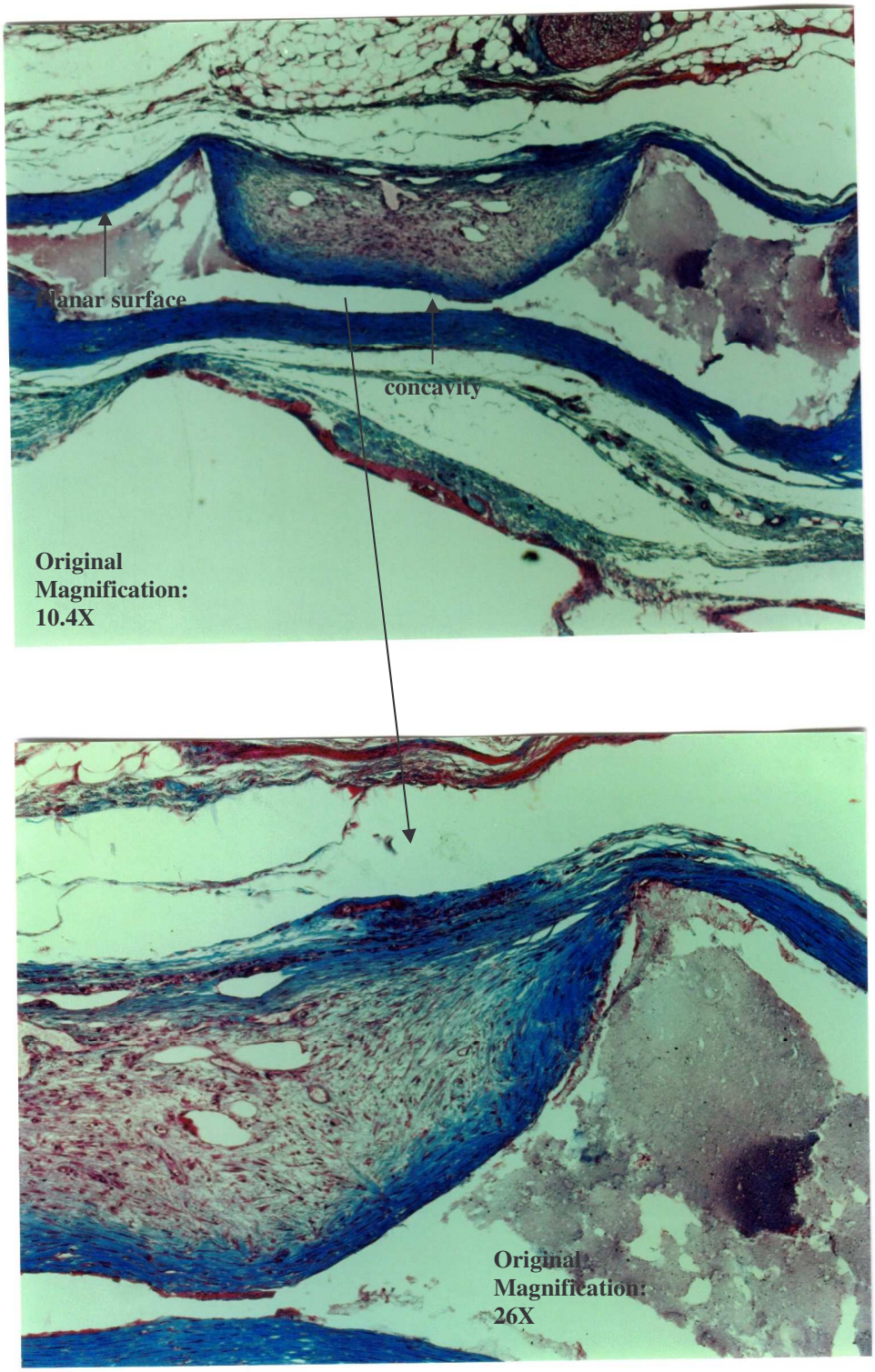
A



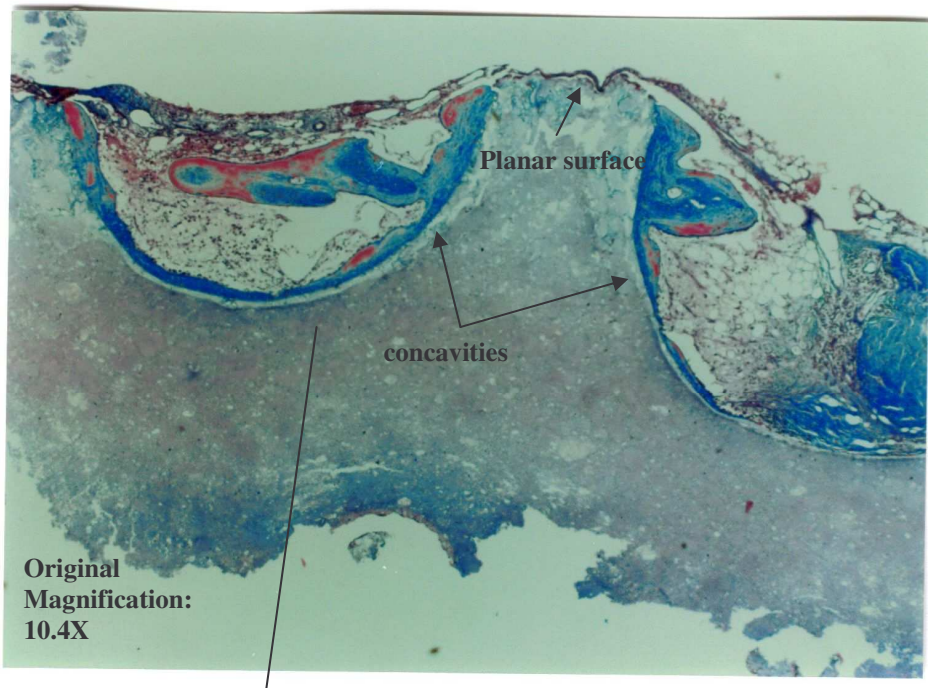
B


Planar surface
concavities
Original
Magnification:
10.4X
Planar surface
Original
Magnification:
26X
Original
Magnification:
26X

C


Planar surface
concavity
Original
Magnification:
10.4X
Original
Magnification:
26X

D


Planar surface
concavities
Original
Magnification:
10.4X

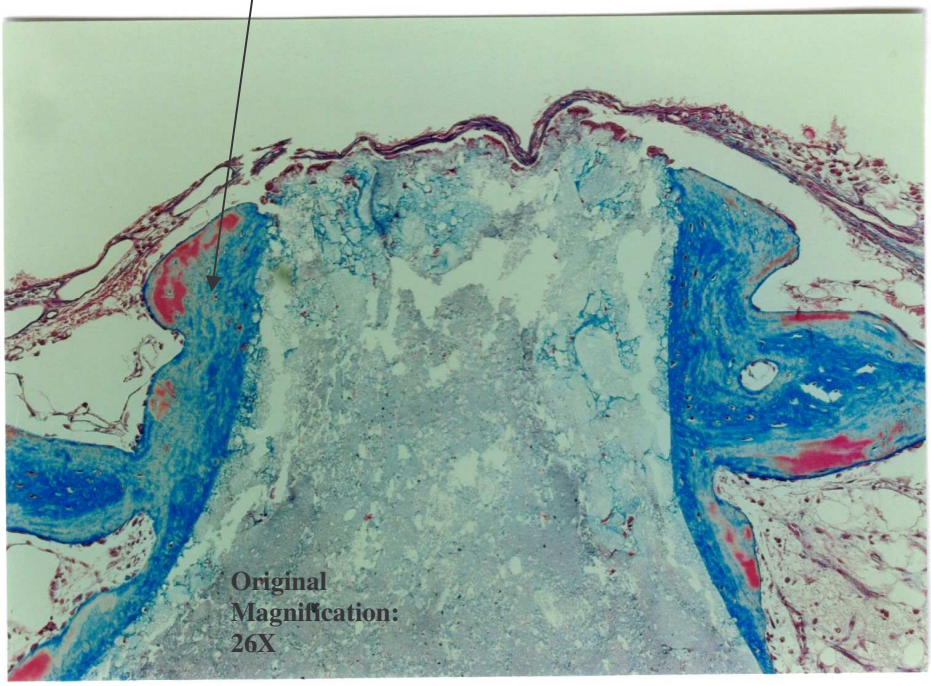
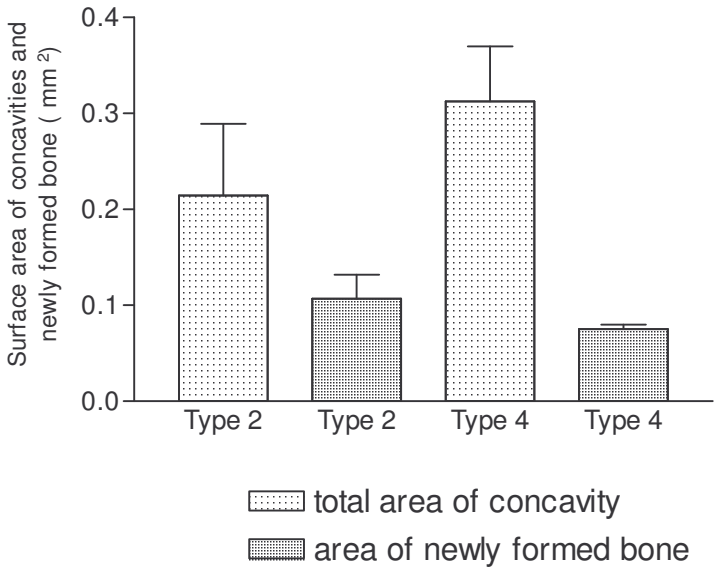

Original
Magnification:
26X

Figure 12. Surface area of newly formed bone

The histological sections of 90 days were analyzed to quantitate the percentage area of the newly formed bone in relation to the total surface area of the concavity.



180 days

Tissue morphogenesis in concavities of the substratum on day 180 after heterotopic implantation of Type 2 (A) and Type 4 (B) biomaterials.

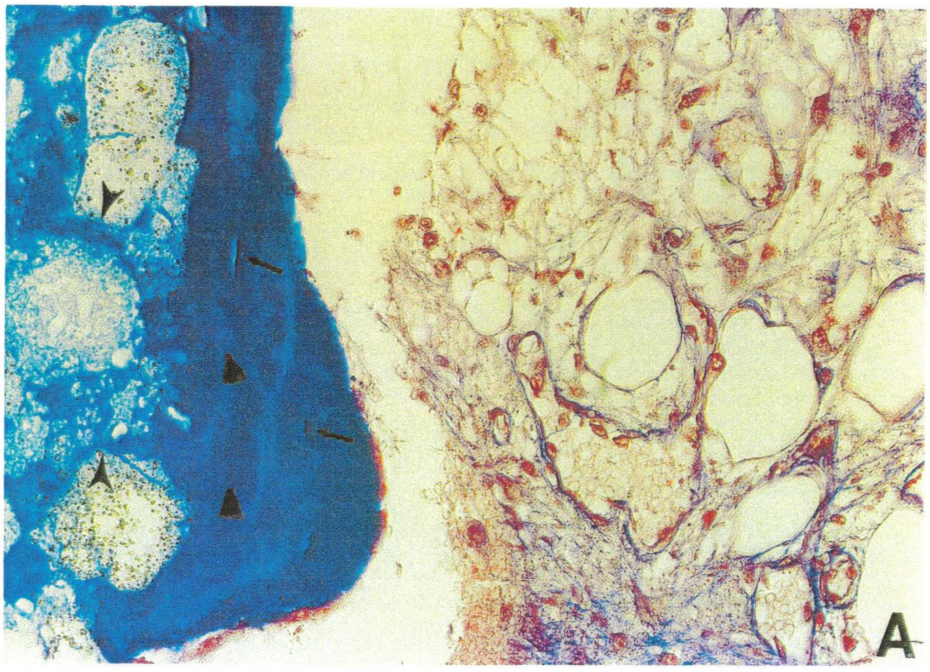
Figure 13: High power photomicrographs of tissues generated in the concavities of HA types 2 and 4 180 days postimplantation.

A: Newly formed bone attached to the substratum (arrow heads). Note Osteocytic cells within new bone (straight arrows) and invading tissue within the microporosity of the substratum (pointy arrow heads)

Original magnification: X101

B: Bone formation (arrow heads) and angiogenic sprouting (pointy arrows). Bone-like tissue invading the microporosity of the substratum (pointy arrow heads)

Original magnification: X101


A

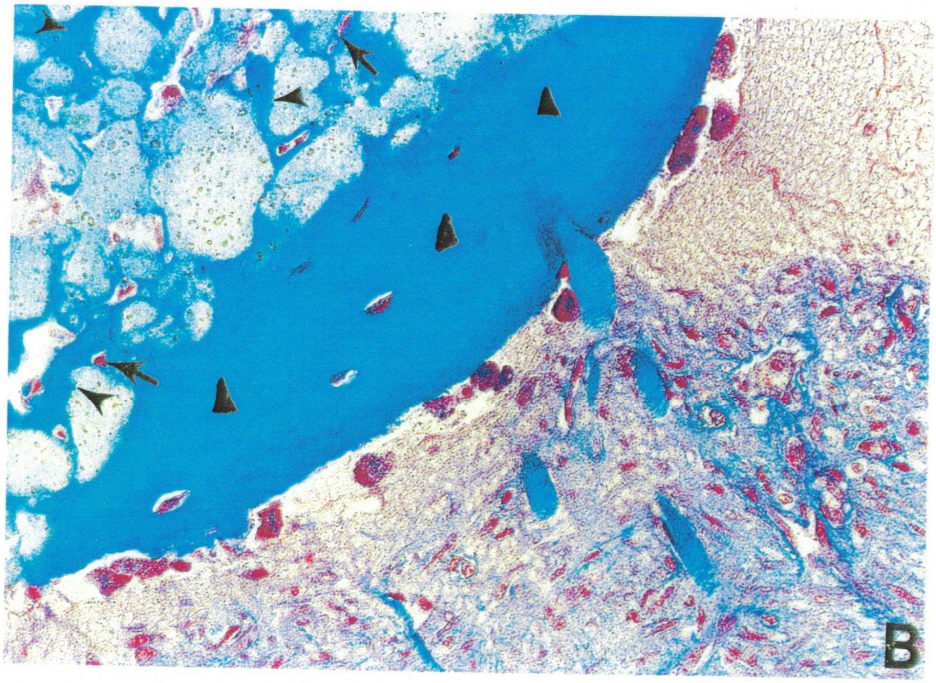
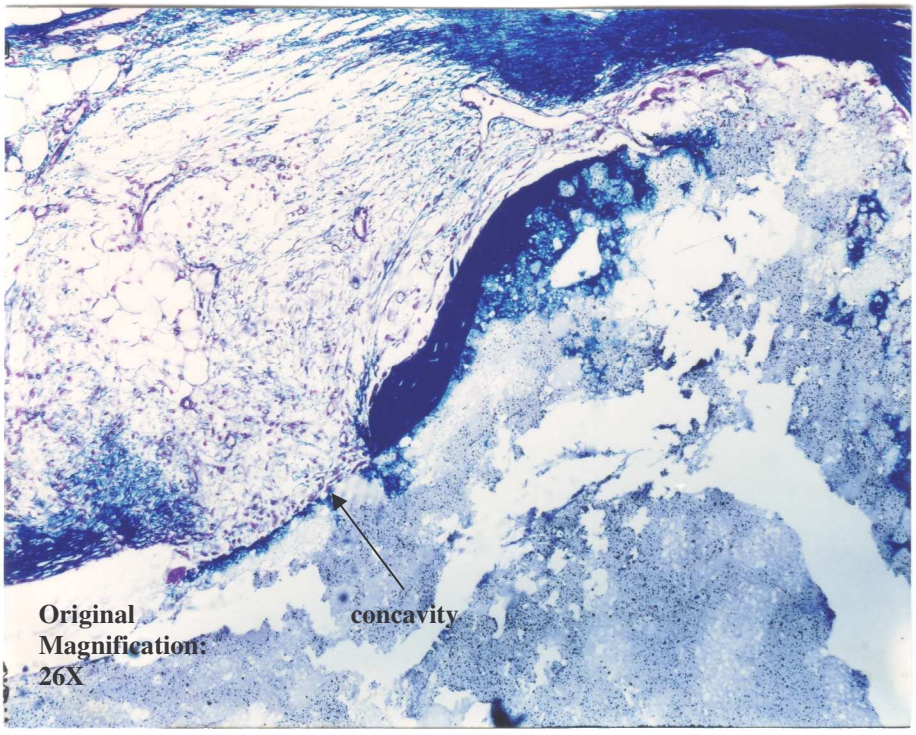

B

Figure 14: Low power photomicrographs showing newly formed bone within the concavities of tissues generated 180 days postimplantation:

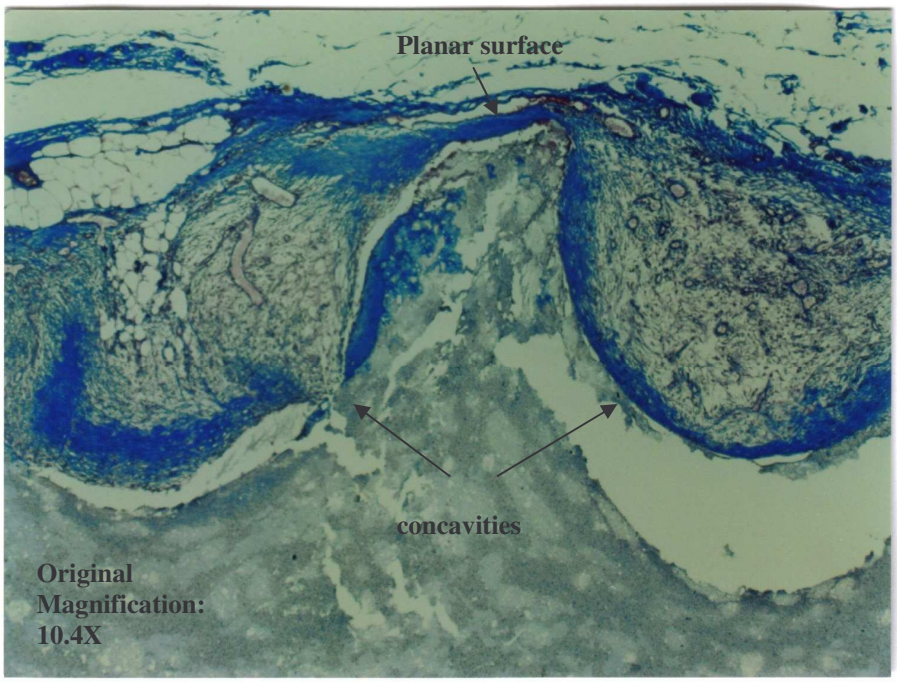
A: Type 2

B: Type 4

A



B


Planar surface
concavities
Original
Magnification:
10.4X

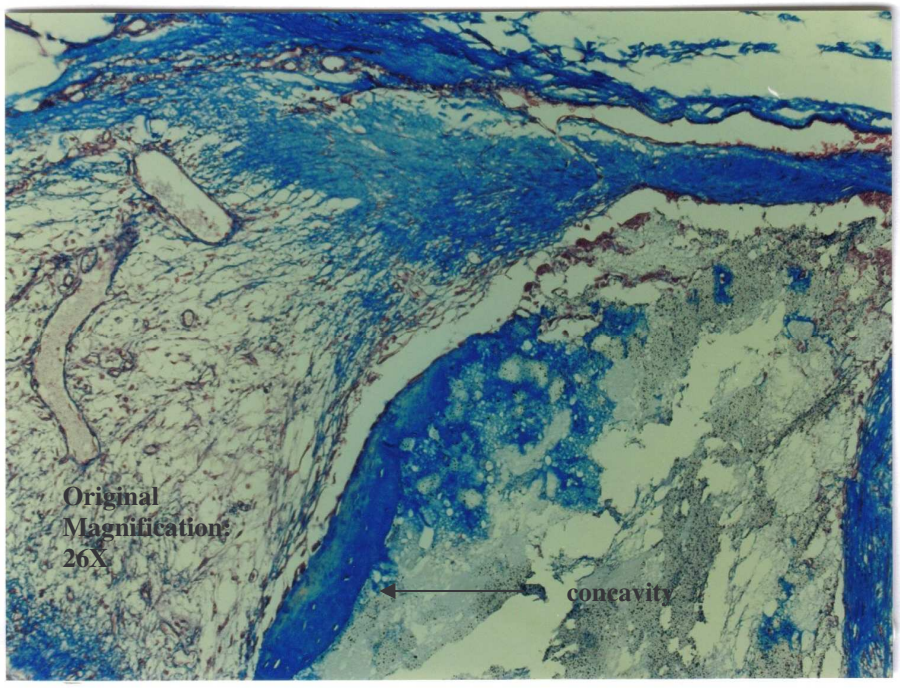

Original
Magnification:
26X
concavity

Figure 15: The histological sections of 180 days were analyzed to quantitate the percentage area of the newly formed bone in relation to the total surface area of the concavity.

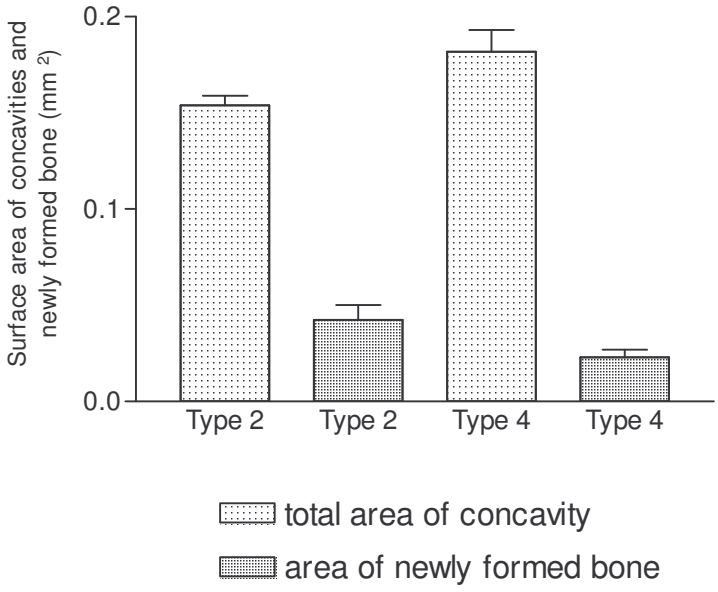
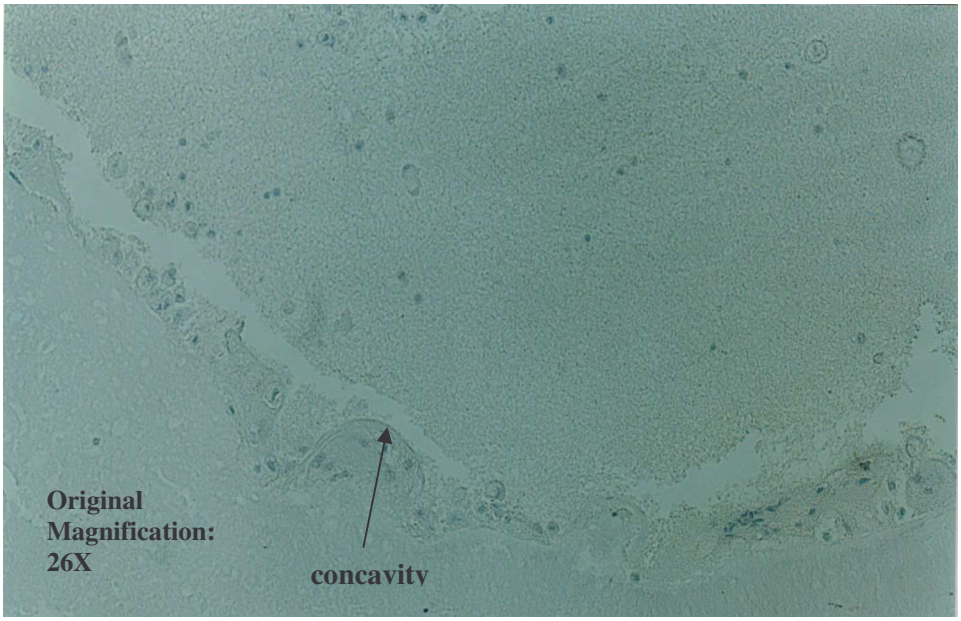


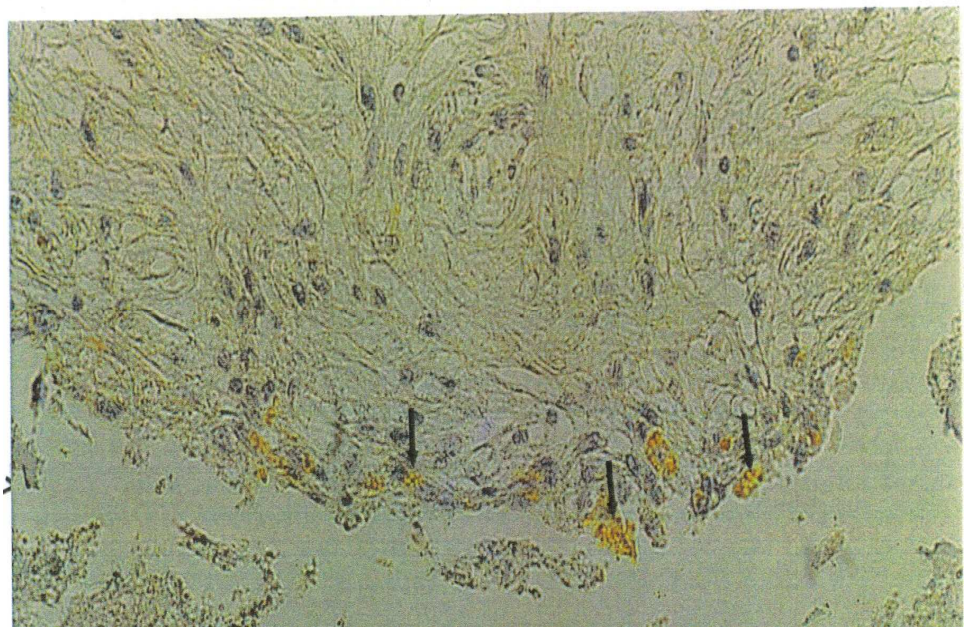
Figure 16. Immunolocalisation of BMP-3 and OP-1 in tissues generated within the concavities of Types 2 and 4 substrata on day 30 after heterotopic implantation.

A: OP-1 control



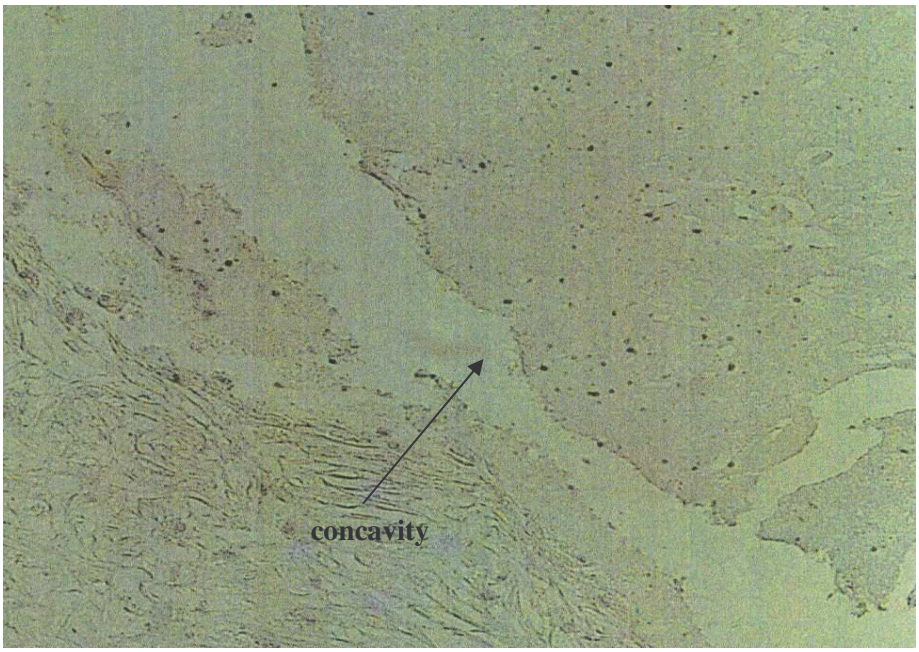
B: Immunolocalisation of OP-1 in sintered hydroxyapatite substratum but harvested from a different animal showing immunolocalisation prominently at the hydroxyapatite interface (arrows).

Original magnification X101



C: BMP-3 control

Original Magnification: X101



D: Immunolocalisation of BMP-3 in osteoblast-like cells predominantly immunolocalised at the substratum interface (arrows).

Original Magnification:X101

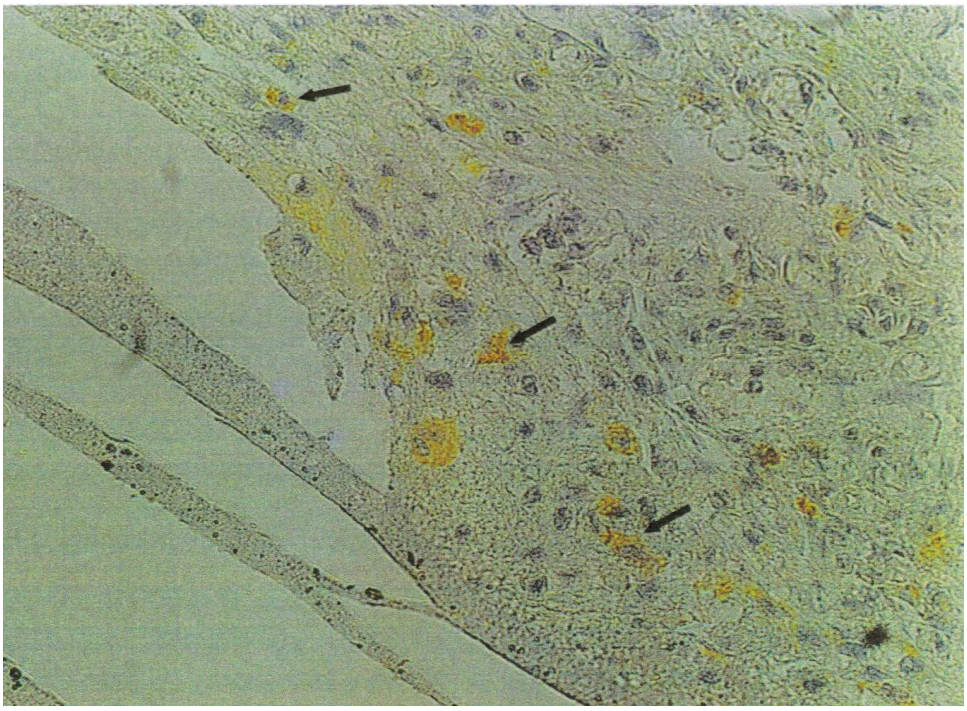


Figure 17. Immunolocalisation of BMP-3 and OP-1 in tissues generated within the concavities of Types 2 and 4 substrata on day 90 after heterotopic implantation.

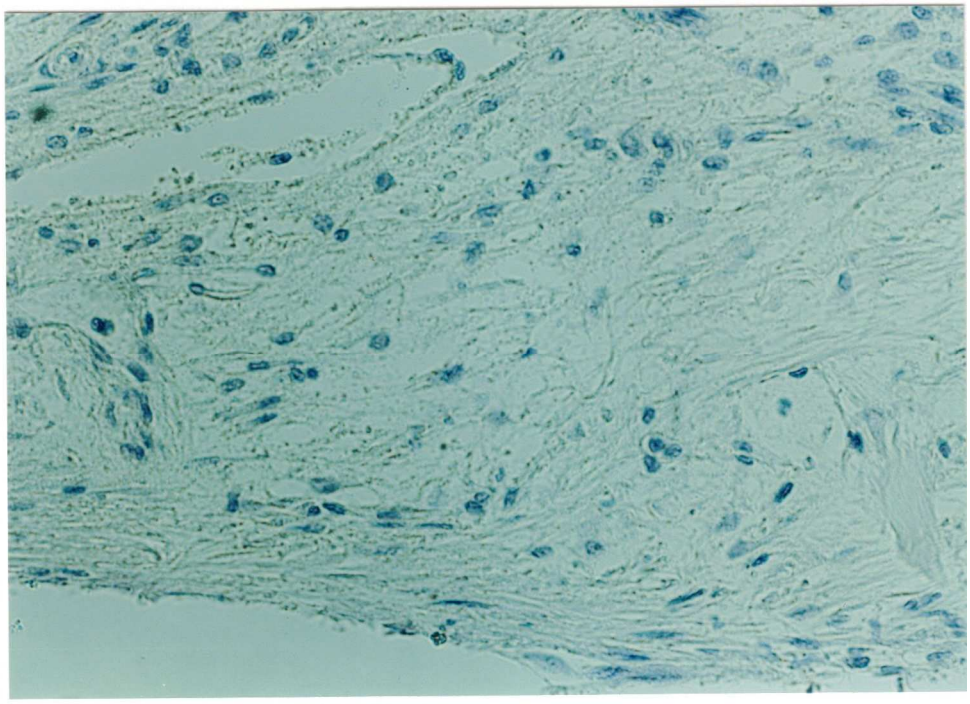
A: OP-1 Control

B: OP-1 imunolocalisation in osteoblast-like cells within the concavity (arrows)

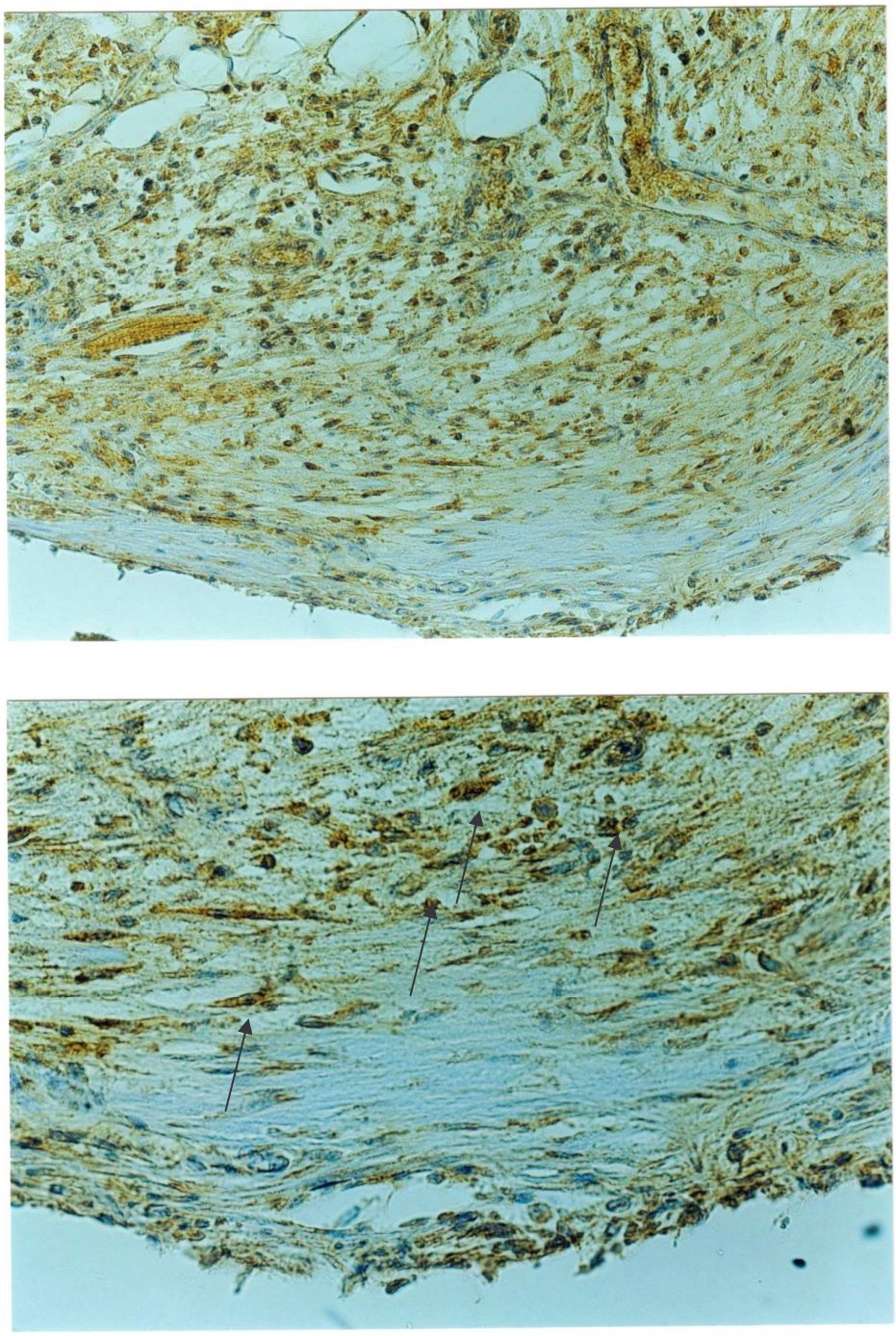
C: BMP-3 Control

D: BMP-3 immunolocalisation imunolocalisation in osteoblast-like cells within the concavity (arrows)

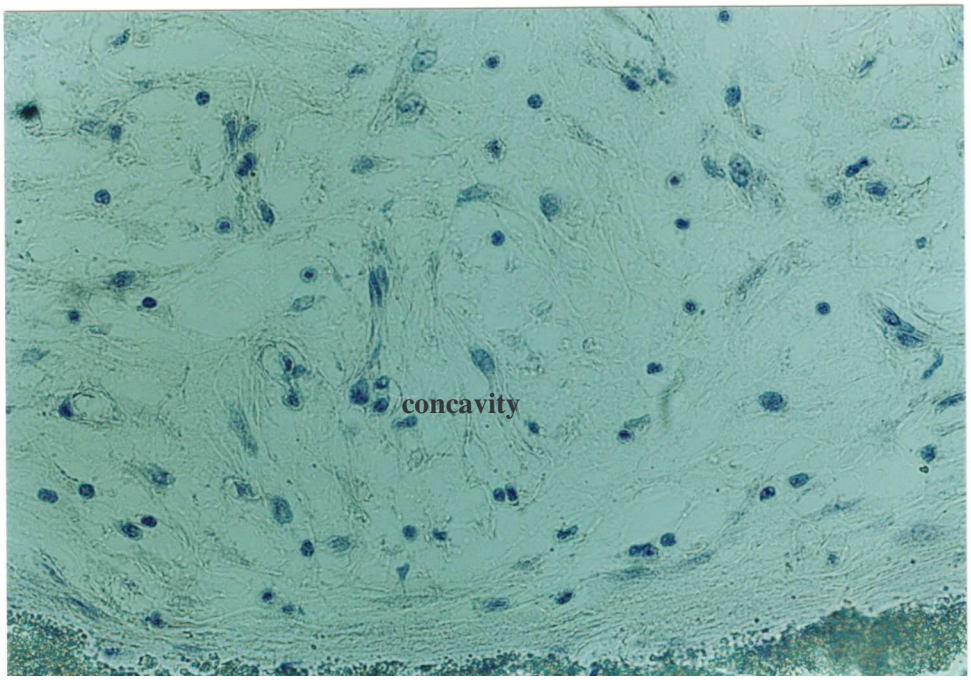
A



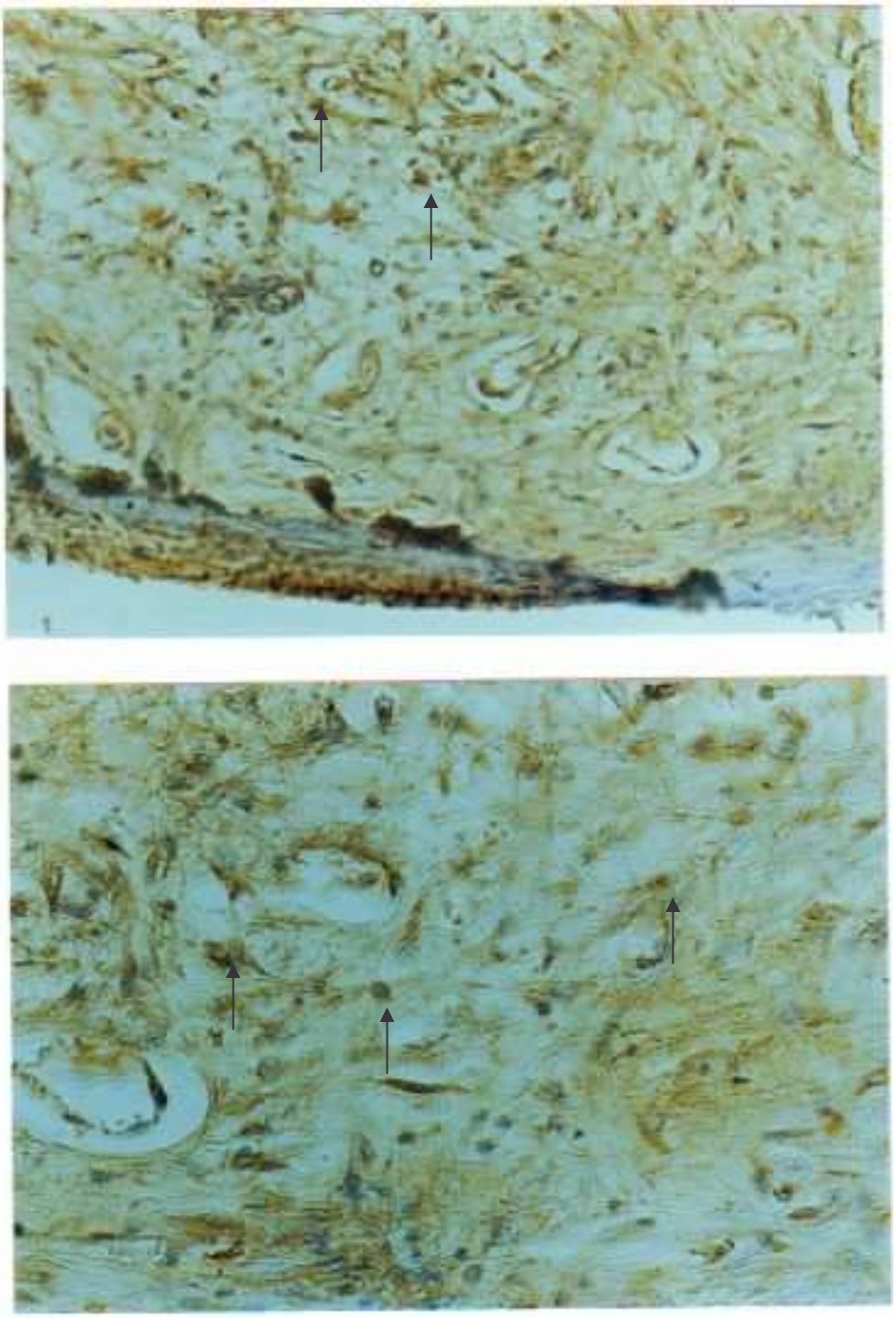
B



C



D



4.4 Northern Blot Analyses

Total RNA was extracted from pooled tissues and hybridized with radiolabelled (P32 alpha labeled) cDNA for OP-1, BMP-3, collagen type IV, collagen type II, TGF-β1 and gamma actin, as control. The results are shown in Table 1. Gamma actin was expressed strongly at 1.9 kilobases (kb) in all types of substrata on all time periods. Collagen type II and TGF-β1 were not expressed in all types of substrata on all time periods. Signal quantitation was performed using a gel documentation system (Gel Documentation and Analysis system, Syngene, U.K) (Matsaba *et al.*, 2001) and the results were normalized against gamma actin as percentages.

4.4.1 30 days implantation

mRNA analysis for OP-1 showed positive signals at 4.0 kb for all Types of substrata (Fig. 7 A and Table 1). However, the signal intensity was shown to be different between the different types with Type 2 showing the highest expression followed by Type 1. Type 3 showed a relatively higher expression of OP-1 than Type 4 though they are both resorbable. mRNA expression for BMP-3 was expressed at 3.0 kb and was relatively higher in Types 2 and 3 as compared to Types 1 and 4 (Fig. 7 A and Table 1). Type IV collagen, expressed as two bands, a minor one at 5.1 kb and a

major one at 4.0 kb was expressed relatively stronger in Type 2 and Type 3 as compared to Types 1 and 4. The presence of type IV collagen indicates an angiogenic response, which is a prerequisite for osteogenesis. Type II collagen and TGF-β1 mRNAs were not expressed (Table 1).

4.4.2 90 days implantation

Northern blot analysis of tissues generated within concavities of all 4 Types of substrata showed clear differences in the expression of OP-1: Types 1 and 4 displayed higher mRNA expression when compared to Types 2 and 3 (Fig. 7 B and Table 1). OP-1 was expressed at 4.0 kb. BMP-3 expressed at 3.0 kb was relatively strong in Type 1 through to Type 4 tissue samples (Fig. 7 B and Table 1). Collagen type IV was relatively strongly expressed at 5.1kb and 4.0 kb though differently between the different substrata types (Fig. 7 B and Table 1).There was no expression of collagen type II and TGF-β1 (Table 1).

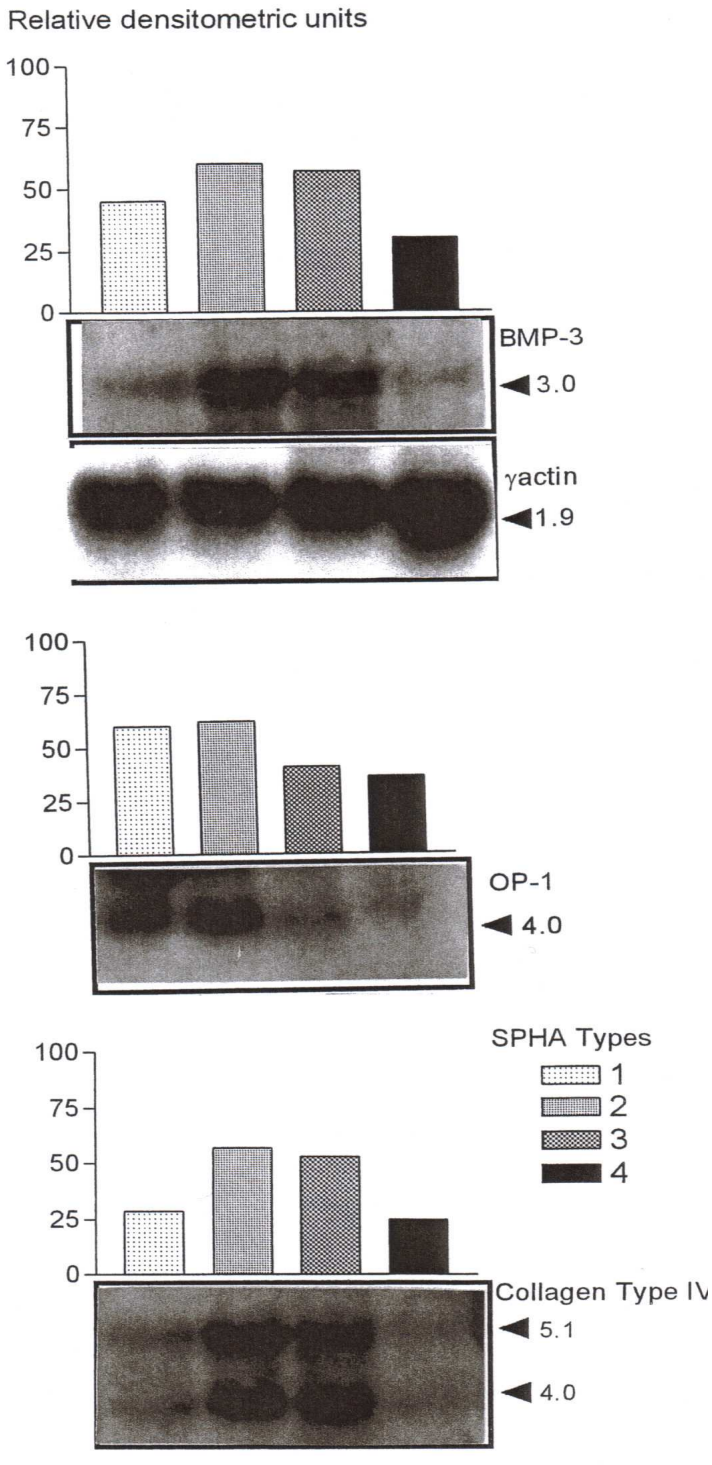
4.4.3 180 days implantation

Northern blot analysis showed a relatively low expression of OP-1 at 4.0 kb in tissues generated in the concavities of both Type 2 and Type 4 (Fig. 7 C and Table 1). There was no expression of BMP-3 in tissues generated from both substrata. Collagen type IV

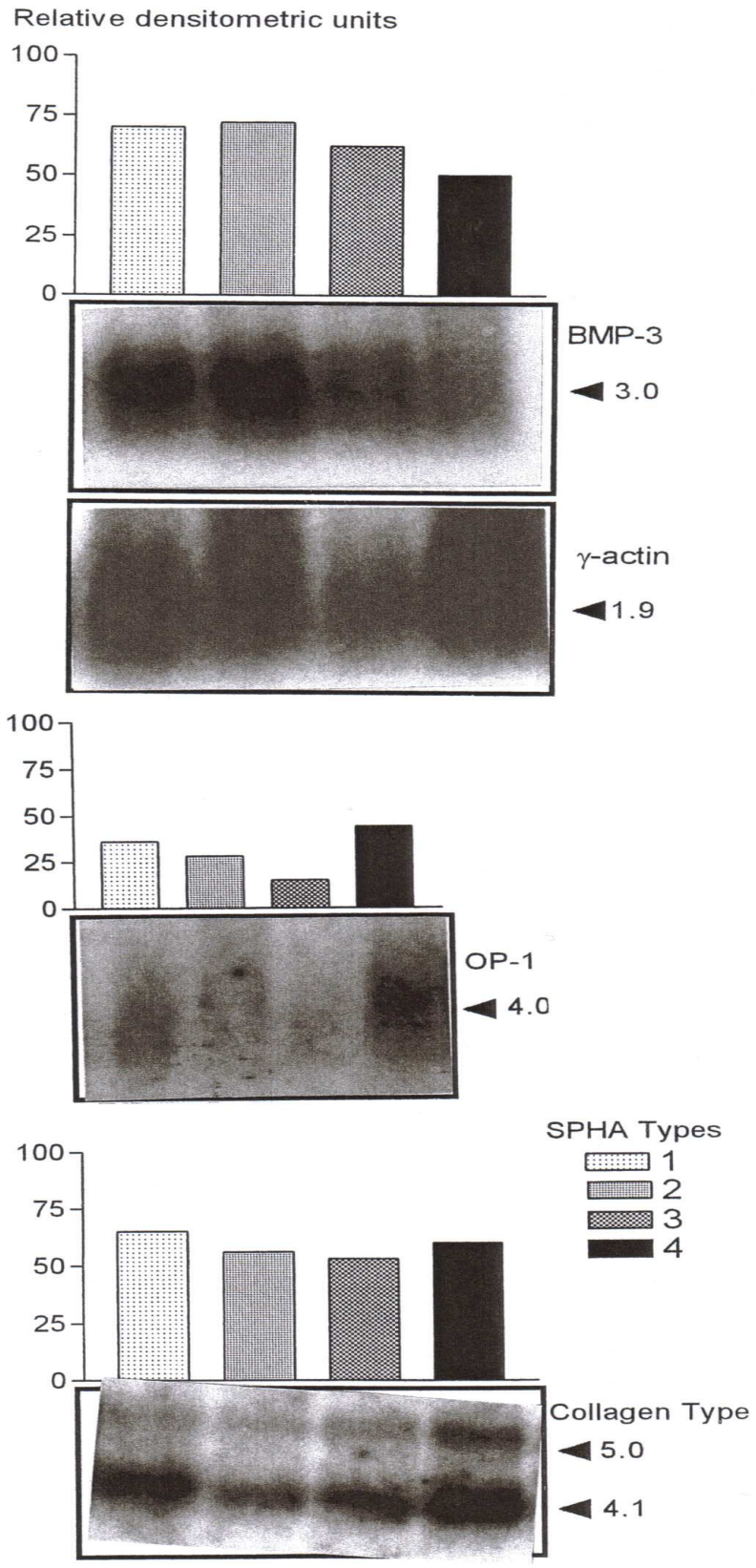
was expressed relatively strong at both 5.1 and 4.0 kb in both tissues generated from both samples (Fig. 7 C and Table 1). There was no expression of Collagen type II and TGFß1.

Figure 18. Northern analysis of mRNA expression of OP-1, BMP-3 and collagen type IV in harvested tissue generated within the concavities of four different types of hydroxyapatite substrata on days 30 (**A**) and 90 (**B**) postimplantation. (N=6) The γ-actin signals were used as standards for size determination and the mRNA levels were normalized against them and expressed as relative densitometric units. On 180 days (**C**) only Types 2 and 4 were implanted (N=4).

A


Relative densitometric units
100
75
50
25
0
BMP-3
3.0
γactin
1.9
100
75
50
25
0
OP-1
4.0
SPHA Types
1
2
3
4
100
75
50
25
0
Collagen Type IV
5.1
4.0

B


Relative densitometric units
100
75
50
25
0
BMP-3
3.0
γ-actin
1.9
100
75
50
25
0
OP-1
4.0
SPHA Types
1
2
3
4
100
75
50
25
0
Collagen Type
5.0
4.1

C

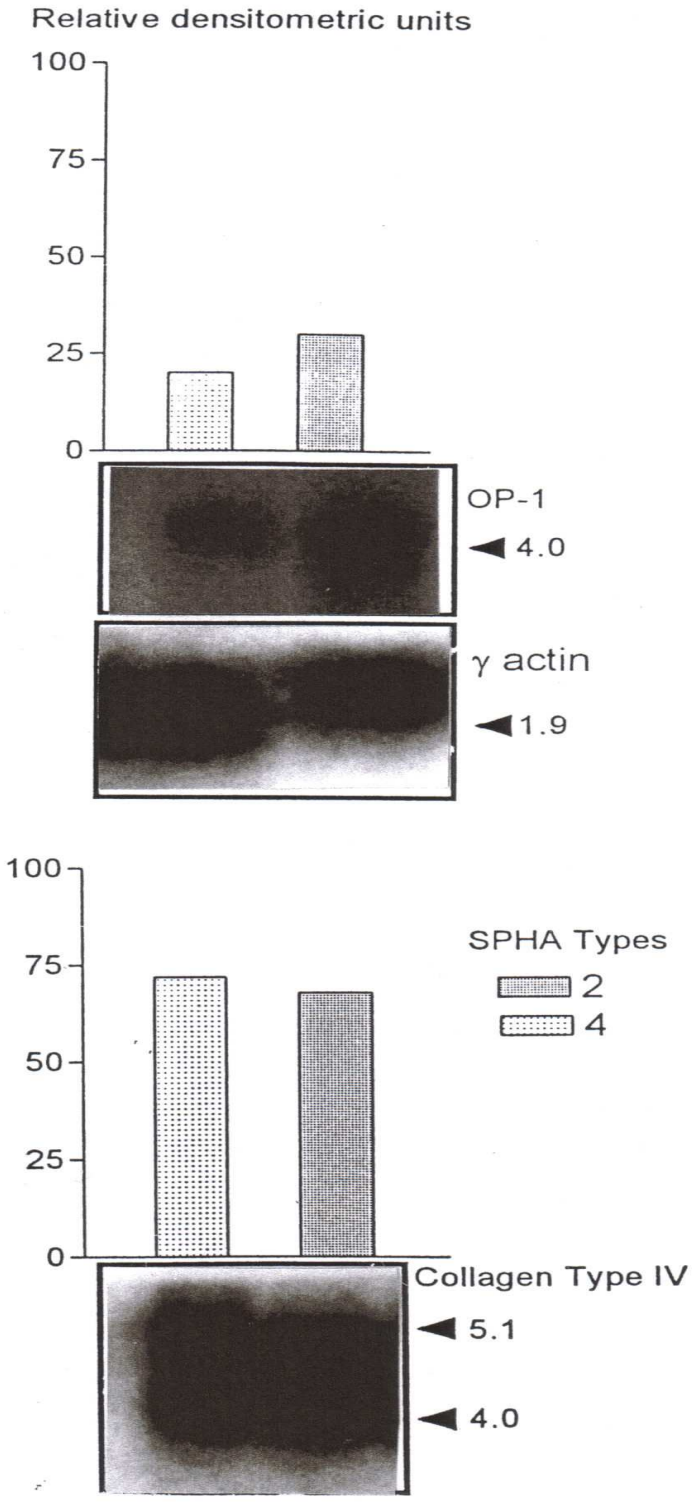

Relative densitometric units
100
75
50
25
0
OP-1
4.0
γ actin
1.9
100
75
50
25
0
SPHA Types
2
4
Collagen Type IV
5.1
4.0

Table 1:Summary of results

	Type 1	**Type 2**	Type 3	**Type 4**
Features	HA (fine) (1 micron size)	HA (coarse) (>1 micron size)	HA/ fine TCP (<100 micron size)	HA/discrete TCP (100-300 micron size)
Post-implantation findings				
30 days				
HISTOLOGY	-	-	-	-
ALKALINE PHOSPHATASE ACTIVITY	X	X	X	X
IMMUNOHISTOCHEMISTRY	-	X (BMP-3 and OP-1)	-	X (BMP- and OP-1)
NORTHERN BLOTS				
OP-1	X	X	X	X
BMP-3	X	X	X	X
Collagen IV	X	X	X	X
Collagen II	-	-	-	-
TGF-beta 1	-	-	-	-

90 days				
HISTO	No bone	X	No bone	X
ALP	X	X	X	X
NORTHERN BLOTS				
OP-1	X	X	X	X
BMP-3	X	X	X	X
Collagen IV	X	X	X	X
Collagen II	-	-	-	-
TGF-beta 1	-	-	-	-
180 days				
HISTO	Not implanted	X	Not implanted	X
ALK P	Not implanted	X	Not implanted	X
NORTHERN BLOTS				
OP-1	-	X	-	X
BMP-3	-	X	-	X
Collagen IV	-	X	-	X
Collagen II	-	-	-	-
TGF-beta 1	-	-	-	-

X= (expression) - = (no expression)

Table2: Intensity of mRNA expression for the probes OP-1, BMP-3, Collagen IV, Collagen II, and TGF-ß1

TIME		30 DAYS				90 DAYS				180 DAYS	
HA		1	2	3	4	1	2	3	4	2	4
	Probes										
	OP-1	++	++	++	++	+	+	+	++	+	+
	BMP-3	++	++	++	+	+++	+++	++	++	-	-
	Collagen IV	+	++	++	+	++	++	++	++	+++	++
	Collagen II	-	-	-	-	-	-	-	-	-	-
	TGF-ß1	-	-	-	-	-	-	-	-	-	-

Key:
- : no expression
+: low expression
++: moderate expression
+++: High expression

5.0 Discussion

The molecular and cellular signals that trigger heterotopic osteoinduction in porous hydroxyapatite implanted in primates are still not well understood. The present study sheds insights into the spontaneous induction of bone formation within the concavities of hydroxyapatite discs. A process referred to as geometric induction of bone formation.

In this study the term geometry refers to concavities of two different dimensions (as described in the materials and methods), which act as microenvironment for induction of bone. The sizes of the concavities were different (figures 1A and 2) to determine the suitable diameter for formation of bone. The presence of bone was observed within the bigger concavities.

Ripamonti *et al*. (1999) reported that the geometry of the HA substratum plays a critical role in spontaneous induction of bone formation. The authors also reported that there was bone formation within the concavities of their biomaterials and that the presence of BMPs as evaluated by immunolocalisation at the interface of the biomaterial suggested two possibilities;

1. BMPs may be secreted from the circulation, adsorbed onto the hydroxyapatite substratum and induce bone as a secondary response.
2. The BMPs may be locally expressed within the concavities and induce bone formation.

It is against this background that the present study was performed, to investigate the two possibilities.

Four different types of substrata were used in this study, where the physical distribution of the co-existing phases was manipulated resulting in different compositions and properties of the final substrata to be implanted. Briefly, types 1 and 2 ceramics were phase pure hydroxyapatite (HA) discs with type 1 prepared from a commercial powder (Plasma Biotal). The Type 2 material was prepared by a solid state reaction between Merck tri-calciumphosphate and calcium with a Ca/P molar ratio of 1.67. Types 3 and 4 samples consisted of a mixture of HA and TCP in the ratio 2:1. The same HA starting powder that was used in type 2 biomaterials was also used in types 3 and 4. The microporosity of the bulk material of each HA sample was as follows: type 1: 39%, type 2: 40%, type 3: 38%, type 4: 37%. The porosity was determined using Archimedes principle as discussed in materials and methods.

Significant differences between the implants were particle size and distribution of the starting powders. The use of relatively fine particles (1 micron) of hydroxyapatite starting powder (Type 1) as opposed to a highly crystalline, coarsened (>1 microns) hydroxyapatite powder (Type 2), or a fine distribution (<100 microns) of TCP in hydroxyapatite matrix (Type 3) as opposed to discreet (100-300 microns) zones of TCP in hydroxyapatite matrix (Type 4) both produced from highly crystalline coarsened powders (Thomas *et al.*, 2003). Phase composition and structure were verified by XRD, FT-IR and SEM.

The XRDs show that all the HA discs (types 1-4) are phase pure, that is, there is only HA (types 1 and 2) or HA and TCP (types 3 and 4) (figure 5 A-D) in the specified discs. The SEMs show the microstructure of the samples (figure 4 A-D). The FTIR show that the high temperature processing conditions did not affect the bonding groups in the HA (OH groups on the HA are intact) (figure 6).

The HA implants were harvested at 30, 90 (types 1-4) and 180 (types 2 and 4) days post-implantation and the induction of bone elicited by the implants was examined using alkaline phosphatase

activity (figure 7), histology (figure 8), and Northern Blots (figure 18) at each time period. Immunohistochemistry was perfomed at 30 days post-implantation to determine the presence of BMPs within the concavities. Alkaline phosphatase activity was used as a marker for bone formation, histological analyses was performed to confirm the osteogenic activity imparted by the biomaterials and northern blots were performed to determine whether the proteins were produced in the concavities or if they are adsorbed from the endogenously circulating proteins.

At 30 days alkaline phosphatase activity was low in the tissues generated by all the four types of substrata ranging from 0.22 units per milligram protein to 0.24 units per milligram protein (figure 7A). There were no significant differences (5%) between alkaline phosphatase activity within the tissues in all four samples implanted.

At 90 days postimplantation, alkaline phosphatase activity was generally low in the tissues generated by all the four types of substrata. The minimum expression was 0.07 units per milligram protein while the maximum expression was 0.27 units per milligram protein (figure 7B). There were no significant (5%)

differences between alkaline phosphatase activity within the tissues in all four biomaterials implanted.

Tissues from both types 2 and 4 showed a relatively low activity with no significant difference (5%) between each other (figure 7C). The minimum activity expressed was 0.05 units per milligram protein and the maximum activity was 0.09 units per milligram protein.

Comparatively, there was no significant difference between alkaline phosphatase activity expressed by tissues generated by Type 1 samples at 30 days and 90 days. Type 2 samples at 30 and 90 days showed a significantly higher amount of alkaline phosphatase at 5% probability level compared to 180 days. Alkaline phosphatase. has been documented as a marker of bone formation (Reddi and Huggins). The authors also reported that alkaline phosphatase activity is low during early bone formation, increases with increase in bone formation then decreases during bone marrow formation.

Histological analyses showed condensed fibrovascular tissue and collagenic material within the concavities of all the four types of HA substrata at 30 days postimplantation (figure 8). Studies by

Ripamonti and Ripamonti *et al*. on porous hydroxyapatite harvested at one month (Ripamonti *et al.,* 1992b), two months (Ripamonti *et al.,* 1993), three months (Ripamonti, 1991; 1996), six months and nine months (Ripamonti, 1991) showed that bone differentiation in porous hydroxyapatite occurs by day 60 after implantation.

The other important observation within the concavities of all harvested HA biomaterials at 30 days was angiogenesis (figure 8). Angiogenesis, which refers to the sprouting of blood vessels from existing ones, as well as vascular invasion, was a prominent histological feature in this study as shown in histology photomicrographs in the results section (figure 8 A-D and figure10A and C). Sprouting blood vessels play a critical role in bone formation because blood is important for delivering oxygen, nutrients and BMPs/OPs to the site of induction (Reddi, 2000; Gerber and Ferrare, 2000; Colnot and Helms, 2001).

The observed angiogenesis within the concavities of the substrata in this study indicate that the specific geometry of the substrata induce vessel ingrowth and capillary sprouting within the mesenchymal tissue that penetrates the porous spaces eventually leading to bone induction. Ripamonti *et al.* (1993) reported data

suggesting that osteogenetic vessels as defined by Trueta (1963) might provide a temporally regulated flow of cell populations that can express the osteogenic phenotype (Ripamonti *et al*., 1999; Ripamonti *et al*., 1993).

Histological examination showed that bone differentiation was localized within the concavities of the substrata and not on the planar surfaces as shown in the photomicrographs of types 2 and 4 in the results section (figure 11 B and D). Modified Goldner's Trichome stain was used to identify bone tissue. With this method bone tissue stains blue on decalcified sections as matrix with lacunae filled by osteocytic cells and often but not always, has osteoblastic cells facing the highly vascularised matrix of the connective tissue. Only HA types 2 and 4 samples induced bone formation at 90 days while sample types 1 and 3 did not show any bone formation at this time period but showed angiogenesis (figures 10 B and D and 11 B and D).

The amount of newly formed bone in type 2 concavities reached 58.2 % while that generated in type 4 reached 28.2 % 90 days postimplantation (figure 12). The amount of newly formed bone was calculated as described in the materials and methods. Newly

formed bone was measured as new bone area in relation to the total area of the concavity in mm^2.

A 180 days postimplantation bone formation was observed in both HA types 2 and 4. The amount of newly formed bone reached 23% in type 2 and 10 % in type 4 (figure15). Angiogenesis was also observed within the concavities (figures 13 and 14).

Immunohistochemistry showed expression of BMP-3 and OP-1 within the concavities in HA types 2 and 4, suggesting the presence of BMPs within the concavities at 30 days post implantation (figure 16). This result agrees with the results of Ripamonti *et al*. (1999) where the authors also suggested the presense of BMPs within the concavities of biomaterials at 30 days post-implantation. OP-1 and BMP-3 were also localised within the concavities 90 days postimplantation (figure 17). However due to the limitations of the technique used, there was some non-specific staining within the concavities as well.

The question remains as to why no bone formation was observed within the concavities of HA types 1 and 3 at 90 days post-implantation. The results suggest that particle size and distribution of the starting powders may have played a critical role

in the induction of bone formation. As has been mentioned, the differences between types 1, 2, 3 and 4 HAs was particle size and distribution of the starting powders. Types 1 and 3, which were both made of fine particles of starting powders did not show any bone formation even in the presence of BMPs. Types 2 and 4 biomaterials, which were both made of coarse starting powders, showed bone formation at 90 days post-implantation.

These results suggest that particle size may play an important role in bone formation.

Complementary DNA (cDNA) probes namely, BMP-3, OP-1, Collagen type II, Collagen type IV and TGF-β1 were used to study gene expression of markers of bone formation. The results showed clear differences in gene expression of the specific markers of bone formation, i.e BMP-3 and OP-1 mRNA expression (figure18). Collagen type IV, a marker for angiogenesis was also expressed (figure 18). Collagen type II and TGF-β1 were not expressed at all time periods in all biomaterials.

OP-1 and BMP-3 expression were observed. OP-1 mRNA was expressed moderately by all types 1-4 biomaterials while BMP-3 mRNA was expressed moderately by types 1-3 and relatively lower by type 4 (figure18). Collagen type IV was expressed

moderately by types 2 and 3 and low by types 1 and 4. Collagen type II and

TGF- β1 were not expressed in all HA types (table 1).

OP-1 expression was relatively low in HA types 1-3 and moderate in type 4 (figures). BMP-3 expression was relatively high in types 1and 2 and moderate in types 3 and 4. Collagen type IV as relatively moderate in all types 1-4 (figure 18). Collagen type IV and TGF-ß1 were not expressed in all HA types (table 1).

There was no expression of BMP-3 mRNA in both HA types 2 and 4. OP-1 mRNA expression was low in both HA types 2 and 4. Collagen type IV mRNA expression was relatively high while Collagen type II and TGF-ß1 mRNAs were not expressed.

Generally, the expression of OP-1 and Collagen type IV was similar both at 90 and 180 days though it differed at 30 days (figures). BMP-3 expression was seen only at 30 days and 90 days, not 180 days (figures). OP-1 was relatively high at 30 days, moderate at 90 days and high at 180 days (figure 18). Collagen type IV was expressed at all time periods and in all types of HA implanted; moderate at 30 days and high at 90 and 180 days (figure 18). This result supports the histological results of all HA

types implanted at all 3 time periods where angiogenesis was one of the major observations (figure 18).

There is a disparity between the histological results and the northern blot results. The northern blot results show expression of BMPs in all types of HA implanted at all time periods (figure18) and yet histologically HA types 1 and 3 did not induce any bone formation at 90 days (figures 9 and 10) and all types 1-4 did not induce bone formation at 30 days. Further studies need to be done to investigate this disparity.

The expression of collagen type IV (figures), which is a major component of basement membranes (Paralkar *et al*., 1990), could give insights towards understanding the morphological evidence of angiogenesis localized in the mesenchymal tissue invading the concavities of the substrata. Angiogenesis is a pivotal event in bone development and in adult bone repair. In both situations, blood vessels grow into hypertrophic cartilage and erode it to produce a scaffold on which osteoblasts settle to produce bone. This vascular response is essential for normal bone formation and bone repair.

There may be other factors that may have inhibited bone formation within the concavities of all HA types at 30 days as well as types 1 and 3 at 90 days even in the presence of BMP expression. This may be explained in further studies into the mechanism of spontaneous induction of bone by HA biomaterials. Expression of BMPs in the absence of bone formation has been reported (Autzen *et al*., 1998; Barnes *et al*., 1995; Hatakeyama *et al*., 1997; Clement *et al*., 1999).

The biomaterials cascade of bone formation involves invasion of the concavities by capillaries resulting in angiogenesis, followed by attachment of mesenchymal cells to the substrata which lead to differentiation of osteoblast-like cells and finally, expression of BMPs/OPs and induction of bone formation. Collagen type II and TGF-β1 were not expressed. Collagen type II is a marker of chondrogenesis, and hence was not expressed suggesting that the cascade of bone formation in this study was intramembranous.

The geometry of the substratum may play a part in initiating a microenvironment that is angiogenic hence conducive for induction of bone in the presence of BMPs within the concavity at a certain time period as shown by HA types 2 and 4. However, HA types 1 and 3 did not show any bone formation within the

concavities even in the presence of BMPs which suggests that there are other factors that also play a critical role in initiating or inhibiting bone formation within the HA concavity.

One factor that has been shown in this study to play a role in the induction or inhibition of bone formation within the concavities is the particle size and distribution of the starting materials where the biomaterials that were made with relatively fine starting powders (types 1 and 3) did not induce bone formation as compared to those that were constructed with relatively coarse starting powders (types 2 and 4).

While all the results observed in this study are significant, they did not provide sufficient basis for explanation for the fact that no bone formation was observed in tissues harvested from HA sample types 1 and 3 at 90 days suggesting that further investigations have to be made into biomaterials to explain this behaviour. Another limitation of the study was the decision to exclude implantation of HA types 1 and 3 for harvesting at 180 days postimplantation based on the fact that bone formation was not observed in the implants 90 days post-implantation. In future studies, all biomaterials implanted for one time period should be

implanted for all periods irrespective of how they behave in between time periods.

6.0 CONCLUDING STATEMENTS

The results of this study revealed that the geometry, which in this study refers to the concavities of specific dimensions, acts as a regulator allowing or inhibiting cell differentiation. There are more mechanisms that need to be studied to unravel this phenomenon of spontaneous bone induction by the geometry of the substratum. The present study, however, has established that it is the effect of the substratum *per se* regulating and driving specific gene expression and the sequential cascade of events leading to bone formation by induction within the concavity in the heterotopic sites of adult baboons. The results of this study suggest that the BMPs are localised within the concavity and initiate bone formation as a secondary response. Further molecular studies need to be carried out using different animal models to shed further insights into the geometric induction of bone formation. This would be of critical importance in clinical contexts.

7.0 REFERENCES

Arun, K. G., Liansheng, S., Paul, R., *et al*., 2002. A 1-year study of osteinduction in hydroxyapatite-derived biomaterials in an adult sheep model: Part 1. Plast. Reconstr. Surg. 109: 619-630.

Asahina, I., Watanabe, M., Sakuri, N., *et al*., 1997. Repair of bone defect in primate mandible using a bone morphogenetic protein (BMP)-hydroxyapatite-collagen composite. J. Med. Dent. Sci. 44: 63-70.

Assoian, R. K. Komoriya, A. and Meyers, C. A., *et al*., 1983. Transforming growth factor beta in human platelets. J. Biol. Chem. 258: 7155-7160.

Beck, L. S., Amento, E. P., and Xu, Y., *et al*., 1993. TGF- ß1 induces bone closure of skull defects: Temporal dynamics of bone formation in defects exposed top rhTGF-ß1. J. Bone Miner. Res. 8: 753-761.

Beck, L. S., Amman, A. J., Aufdemorte, T. B. *et al*., 1991. In vitro induction of bone by recombinant transforming growth factor beta 1. J. Bone Miner. Res. 6: 961-968.

Begley, C. T., Doherty, M. J., Hankey, D. P. *et al*., 1993. The culture of human osteoblasts upon bone graft substitute. Bone. 14: 661-666.

Bentz, H., Thompson, A., Amstrong, R., *et al*., 1991. Transforming growth factor beta 2 enhances the osteoinductive activity of a

bovine bone-derived fraction containing bone morphogenetic protein 2 and 3. Matrix. 11: 269-275.

Bentz, H., Nathan, R. M., Rosen, D., *et al*., 1989. Purification and characterisation of a unique osteoinductive factor from bovine bone. J. Biol. Chem. 264: 20805-20810.

Birnboim, H. C. and Doly, J. 1979. A rapid alkaline extraction procedure for screening recombinant plasmid DNA. Nucleic Acids Res. 7: 1513-1522.

Bonassar, L. J. and Vacanti, C. A. 1998. Tissue engineering: The first decade and beyond.J. Cellular Biochem. Supplements. 30-31: 297-303

Bonfiglio, M. and Jeter, W. S. 1972. Immunological responses to bone. Clin. Orthop. 87: 19-27.

Bos, G. D., Goldberg, V. M., Zika, J. M., *et al*., 1983. Immune responses of rats to frozen bone allografts. J. Bone Joint Surgery. 65A: 239-246.

Bostrom, M., Lane, J. M., Tomin, E., *et al*., 1996. Use of bone morphogenetic protein-2 in the rabbit ulna nonunion model. Clin. Orthop. 327: 272-282.

Bouler, J. M., LeGeros, R. Z., Daculsi, G. 2000. Biphasic calcium phosphates: influence of three synthesis parameters on the HA/beta-TCP ratio. J. Biomed. Mater. Res. 51: 680-684.

Cao, Y., Linden, P., Shima, D., *et al*., 1986. *In vivo* angiogenic activity of hypoxia induction of heterodimers of placenta growth factor/vascular endothelial growth factor. J. Clin. Invest. 98: 2507-2511.

Carnesale, P. L. and Spankus, J. D. 1961. Clinical comparative study of autogenous and homogenous bone grafts. J. Bone Joint Surg. 41A: 887-894.

Cate, R. L., Mattaliano, R. J. and Hession, C. 1986. Isolation of the bovine and human genes for Mullerian inhibiting substance and expression of the human gene in animal cells. Cell: 45: 685-698.

Centrella, M., Casinghino, S., Kim, J. *et al*., 1995. Independent changes in type I and type II receptors for transforming growth factor ß induced by bone morphogenetic protein-2 parallel expression of the osteoblast phenotype. Mol Cell Biol. 15: 3273-3281.

Centrella, M., Horowitz, M. C. and Wozney, John. 1994. Transforming growth factor beta gene family members and bone. Endocrine Reviews. 15: 27-39.

Chang, B. S., Lee, C. K., Hong, K. S., *et al*., 2000. Osteoconduction of porous hydroxyapatite with various pore configurations. Biomaterials. 21: 1291-1298.

Chang, S. C., Hoang, B., Thomas, J. T., *et al*., 1994. Cartilage-derived morphogenetic proteins, new members of the transforming growth factor beta superfamily predominantly

expressed in long bones during embryonic development. J. Biol. Chem. 269: 28227-28234.

Christel, P. S. 1992. Biocompatibility of surgical grade dense polycrystalline alumina. Clinical Orthopedics. 282: 10-18.

Clark, D. A. and Coker, R. 1998. Transforming growth factor-beta (TGF- ß). Int. J. Biochem. Cell. Biol. 30: 293-298.

Cohen, S. N., Chang, A. C. and Hsu, L. 1972. Nonchromosomal antibiotic resistance in bacteria: genetic transformation of *Escherichia coli* by R factor DNA. Proc. Natl. Acad. Sci. USA. 69: 2110-2114.

Colnot, C. I. And Helms, J. A. 2001. A molecular analysis of matrix remodelling and angiogenesis during long bone development. Mech Dynamics. 100: 245-250.

Cong, Z., Jianxin, W. and Xingdong, Z. 2000. Osteoinductivity and biomechanics of a porous ceramic with autogenic periosteum. J Biomed Mater Res. 52: 354-359.

Cook, S. D. and Rueger, D. 1996. Osteogenic protein-1. Clin. Orthop. 324: 29-38

Cook, S. D., Wolfe, M. W. and Salkeld, S. L. *et al.*, 1995. Effect of recombinant human osteogenic protein-1 on healing of segmental defects in non human primates. J. Bone Joint Surg. 77: 734-746.

Cook, S. D., Baffes, G. C., and Wolfe, M. W. *et al*., 1994. Recombinant human bone morphogenetic protein-7 induces healing in canine long bone segmental defect model. Clin. Orthop. 301: 302-311.

Cook, S. D., Thomas, K. A. and Kay, J. F., *et al*., 1987. Hydroxyapatite-coated porous titanium for use as an orthopedic biologic attachment system. Clin. Orthop. 230: 303-311.

Cook. S. D., Thomas, K. A. and Kay, J. F., *et al*., 1986. Hydroxyapatite coated titanium for orthopedic implantation. Clin. Orthop. 232: 225-243.

Cooke, F. W. 1992. Ceramics in orthopedic surgery. Clin. Orthop. 276: 135-146.

Cunningham, N. S., Jenkins, N. A. and Gilbert, D. J., *et al*., 1995. Growth/ differentiation factor-10: A new member of the transforming growth factor beta superfamily related to bone morphogenetic protein-3. Growth factors. 12: 99-109.

Cunningham, N. S., Paralkar, V. and Reddi, A. H. 1992. Osteogenin and recombinant bone morphogenetic protein-2B are chemotactic for human monocytes and stimulate transforming growth factor ß1 mRNA expression. Proc. Natl. Acad. Sci. USA. 89: 11740-11744.

de Bortolli , C. Chailley-Heu, B. and Bourbon, J. R. 1995. Production of transforming growth factor (TGF) beta by fetal lung cells. Biol. Cell. 84:215-218.

De bruijn, J. D., Dalmeijer, R. de Groot, K. 1999. Osteoinduction by microstructured calcium phosphates. Transactions of the 25th Annual Meeting Society for Biomaterials, RI, USA. 235

de Groot, K. 1980. Bioceramics consisting of calcium phosphate salts. Biomaterials. 1: 47-50.

De Larco, J. E. and Torado, G. J. 1978. TITLE. Proc. Natl. Acad. Sci. USA. 75: 4001-4005.

Denissen, H., Montanari, C., Martinetti, R. *et al*., 2000a. Alveolar bone response to submerged bisphosphonate-complexed hydroxyapatite implants. J. Periodontol. 71: 279-286.

Denissen, H., Martinetti, R., van Lingen, A., *et al*., 2000b. Normal osteoconduction and repair in and around submerged highly bisphosphonate-complexed hydroxyapatite implants in rat tibiae. J. Periodontol. 71: 272-278.

Derynck, R. 1994. The biological complexity of transforming growth factor-ß. In: The Cytokine Handbook. A Thompson, editor. Academic Press, Boston. 319-342.

Derynck, R., Lindquist, P. B. and Lee, A., *et al*., 1988. A new type of transforming growth factor-beta, TGF-beta 3. EMBO J. 7: 3737-3743.

Derynk, R., Jarret, J. A., Chen, E. Y., *et al*. 1985. Human transforming growth factor–ß complementary DNA sequence and expression in normal and transformed cells. Nature. 316: 701-705.

Dhert, W. J. A., Klein, C. P. A. T., Wolke, J. G. G., *et al.*, 1991. A mechanical investigation of fluoropatite, magnesium whitlockite and hydroxyapatite plasma-sprayed coating in goats. J. Biomed. Mater. Res. 25: 1183-1200.

Dreyer, J. J. and Du Bruyn, D. B., 1968. Composition of a food mixture developed at the NNIR for supplementation of predominantly cereal diets. South African Medical Journal. 22: 600-604.

Duneas, N. Crooks, J. and Ripamonti, U. 1998. Transforming Growth factor beta 1: Induction of bone Morphogenetic protein genes expression during endochondral bone formation in the baboon, and synergistic interaction with osteogenic protein-1 (BMP-7). Growth Factors. 15: 259-277.

Ennerking, W. F., Buchardt, H. Puhl, J. J., *et al.*, 1975. Physical and biological aspects of repairin dog cortical-bone transplants. J. Bone Joint Surg. (Am). 57: 237-252.

Erlebacher, A. and Derynck, R. 1996. Increased expression of TGF-ß2 in osteoblasts results in osteoporosis-like phenotype. J. Cell Biol. 132: 195-210.

Fajardo, L. F., Prionas, S. D., Kwan, H. H., *et al.*, 1996. Transforming growth factor-β1 induces angiogenesis *in vivo* with a threshold pattern. Lab. Invest. 74: 600-608.

Feldman, D. and Estridge, T. 1984. Factors affecting soft tissue ingrowth into porous implants. Transactions 2nd World congress Biomaterials Society. 10th annual meeting. pp 37.

Ferretti, C. and Ripamonti, U. 2002. Human segmental mandibular defects treated with naturally-derived bone morphogenetic proteins. J. Craniofac. Surg. 13: 434-444.

Fine, A. Poliks, C. F. and Smith, B. D. 1990. The accumulation of type 1 collagen mRNAs in human embryonic lung fibroblasts stimulated by transforming growth factor beta. Connect. Tissue Res. 24: 237-247.

Foidart, J. M. and Reddi, A. H. 1980. Immunofluorescent localization of type IV collagen and laminin during endochondral bone differentiation and regulation by pituitary growth hormone. Dev. Biol. 75: 130-136.

Forage, R. G., Ring, J. M., Brown, R. W., *et al*., 1986. Cloning and sequence analysis of cDNA species coding for the two sub units of inhibin from bovine follicular fluid. Proc. Natl. Acad. Sci. USA. 83: 3091-3095.

Friedlaender, G. E., Perry, C. R., Cole, J. D., *et al*., 2001. Osteogenic protein-1 (bone morphogenetic protein-7) in the treatment of tibial nonunions. J. Bone Joint Surg. (Am). 83A: S151-58.

Fujisawa, R., Muzino, M., Nodasaka, Y. *et al*., 1997. Attachment of osteoblastic cells to hydroxyapatite crystals by a synthetic peptide (Glu7-pro-Arg-Gly-Asp-Thr) containing two functional sequences of bone sialoprotein. Matrix Biol. 16: 21-28.

Fujisawa, R., Nodasaka, Y. and Kuboki, Y. 1995. Further characterisation of interaction between bone sialoprotein (BSP) and collagen. Calcif. Tissue Int. 56: 140-144.

Fujiu, T. and Ogino, M. 1984. Difference of bond bonding behavior among surface active glasses and sintered apatite. J. Biomed. Mater. Res. 18: 845-859.

Furlong, R. J. and Osborn, J. F. 1991. Fixation of hip prostheses by hydroxyapatite ceramic coatings. J. Bone Joint Surg. 73-B: 741-745.

Galaev, I.Y. and Mattiason B. 2000. 'Smart' polymers and what they could do in biotechnology and medicine. Trends Biotech. 17. 335-340.

Geesink, R. G. T., Groot, K. and de Klein, C. P. A. T. 1988. Bonding of bone to apatite-coated implant. J. Bone Joint Surg. 70-B: 17-22.

Gentry, L. E., Webb, N. R., Lim, J. G. *et al.*, 1987. Type-1 transforming growth factor beta: Amplified expression and secretion of mature and precursor polypeptides in Chinese hamster ovary cells. Mol. Cell Biol. 7: 3418-3427.

Gerber, H. P. and Ferrare, N. 2000. Angiogenesis and bone growth. Trends Cardiovasc Med. 10: 223-228.

Gerhart, T. N., Kirker-head, C. A., Kritz, M. J., et al., 1993.Healing segmental femoral defects in sheep using recombinant human bone morphogenetic protein. Clin. Orthop. 293: 317-326.

Goshima, J., Goldberg, V. M. and Caplan, A. I. 1991. The osteogenic potential of culture-expanded rat marrow mesenchymal cells assayed *in vivo* in calcium phosphate ceramic blocks. Clin. Orthop.262: 298-.

Graham, NB. 1998. Hydrogels: their future, Part I. Med Device Technol. 9: 18-22.

Grauer, J. N., Patel, T. C. and Erulkar, J. S., *et al*., 2001. Evaluation of OP-1 as a graft substitute for intertransverse process lumbar fussion. Spine. 26: 127-133.

Graves, D. T., Owen, A. J.and Barth, R. K. *et al*., 1984. Detection of c-sis transcripts and synthesis of PDGF-like proteins by human osteosarcoma cells. Science. 226: 972-974.

Green, J. P., Wojno, T. H., Wilson, M. W., *et al*., 1995. Bone formation in hydroxyapatite orbital implants. Am J Opthalmology. 120: 681-682.

Guillemin, G., Patat, J. L., Fournie, J., *et al*., 1987. The use of coral as a bone graft substitute. J. Biomed. Mat. Res. 21: 557-567.

Hammonds, R. G., Schwall, R., Dudley A.,. *et al*., 1991. Bone inducing activity of mature BMP-2b produced from a hybrid BMP-2a/2b precursor. Mol. Endocrinol. 5: 149-155.

Harris, W. H. and Heaney, R.P. 1969. Skeletal renewal and metabolic bone disease. N. Engl. J. Med. 280:193-202.

Hayek, A., Culler, F. L., Beattie, G. M., *et al*., 1987. An *in vivo* model for the study of angiogenic effects of basic fibroblast growth factor. Biochem. Biophys Res Commun. 147: 876-880.

Heimke, G. 1990. Use of aluceramics in medicine. In: Hulbert, J. E., Hulbert, S. F. eds. Bioceramics. Indiana: Rose-Hulman Institute of Technology. 3: 19-30

Heine, U. I., Munoz, E. F., Flanders, K. C., *et al*., 1987. Role of transforming growth factor beta in the development of the mouse embryo. J Cell Biol. 105: 2861-2876.

Helder, M. N., Özkaynak, E., Sampath, T. K., 1995. Expression pattern of osteogenic protein-1 (Bone morphogenetic protein-7) in human and mouse development. J. Histochem.Cytochem. 43: 1035-1044.

Hench, L. L. and Wilson, J. 1984. Surface-active biomaterials. Science. 226: 630-636.

Hench, L. L., Splinter, R. J. and Allen, W. C., *et al*., 1971. Bonding mechanisms at the interface of ceramic prosthetic materials. J. Biomed. Mater. Res. Symp. 2: 117-141.

Herr, G., Hartwig, C. H., Boll, C., et al., 1996. Ectopic bone formation by composites of BMP and metal implants in rats. Acta. Orthop. Scand. 67: 606-610.

Hoffman, AS. 1995. “Intelligent” polymers in medicine and biotechnology. Artif Organs. 19: 458-467.

Holand, W., Vogel, W. and Nauman, K. *et al*., 1985. Interface reactions between machinable bioactive glass-ceramics and bone. J. Biomed. Mater. Res. 19: 303-312.

Holmes, E. R., Bucholz, W. R., and Mooney, V. 1987. Porous hydroxyapatite as a bone graft substitute in diaphyseal defects: A histometric study. Journal of Orthopedic Research. 5: 114-121.

Hostikka, S. L. and Trygvasson, K. 1988. The complete primary structure of the alpha 2 chain of human type IV collagen and comparison with the alpha 1 (IV) chain. J. Biol. Chem. 263: 19488-19493.

Hotten, G. C., Matsumoto, T., Kimura, M., *et al*., 1996 Recombinant human growth/differentiation factor 5 stimulates mesenchyme aggregation and chondrogenesis responsible for the skeletal development of the limbs. Growth Factors. 13: 65-74.

Huipin, Y., Zongjian, Y., Joost, D. e*t al*., 2001. Material-dependent bone induction by calcium phosphate ceramics: a 2.5 year study in dog. Biomaterials. 22: 2617-1623

Hulbert, S. F. 1990. The use of ceramics in medicine. In: Hulbert, J. E., Hulbert, S. F. eds. Bioceramics. Indiana: Rose-Hulman Institute of Technology. 3: 1-17.

Hulbert, S. F., Young, F. A., Mathews, R. S., *et al*., 1970. Potential ceramic materials as permanently implantable skeletal prostheses. J. Biomed. Mater. Res. 4: 433-456.

Itatani, C. and Marshall, G. J. 1984. Cellular responses to implanted replaniform hydroxyapatite. Trans. Orthoped. Res. Soc. 9: 123.

Ito, Y. 1997. “Intelligent biomaterials for tissue engineering" in “Advances in Biomaterials Science” ed. Akaike, T., Okano, T., Akashi, M., Terano, T. and Yui, N. CMC Co. Ltd. Tokyo. pp.421-432.

Itoh, S., Kikuchi, M., Takakuda, K., *et al*., 2000. The biocompatibility and osteoconductive activity of a novel hydroxyapatite/collagen composite biomaterial, and its function as a carrier of rhBMP-2. 54: 445-453.

Jarcho, M. 1986. Biomaterials aspects of calcium phosphates: Properties and applications. Dental clinics of North America. 30: 25-47.

Jarcho, M. 1981. Calcium phosphate ceramics. Clin. Orthop. 157: 259-278.

Jarcho, M., Gumaer, K. I., Doremus, R. H. and Drobeck, H. P. 1977. Tissue cellular, and subcellularevents at a bone ceramic interface. J. Bioeng. 1: 79-92.

Jin, QM., Takita, H., Kohgo, T., *et al*., 2000. Effects of geometry of hydroxyapatite as a cell substratum in BMP-induced ectopic bone formation. J Biomed Mater Res. 52: 491-499.

Johnson, E. E., Urist, M. R. and Finerman, G. A. M. 1988. Bone morphogenetic protein augmentation grafting of resistant femoral nonunions. A preliminary report. Clin. Orthop. 230:257-265.

Jones, C. M., Simon-Chazottes, D., Guenet, J-L., *et al*., 1992. Isolation of Vgr-2, a novel member of the transforming growth factor-ß-related gene family. Mol. Endocrinol. 6: 1961-1968.

Kato, K., Aoki, H., Tabata, T. *et al*., 1979. Biocompatibility of apatite ceramics in mandibles. Biomater. Med. Device Artif. Organs. 7: 291-297.

Kawai, T., Mieki, A., Ohno, Y., *et al*., 1993. Osteoinductive activity of composites of bone morphogenetic protein and pure titanium. Clin. Orthop. 290:296-305.

Kessler, E., Takahara, K., Biniaminov. L., *et al*., 1996. Bone morphogenetic protein-1: the type-1 procollagen-C proteinase. Science. 271; 360.

Kibblewhite, D. J., Bruce, A. G. and Strong, D. M., 1993. Transforming growth factor beta accelerates osteoinduction in a craniofacial onlay model. Growth Factors. 9: 185-193.

Kingsley, D. 1994. The TGF-ß superfamily: new members, new receptors and new genetic tests of functions in different organisms. Genes and Development. 8:133-146.

Kingsley, D. 1994. What do BMPs do in mammals? Clues from the mouse short ear mutation. TIGS. 10: 16-21.

Kitsugi, T., Yamamuro, T. and Kokubo, T. 1989. Bonding behavior of a glass-ceramic containing apatite and wollastonite in segmental replacement of the rabbit tibia under load-bearing conditions. J. Bone and Joint Surg. 71A: 264-272.

Klein, C. P. A., T., De Groot, K., Chen, W. *et al*., 1994. Osseous substance formation induced in porous calcium phosphate ceramics in soft tissues. Biomaterials. 15: 31-34.

Kothapalli, R., Buyuksal, I., Wu, S. Q., *et al*., 1997. Detection of ebaf, a novel human gene of the transforming growth factor beta superfamily association of gene expression with endometrial bleeding. J. Clin. Invest. 99: 2342-2350.

Krajewski, A., Ravaglioli, A., Mongiorgi, R., *et al*., 1988. Mineralization and calcium fixation within a porous apatitic ceramic material after implantation in the femur of rabbits. J. Biomed. Mater. Res. 22: 445-457.

Kuboki, Y., Jin, Q. and Takita, H. 2001. Geometry of carriers controlling phenotypic expression in BMP-induced osteogenesis and chondrogenesis. The Journal of Bone and Joint Surgery. 83A: S1-105-115.

Kuboki, Y., Sasaki, M. and Saito, A. 1998. Regeneration of periodontal ligament and cementum by BMP-applied tissue engineering.. Eur. J. Oral Sci. 106: 197-203.

Kuboki, Y., Takita, H., Tsuruga, E., *et al*., 1998. BMP-induced osteogenesis on the surface of hydroxyapatite with geometrically feasible and non feasible structures: topology of osteogenesis. J Biomed Mater Res. 39: 190-199.

Kuboki, Y., Saito, T., Murata, H., *et al*., 1995. Two distinctive BMP carriers induce zonal chondrogenesis and membranous ossification respectively; geometrical factors of matrices for cell differentiation. Connect. Tissue. Res. 32: 219-226.

Kuboki, Y., Yamagushi, H., Yokoyama, A., *et al*., 1991. The bone biomaterials interface. Osteogenesis induced by BMP-coated biomaterials. Biochemical principles of bone reconstruction in dentistry. In: The Bone Biomaterial Interface, University of TorontoPress, Toronto, p 127-138.

Kulkarni, A. B., Huh, C. G. Becker, D., *et al*., 1993. Transforming growth factor beta 1 null mutation in mice causes excessive inflammatory response and early death. Proc. Natl. Acad. Sci. USA. 90: 770-774.

Kurioka, K., Umeda, M., Teranobu, O. and Komori, T. 1999. Effects of various properties of hydroxyapatite ceramics on osteoinduction and stability. 45: 149-163.

Lacroix, P., 1945. Recent investigation on the growth of bone. Nature. 156: 576

Langer, R. 2000. Biomaterials in drug delivery and tissue engineering: one laboratory's experience. Acc Chem Res. 33: 94-101.

Larsen, H. D., Finger, I. M., Guera, L. R., *et al*., 1983. Prosthodontic management of the hydroxyapatite denture patient: A preliminary report. J. Prosthet. Dent. 49: 461-470.

Lee, S. C., Shea, M. and Battle, M. A. *et al*,. 1994. Healing of large segmental defects in rat femurs is aided by rhBMP-2 in PLGA matrix. J. Biomed. Mater. Res. 28: 1149-1156.

Lehnet, S. A. and Akhust, R. J. 1988. Embryonic expression pattern of TGF-ß type-1 RNA suggests both paracrine and autocrine mechanisms of action. Development. 104: 263-273.

Letterio, J. J. and Bottinger, E. P. 1998. TGF-beta knockout and dominant-negative receptor transgenic mice. Miner. Electrolyte Metab. 24: 161-167.

Lotz, M. and Seth, P. 1993. TGF-beta and HIV infection. Ann. N Y Acad. Sci. 23: 501-511.

Lowry, O. H., Rosebrough, N. J. and Farr, A. L., *et al.* 1951. Protein measurement with the Folin Phenol reagent. J. Biol. Chem. 193: 265-275.

Luyten, F. P., Cunnningham, N. S., Ma, S., *et al*., 1989. Purification and partial amino acid sequence of osteogenin, a

protein initiating bone differentiation. J. Biol. Chem. 264: 13377-13380.

Lyons, K. M., Hogan, B. L. M. and Robertson, E. J. 1995. Colocalization of BMP-7 and BMP-2 RNAs suggests that these factors cooperatively mediate tissue interactions during murine development. Mech. Dev. 50: 71-83.

Lyons, K. M., Graycar, J. L., Lee, A., *et al*., 1989. Vgr-1, a mammalian gene related to Xenopus Vg-1 and a new member of the transforming growth factor ß superfamily. Proc. Natl. Acad. Scie. USA. 86: 4554-4558.

Machwate, M., Zerath, E. Holy, X. *et al*., 1995. Systemic administration of transforming growth factor beta-2 prevents the impaired bone formation and osteopenia induced by unloading in rats. J. Clin. Invest. 96: 1245-1253.

Magan, A. and Ripamonti, U., 1996. Geometry of porous hydroxyapatite implants influences osteogenesis in baboons (*Papio ursinus*). The Journal of craniofacial surgery. 7: 71-78.

Mahmood, J., Takita, H., Ojima, Y., et al., 2001. Geometric effect of matrix upon cell differentiation: BMP-induced osteogenesis using a new bioglass with a feasible structure. J. Biochem. 129: 163-171.

Mankin, H. J., Gebhardt, M. C. and Tomford, W. W. 1987. The use of frozen cadaveric allografts in the management of patients with

brain tumours of the extremities. Orthop. Clin. North Am. 18: 275-289.

Marcelli, C., Yates, A. J. and Mundy, G. R. 1990. In vivo effects of human recombinant transforming growth factor beta on bone turnover in normal mice. J. Bone Miner. Res. 5: 1087-1096.

Mason, A. J., Hayflick, J. S., Ling, N., *et al*., 1985. Complementary DNA sequences of ovarian follicular fluid inhibin show precursor structure and homology with transforming growth factor-ß. Nature. 318: 659-663.

Massague, J. 1990. The transforming growth factor-beta family. Annu. Rev. Cell. Biol. 6: 597-641.

Matsaba, T., Ramoshebi, L. N. and Crooks, J. *et al*., 2001. Transforming growth factor-ß1 supports the rapid morphogenesis of heterotopic endochondral bone initiated by human osteogenic protein-1 via the synergistic upregulation of molecular markers. Growth Factors.19: 73-86.

Mayer, M., Hollinger, J., Ron, E., *et al*., 1996. Maxillary alveolar cleft repair in dogs using recombinant human bone morphogenetic protein 2 and a polymer carrier. Plast. Reconstr. Surg. 98: 247-259.

Mayo, K. E., Cerelli, G. M., Spiess, J., *et al*., 1986. Inhibin-A subunit cDNAs from porcine ovary and human placenta. Proc. Natl. Acad. Sci. USA. 83: 5849-5853.

McDavid, P. T., Boone, M. E., Kafrawry, A. H., *et al*., 1979. Effects of autogenous marrow and calcitonin on reactions to a ceramic. J. Dent. Res. 58: 1478-1483.

Metsger, D. S., Driskel, T. D. and Paulsrud, J. R. 1982. Tricalcium phosphate ceramic a resorbable bone implant. Review and current status. J. Am. Dent. Assoc. 105: 1035-1038.

Miki, T., Masaka, K. and Imai, Y., *et al*., 2000. Experience with freeze-dried PGLA/HA/rhBMP-2 as a bone graft substitute. J. Maxillofac. Surg. 28: 294-299.

Millan, F. A., Dehnez, F. and Konaiah, P. *et al*., 1991. Embryonic gene expression patterns of TGF-ß 1, -ß2, and -ß3 suggest differential development functions in vivo. Development. (Camb). 11: 131-144.

Miller, T. A., Ishida, K., Kobayashi, M, *et al*., 1991. The induction of bone by an osteogenic protein and the conduction of bone by porous hydroxyapatite: a laboratory study in the rabbit. Plast. Reconstr. Surg. 87: 87-95.

Miyamoto, S., Takaoka, K., Okada, T., *et al*., 1993. Polylactic acid-polyethylene glycol block copolymer: a new biodegradable synthetic carrier for bone morphogenetic protein. Clin. Orthop. 294: 333-343.

Mundy, G. R., (1996) Regulation of bone formation by bone morphogenetic proteins and other growth factors. Clinical Orthopedics and Related Research. 323: 24-28.

Mundy, G. R. 1995. Local control of bone formation. Clin. Othop. 313: 19-26.

Murata, M., Inoue, M., Arisue, M., Kuboki, Y. and Nagai, N. 1998. Carrier-dependency of cellular differentiation induced by bone morphogenetic protein in ectopic sites. Int J Oral Maxillofac Surg. 27: 391-396.

Noda, M. and Camilliere, J. J. 1989. In vivo stimulation of bone formation by transforming growth factor beta. Endocrinology. 124: 2291-2294.

Ogawa, Y., Schmidt, D. K. and Nathan, R. M., *et al*., 1992. Bovine bone activin enhances bone morphogenetic protein-induced ectopic bone formation. J. Biol. Chem. 267: 14233-14237.

Ohgushi, H., Dohi, Y. and Tamai, S. *et al*., 1993. Osteogenic differentiation of marrow stromal stem cells in porous hydroxyapatite. J. Biomed. Mat. Res. 27: 1401-1407.

Ohgushi, H., Okumura, M., Tamai, S., *et al*., 1990. Marrow-cell induced osteogenesis in porous hydroxyapatite and tricalcium phosphate: A comparative histomorphometric study of ectopic bone formation. J. Biomed. Mater. Res. 24: 1563-1570.

Ohgushi, H., Goldberg, V. M. and Caplan, A. I. 1989. Heterotopic Osteogenesis in porous ceramics induced by marrow cells. J. Orthop. Res. 7: 568-578.

Okumora, M., Ohgushi, H. and Tamai, S., *et al*., 1991. Primary bone formation in porous hydroxyapatite ceramic: a light and

scanning electron microscopic study. Cells and Materials. 1: 29-34.

Ono, I., Inoue, M. and Kuboki, Y. 1996. Promotion of the osteogenetic activity of recombinant human bone morphogenetic protein by prostaglandin E1. Bone. 19: 581-588.

Ono, I., Gunji, H. and Suda, K., *et al*., 1995. Bone induction of hydroxyapatite combined with bone morphogenetic protein and covered with periosteum. Plast. Reconstr. Surg. 95: 1265-1272.

Ono, I., Ohura, T. and Murata. M. *et al*., 1992. A study on bone induction in hydroxyapatite combined with bone morphogenetic protein. Plast. Reconstr. Surg. 90: 870-879.

Özkaynak, E., Schnegelsberg, P. N. J. and Opperman, H. 1991. Murine osteogenic protein (OP-1): High levels of mRNA in kidney. *Biochem. Biophys.* Res. Commun. 179: 116-123.

Padget, R. W., St Johnston, R. D. and Gelbar, W. M. 1987. A transcrit from a drosophila pattern gene predicts a protein homologous to the transforming growth factor beta family. Nature. 325: 81-84.

Paralkar, V. M., Nandedkar, A. K. N., Pointer, R. H., *et al*., 1990. Interaction of osteogenin, a heparin binding bone morphogenetic protein, with type IV collagen. J. Biol. Chem. 265: 17281-17284.

Parrish, F. F. 1972. Homograft of bone. Clin. Orthop.87: 36-42.

Pelton, R. W., Hogan, B. L., and Miller, D. A. 1990. Differential expression of genes encoding TGFs ß 1, 2, 3 during murine palatal formation. Dev. Biol. 141: 456-460.

Pelton, R. W., Nomura, S., Moses, H. L., *et al*., 1989. Expression of transforming growth factor beta 2 RNA during murine embryogenesis. Development, 106: 759-767.

Pieench, J. F. 1982. Extraskeletal implantation of a porous hydroxyapatite ceramic. J. Dent. Res. 61: 1458-1460.

Raghu, G., Masta, S., Meyers, D. *et al*., 1989. Collagen synthesis by normal and fibrotic human lung fibroblasts and the effect of transforming growth factor-beta. Am. Rev. Respir. Dis. 140: 95-100.

Rameshwar, P., Poddar, A., Zhu, G. and Gascon, P. 1997. Receptor induction regulates the synergistic effects of substance P with IL-1 and platelet-derived growth factor on the proliferation of bone marrow fibroblasts. J. Immun. 158: 3417-3424.

Ramoshebi, L. N. and Ripamonti, U. 2000. Osteogenic protein-1, a bone morphogenetic protein, induces angiogenesis in the chick chorioallantoic membrane and synergizes with basic fibroblast growth factor and transforming growth factor-ß1. Anat. Rec. 259: 97-107.

Ravaglioli, A., Krajewski, A., Biasini, V. *et al*., 1992. Interface between hydroxyapatite and mandibular human bone tissue. Biomaterials. 13: 162-167.

Reardon, W., Winter, R. M., Rutland, P., *et al*., 1994. Mutations in the fibroblast growth factor receptor 2 gene cause Crouzone syndrome. Nature Gene. 9: 98-103.

Reddi, A. H. and Kuettner, K. E. 1998: Vascular invasion of cartilage: correlation of morphology with lysozyme, glycosaminoglycans, protease-inhibitory activity during endochondral bone development. Dev. Biol. 82: 217-223.

Reddi, A. H. 1997. Bone morphogenetic proteins: An unconventional approach to isolation of first mammalian morphogens. Cytokine Growth Factor Rev. 8: 11-20.

Reddi, A. H. 1996. BMP-1. Resurrection as procollagen C proteinase. Science. 271: 463.

Reddi, A. H. 1994a. Bone and cartilage differentiation. Curr. Opin. Genet. Dev. 4: 737-744.

Reddi, A. H. 1994b. Symbiosis of biotechnology and biomaterials: applications in tissue engineering of bone and cartilage. J. Cell. Biochem. 56: 192-195.

Reddi, A. H., 1992. Regulation of cartilage and bone differentiation by bone morphogenetic proteins. Curr. Opi. Cell Biol. 4: 850-855.

Reddi, A. H. 1981. Cell biology and biochemistry of endochondral bone development. Coll. Rel. Res. 1: 209-226.

Reddi, A. H. 1974. Bone matrix in the solid state: geometric influence on the differentiation of fibroblasts. Adv. Biol. Med. Phy. 15: 1-18.

Reddi, A. H. and Huggins, C. B. 1973. Influence of geometry of transplanted tooth and bone on transformation of fibroblasts. Proc. Soc. Exp. Biol. Med. 143: 634-637.

Reddi, A. H. and Huggins, C. B., 1972. Biochemical sequences in the transformation of normal fibroblasts in adolescent rat. Proc. Natl. Acad. Sci. USA. 69, 1601-1605.

Richter, P. W., Thomas, M. E. and van Deventer, T. 1999. Macroporous hydroxyapatite bioceramics by solid freeform fabrication: towards custom implants. S. Afr. J. Sci. 95: 325-326.

Ripamonti, U., Crooks, J. and Rueger, D., *et al.*, 2001. Induction of bone formation by recombinant human osteogenic protein-1 and sintered porous hydroxyapatite in adult primates. . Plast. Reconstr. Surg. 107:977-988.

Ripamonti, U., Ramoshebi, L. N., Matsaba, T., *et al.*, 2001. Bone induction by BMPs/OPs and related family members in primates: The critical role of delivery systems. J.B.J.S. 83-A: S1-116-117.

Ripamonti, U. Prospects for tissue engineering of bone. Chapter XI-3. 2000. In K Sames (Ed.), Regeneration Medicine, Ecomed. pp. 1-7.

Ripamonti, U., Crooks, J., Matsaba, T. and Tasker, J. 2000a. Induction of endochondral bone formation by recombinant human

transforming growth factor-β2 in the baboon (*Papio ursinus*). Growth Factors. 17: 269-285.

Ripamonti, U., Van den Heever, B., Crooks, J., *et al*., 2000b. Long term evaluation of bone formation by osteogenic protein 1 in the baboon and relative efficacy of bone-derived bone morphogenetic proteins delivered by irradiated xenogeneic collagenous matrices. J. Bone. Miner. Res. 15. 1798-1809.

Ripamonti, U. 2000c. Smart biomaterials with intrinsic osteoinductivity: geometric control of bone differentiation, in Bone Engineering (Davies, J. E., ed.) EM2 Corporation Toronto, Canada.pp 215-221.

Ripamonti, U., Crooks, J. and Kirkbride, AN. 1999. Sintered porous hydroxyapatites with intrinsic osteoinductive activity: geometric induction of bone. S. Afr. J. Sci. 95: 335-343.

Ripamonti, U. and Duneas, N. 1998. Tissue morphogenesis and regeneration by bone morphogenetic proteins. Plast. Reconstr. Surg. 101: 227-239.

Ripamonti, U. and Reddi, A. H. 1997. Tissue engineering and morphogenesis of periodontal tissues by bone morphogenetic proteins. Crit. Rev. Oral. Biol. Med. 8: 154-163.

Ripamonti, U., Duneas, N., van den Heever, B., Bosch, C. and Crooks, J. 1997. Recombinant transforming growth factor β1 induces endochondral in the baboon and synergizes with recombinant osteogenic protein 1 (bone morphorgenic protein-7) to initiate rapid bone formation. J. Bone. Miner. Res.12: 1584-1595.

Ripamonti, U. 1996. Osteoinduction in porous hydroxyapatite implanted in heterotopic sites of different animal models. Biomaterials. 17: 31-35.

Ripamonti, U. and Duneas, N. 1996. Tissue engineering of bone by osteoinductive biomaterials. Mat. Res. Soc. Bull. 21: 36-39.

Ripamonti, U., Van den Heever, B., Sampath, T. K., *et al*., 1996a. Complete regeneration of bone in the baboon by recombinant human osteogenic protein-1 (hOP-1, bone morphogenetic protein -7). Growth Factors. 13: 273-289.

Ripamonti, U. Heliotis, M. and Rueger, D. C. *et al*., 1996b. Induction of cementogenesis by recombinant human osteogenic protein 1(hOP-1/BMP-7) in the baboon (Papio ursinus). Arch. Oral Biol. 41: 121-126.

Ripamonti, U. and Reddi, A. H. 1995. Bone morphogenetic proteins: Applications in plastic and reconstructive surgery. Adv. Plast. Reconstr. Surg. 11: 47-74.

Ripamonti, U. and Vukicevic, S. 1995. Bone Morphogenetic proteins: from developmental biology to molecular therapeutics. S. Afr. J. Sci. 91: 277-280.

Ripamonti, U, Ma, S., Cunningham, N. Yeates, L., and Reddi, A. H., 1993a. Reconstruction of the bone-bone marrow organ by osteogenin, a bone morphogenetic protein and demineralised bone matrix in calvarial defects of adult primates. Plast. Reconstr. Surg. 91: 27-368.

Ripamonti, U., Yeates, L., van den Heever, B. 1993b. Initiation of heterotopic osteogenesis after chromatographic adsorption of osteogenin, a bone morphogenetic protein, onto hydroxyapatite. Biochem. Biophys. Res. Commun. 193: 509-517.

Ripamonti, U. 1992. Calvarial reconstruction in baboons with porous hydroxyapatite. J. Craniofac. Surg. 3:149-159.

Ripamonti, U., Ma, S. Cunningham, N. S., et al., 1992a. Initiation of bone regeneration in adult baboons by osteogenin, a bone morphogenetic protein. Matrix. 12: 369-380.

Ripamonti, U. Ma, S. and van den Heever, B. *et al*., 1992c. Osteogenin, a bone morphogenetic protein, adsorbed on porous hydroxyapatite substrata induces rapid bone differentiation in calvarial defects of adult primates. Plast. Reconstr. Surg. 90: 382-393.

Ripamonti, U., Ma, S. and Reddi, A. H. 1992d. The critical role of geometry of porous hydroxyapatite delivery system in induction of

bone by osteogenin, a bone morphogenetic protein. Matrix. 12: 202-212.

Ripamonti, U., Ma, S. S., and Reddi, A. H. 1992e. Induction of bone in composites of osteogenin and porous hydroxyapatite in baboons. Plast. Recons. Surg. 89: 731-739.

Ripamonti, U. 1991a. Bone induction in non human primates. An experimental study on the baboon (Papio ursinus). Clinical Orthopaedics, 269: 284-294.

Ripamonti, U. 1991b. The morphogenesis of bone in replicas of porous hydroxyapatite obtained from conversion of calcium carbonate exoskeletons of coral. J. Bone. Joint. Surg. 73A: 692-703.

Ripamonti, U. 1990. Inductive bone matrix and porous hydroxyapatite composites in rodents and nonhuman primates. In handbook of Bioactive Ceramics, vol. 11: Calcium phosphate and Hydroxyapatite Ceramics, eds.
Yamamuro, J. Wilson-Hench, L. L. Hench, pp. 245-253. CRC Press Boca Raton.

Roberts, A. B., Seong-jin, K. and Paturu, K. *et al.*, 1991. Transcription control of expression of the TGF betas. Annals New York Academy of Sciences. 43-58.

Roberts, A. B. and Sporn, M. B. 1990. The transforming growth factor beta. In: Sporn, M. B., Roberts, A. B., (eds.). Handbook of experimental pharmacology Vol. 95, Part1. Springer-Verlag, Heidelberg Germany. 419-472.

Roberts , A. B., Sporn, M. B., Assoian, R. K., *et al*., 1986. Transforming growth factor type β: rapid induction of fibrosis and angiogenesis in vivo and stimulation of collagen formation in vitro. Proc. Natl. Acad. Sci. USA. 83: 4167-4171.

Roberts, A. B., Anzano, M. A. and Lamb, L. C. *et al*., 1981. New class of transforming growth factors potentiated by epidermal growth factor isolation from non-neoplastic tissues**.**. Proc. Natl. Acad. Sci. USA. 78: 5339-5343.

Roberts, A. B., Lamb, L. C., Newton, D. L., *et al*., 1980. Transforming growth factors: isolation of polypeptides from virally and chemically transformed cells by acid/ethanol extraction. Proc. Natl. Acad. Sci. USA. 77: 3494-3498.

Rodeo, S. A., Suzuki, K. and Deng, X. *et al*., 1999. Use of recombinant human bone morphogenetic protein-2 to enhance tendon healing in a bone tunnel. The American Journal of Sports Medicine. 27: 476-488.

Rosen, D., Miller, S. C. and Deleon, E., *et al*., 1994. Systemic administration of recombinant transforming growth factor-beta 2 (rhTGF-ß2) stimulates parameters of cancellous bone formation in juvenile and adult rats. Bone. 15: 355-359.

Rousseau, F. Bonaventure, J. and Legeal-Mallet, L., *et al*., 1994. Mutations in the gene encoding fibroblast growth factor receptor 3 in anchodroplasia. Nature. 371:252-254.

Rutherford, R. B., Wahle, J. and Tucker, M., *et al*., 1993. Induction of reparative dentine formation in monkeys by recombinant human osteogenic protein-1. Arch. Oral Biol. 38: 571-576.

Sampath, T. K., Rashka, K. E., Doctor, J. S., *et al*., 1993. Drosophila TGF-β superfamily proteins induce endochondral bone formation in mammals. Proc.Natl. Acad. Sci. USA. 90: 6004-6008.

Sampath, T. K., Maliakal, J. C., Hauschka, P. V., *et al*., 1992. Recombinant human osteogenic protein-1 (hOP-1) induces new bone formation *in vivo* with a specific activity comparable with natural bovine osteogenic protein and stimulates osteoblast proliferation and differentiation in vivo. J. Biol. Chem. 267. 20352-20362.

Sampath, T. K., Muthukumaran, N. and Reddi, A. H., 1987. Isolation of osteogenin, an extracellular matrix-associated bone-inductive protein, by heparin affinity chromatography. Proc. Natl. Acad. Sci. USA. 84: 7109-7113.

Sampath ,T. K. and Reddi, A. H. 1984. Importance of geometry of the extracellular matrix in endochondral bone differentiation. J. Cell. Biol. 98: 2192-2197.

Sampath, T. K. and Reddi, A. H. 1984. Distribution of bone inductive proteins in mineralised extracellular matrix. Biochem. Biophys. Res. Commun. 119: 949-961

Sampath, T. K. and Reddi, A. H. 1981. Dissociative extraction and reconstitution of extracellular matrix components involved in local bone differentiation.Proc. Natl. Acad. Sci. USA. 78: 7599-7603.

Sasano, Y., Kamakura, S., Nakamura, M., *et al*., 1995. Subperiosteal implantation of octacalcium phosphate (OCP) stimulates both chondrogenesis and osteogenesis in the tibia, but only osteogenesis in the parietal bone of a rat. The Anatomical Records.242: 40-46

Sasano, Y., Ohtani, E., Narita, K., *et al*., 1993. BMPs induce direct bone formation in ectopic sites independent of the endochondral ossification in vivo. Anatomical Records. 236: 373-380.

Schmidt, P. D., Bible, C. G., Mcmaster, G. K., *et al*., 1991. Differential expression of TGF-ß1, ß2 and ß3 genes during mouse embryogenesis. Development. 111: 117-130.

Schreiber, A. B., Winkler, M. E. and Derynck, R. 1986. Transforming growth factor-α: a more potent angiogenic mediator than epidermal growth factor. Science. 232: 1250-1253.

Schwall, R. H., Nikolic, K. and Szonyi, E., *et al*., 1988. Recombinant expression and characterisation of human activin A. Mol. Endocrinol. 3: 1237-1241.

Sekiya, H., Mikuni-Takagaki, Y., Kondoh, T. and Seto, K. 1999. Synergistic effect of PTH on the mechanical responses of human alveolar osteocytes. Biochem. Biophys. Res. Commun. 264: 719-723.

Shah, M., Foreman, D. M. and Ferguson, M. W. J. 1995. Neutralization of TGF-ß1 and TGF-ß2 or exogenous addition of TGF-ß3 to cutaneous rat wounds reduces scarring. J. Cell Science. 108: 985-1002.

Shinozaki, M., Kawara, S. and Hayashi, N., *et al*., 1997. Induction of subcutaneous tissue fibrosis in newborn mice by transforming growth factor-ß simultaneous application with basic fibroblast growth factor causes persistent fibrosis. Biochem. Biophys. Res. Commun. 237: 292-297.

Shors, E. C., White, E. W. and Kopchok, G. 1989. Biocompatibility, osteoconduction and biodegradation of porous hydroxyapatite, tricalcium phosphate, sintered hydroxyapatite and calcium carbonate in rabbit bone defects. Mat. Res. Symp. Proc. 110: 211-217.

Si, X., Jin, Y. and Yang, L. (1998) Induction of new bone by ceramic bovine bone with recombinant human bone morphogenetic protein-2 and transforming growth factor beta. Int. J. Maxillofac. Surg. 27. 310-314.

Sillet, H. K., Cruickshank, S. M. and Southgate, J. 2001. Transforming growth factor beta Promotes 'death by neglect' in post-activated human T cells. Immunology. 102: 310-316.

Sires, B. S., Holds, J. B., Kincaid, M. C., *et al*., 1997. Osteogenin enhanced bone specific differentiation in hydroxyapatite orbital implants. Ophthalmol. Plst. Reconstr. Surg. 13: 244-251

Soballe, K., Gotfredsen, K., Brockstedt-Rasmussen, H., *et al*., 1989. Histologic analysis of a retrieved hydroxyapatite-coated femoral prosthesis. Clin. Orthop. 272: 255-258.

Sprugel, K. H., McPherson, J. M. and Clowes, A. W. 1987. Effects of growth factors in vivo. Cell ingrowth into porous subcutaneous chambers. Am. J. Pathol. 129: 601-613.

Storm, E. E., Huynh, T. V. and Copeland, N. G. 1994. Limb alterations in brachypodism mice due to mutations in a new member of the TGF-ß superfamily. Nature. 368: 639-643.

Takahashi, T., Tominaga, T. and Watabe, N., *et al*., 1999. Use of porous hydroxyapatite graft containing recombinant human bone morphogenetic protein-2 for cervical fusion in a caprine model. J. Neurosurg. (Spine 2). 90: 224-230.

Takaoka, K., Koezuka, M. and Nakahara, H. 1991. Telopeptide-depleted bovine skin collagen as a carrier for bone morphogenetic protein. J. Orthop. Res.9: 902-907.

Takaoka, T., Okumura, M., Ohgushi, H., *et al*., 1996. Histological and biochemical evaluation of osteogenic response in porous hydroxyapatite coated alumina ceramics. Biomaterials. 17: 1499-1505.

Takaoka, K., Nakahara, H., Yoshikawa, H., *et al*., 1988. Ectopic bone induction on and in porous hydroxyapatite combined with collagen and bone morphogenetic protein. Cli. Orthop. 234: 250-254.

ten Djike, P., Hanse, P., Iwata, K. K., *et al*., 1988. Identification of another member of the transforming growth factor type beta gene family. Proc. Natl. Acad. Sci. USA. 85: 4715-4719.

Thomas, M., Richter, W., Matsaba, T., Ramoshebi, N., Teare, J., Renton, L., Ripamonti, U. 2003. Gene expression and bone induction regulated by bioceramic substratum. Key Engineering Materials. 240-242.: 639-642.

Thomas, M. E., Richter, P. W., van Deventer, T., *et al*., 1999. Macroporous synthetic hydroxyapatite bioceramics for bone substitute applications. South African Journal of Science. 95: 359-362.

Toth, J. M., Lynch, K. L., Hackbarth, D. A., et al., 1993. Ceramic-induced osteogenesis following subcutaneous implantation of calcium phosphates. Bioceramics.6: 9-13

Tracy, B. M. and Doremus, R. H. 1984. Direct electron microscopy studies of the bone hydroxyapatite interface. J. Biomed. Mater. Res. 1984: 719-726.

Trueta, J. 1963. The role of the vessels in angiogenesis. J. Bone Joint Surg. 45B: 402-418.

Tsuruga, E., Takita, H., Itoh, H., Wakisaka, Y. and Kuboki, Y. 1997. Pore size of porous hydroxyapatite as the cell substratum controls BMP-induced osteogenesis. J Biochem. 121: 317-324.

Tucker, A. S., Matthews, K. L., and Sharpe, P. T., 1998. Transformation of tooth type induced by inhibition of BMP signalling. Science. 282: 1136-1138.

Urist, M. R., Nilsson, O., Rasmussen, J., *et al*., 1987. Bone regeneration under the influence of bone morphogenetic protein (BMP) beta tricalcium phosphate (TCP) composite in skull trephine defects in dogs. Clin. Orthop. 214:295-304.

Urist, M. R. Lietze A and Dawson E. 1984. β-tricalcium phosphate delivery system for bone morphogenetic protein. Clinical orthopedics. 187: 277-280.

Urist, M. R. 1980. Heterotopic bone formation. In: Fundamental and clinical bone physiology. Urist, M. R. ed. J. B. Lippincott Company, Philadelphia. Pp 369-393.

Urist, M. R. 1965. Bone: Formation by autoinduction. Science. 159: 893-899.

Van Eeden, S. P. and Ripamonti, U. 1994. Bone differentiation in porous hydroxyapatite is regulated by the geometry of the substratum: implications for reconstructive craniofacial surgery. Plast. Reconstr. Surg. 93: 959-966.

Vargervik, K.1992. Critical sites for new bone formation: In: Habal MB, Reddi Ah, editors. Bone grafts and Bone substitues. Philadelphia: Saunders. 112-120.

Vukicevic, S., Kopp, J. B., Luyten, F. P., *et al*., 1996. Induction of nephrogenic mesenchyme by osteogenic protein-1 (bone

morphogenetic protein-7). Proc. Natl. Acad. Sci. USA. 93: 9021-9026.

Wang, C., Stewart, R. J. and Kopecek, J. 1999. Hybrid hydrogels assembled from synthetic polymers and coiled-coil protein domains. Nature. 397: 417-420.

Wang, E. A., Rosen V, D'Alessandro J. S., *et al*., 1990. Recombinant human bone morphogenetic protein induces bone formation. Proceedings, National Academy of Science.USA. 87: 2220-2224.

Wataya-kaneda, M., Hashimoti, K. and Kato, M., *et al*., 1994. Differential localisation of transforming growth factor beta precursor isotype in normal human skin. J. Dermatol Sci. 8: 38-44.

Weeks, D. L. and Melton, D. A. 1987. A material mRNA localized to the vegetal hemisphere in Xenopus eggs codes for a growth factor related to TGF-ß. Cell. 51: 861-867.

White, E. and Shors, E. 1986. Biomaterial aspects of Interpore-200 porous hydroxyapatite. Dental Clinics of North America. 30: 49-67.

Williams, D. 1997. Ceramics transformed: manipulating crystal structures to toughen bioceramics. Med Device Technol. 8: 6-8.

Wozney, J. M. 1992. The bone morphogenetic protein family and osteogenesis. Mol. Reprod.Dev. 32: 160-167.

Wozney, J. M., Rosen, V. and Celeste, A. J., *et al*., 1988. Novel regulators of bone formation: Molecular clones and activities. Science 242: 1528-1534.

Xhang, X. 1991. A study of porous block HA ceramics, its osteogenesis. In: Ravaglioli AA, Krajewski A, editors. Bioceramics and the human body. Amsterdam: Elsevier Science. 408-415.

Yamada, S., Heymann, D., Bouler J. M., et al., 1997. Osteoclastic resorption of calcium phosphate ceramics with different hydroxyapatite/beta-tricalcium phosphate ratios. Biomaterials. 18: 1037-1041

Yamasaki, H. 1990. heterotopic bone ormation around porous hydroxyapatite ceramics in the subctis of dogs. Jpn J. Oral Biol. 32: 190-192

Yamasaki, H. and Sakai, H. 1992.Osteogenic response to porous hydroxyapatite ceramics under the skin of dogs. Biomaterials. 13: 308-312.

Yan, J., Xiang, W., Baolin, L., *et al*., 1994. Early histologic response to titanium implants complexed with bovine bone morphogenetic protein. J. Prosthet. Dent. 71: 289-294.

Yang, Z., Yuan, Huipin., Tong , W et al., 1996. Osteogenesis in extraskeletally implanted porous calcium phosphate ceramics: variability among different kinds of animals. Biomaterials. 17: 2131-2137.

Yoshikawa, T., Ohgushi, H. and Tamai, S. 1996. Immediate bone forming capability of prefabricated osteogenic hydroxyapatite. Journal of Biomedical Materials Researh. 32: 481-492.

Yuan, H., Li, Y., Yang, Z., *et al*., 1997. Calcium phosphate ceramic-induced osteogenesis in rabbits. In: Zhang X, Ikada Y, editors. Biomedical materials research in the Far East (III). Kyoto: Kobunshi kankokai. 228-229

Yuan, H., Yang, Z., Li, Y., *et al*., 1998. Materials in Medicine. J. Mater. Sci: 9:723.

Yuan, H., Li, Y., de Bruijn, J., D., *et al*., 2000. Tissue esponses of calcium phosphate cement: a study in dogs. Biomaterials. 21: 1283-1290

Yuan, H., de Bruijn, J., D., Li, Y., *et al*., 2001. Bone frmation induced by calcium phosphate ceramics in soft tissue of dogs: a comparative study between alpha-TCP and beta-TCP. J Mater Sci:Mater Med. 12: 7-13

8.0 APPENDICES

Appendix 1

Substrate solution- 0.01M para-nitrophenyl phosphate (PNPP) in distilled water

Buffer solution- 0.1 M sodium barbitone in distilled water pH 9.3

Base solution- 0.1 N (Sodium hydroxide) NaOH in distilled water

Homogenising buffer- 0.15 M (Sodium chloride) NaCl, 0.003 M Sodium

bicarbonate ($NaHCO_3$) in distilled water

Appendix 2

Bovine serum albumin (BSA) stock: 1 mg/ml in distilled water

Protein stock solution: 2% Na_2Co_3 (w/v) in 0.1 N NaOH

Copper Reagent: To 100 ml of protein stock solution, were added 1 ml of 2% Na Tartrate and 1 ml of 1% (w/v) $CuSO_4.5\ H_2O$.

Phenol reagent: 2 N Folin Ciocalteau diluted 1:1 with distilled water.

Appendix 3

Stable Iron Haematoxylin

Fuschin Ponceau

Orange G Molybdate

Methyl Blue

Appendix 4

Buffer : Sodium Chloride: 17.0 g
Di-sodium Hydrogen Orthophosphate: 2.8 g

Potassium Dihydrogen Orthophosphate: 0.4 g

Potassium Chloride: 0.4 g

Distilled Water: 2000 ml

Appendix 5

0.1% diethylpyrocarbonate (DEPC) in milli Q water

Tri- Pure isolation reagent

Chloroform

100% isopropanol

75% ethanol

lauryl sarcosine/EDTA solution

Appendix 6

Electrophoresis buffer, 5X concentrate

0.1 M Mops

40 mM sodium acetate, pH 7.0

5 mM EDTA

Gel loading buffer:

50% glycerol

1 mM EDTA

0.25% bromophenol blue

0.25% xylene cyanol FF

Appendix 7

Formamide

Formaldehyde

RNA gel loading buffer

0.5µg/ml ethidium bromide

DEPC treated water

Appendix 8

Formamide

Formaldehyde

RNA gel loading buffer

0.5µg/ml ethidium bromide

DEPC treated water

Appendix 9

Luria Bertani (LB) medium

Agar

$CaCl_2$

Glycerol

Appendix 10

LB medium
Distilled water

Appendix 11

High Pure Plasmid Kit

LB medium

Tris-HCl buffer

Appendix 12
Tris borate (TBE) buffer

DNA megaprime labeling kit RPN 1606

alpha- ^{32}P dCTP

DNA purification kit

Appendix 13

Sonicated fish sperm DNA

QuikHYB

SSC (Saline Sodium Citrate)

SDS (Sodium Dodecyl Sulphate)